Available online at www.sciencedirect.com
SCIENCE DIRECT®
Coordination Chemistry Reviews 246 (2003) 247–289
COORDINATION CHEMISTRY REVIEWS
www.elsevier.com/locate/ccr

Review

Polycatenation, polythreading and polyknotting in coordination network chemistry☆

Lucia Carlucci, Gianfranco Ciani*, Davide M. Proserpio

Dipartimento di Chimica Strutturale e Stereochimica Inorganica (DCSSI), Università di Milano, Via G. Venezian 21, 20133 Milano, Italy

Received 25 February 2003; accepted 14 July 2003

Contents

Abstract

The use of crystal engineering concepts has produced a variety of coordination networks, many of which exhibit novel and fascinating types of entanglements of individual motifs. This review analyses the structures of a number of entangled polymeric networks reported in these years by many groups. A topological classification of the different interlocked and interweaved species is attempted. Wide classes of polycatenated and polythreaded species have been recognized and other *phenomena*, as polyknotting (self-penetration) and interweaving of 1D chains, are also discussed. Unexpected topological features and new linkages, that were previously overviewed, have been discovered, including the first examples of infinite Borromean links.

Keywords: Coordination networks; Entanglements; Polycatenane; Polyrotaxane; Polyknot

☆ After the submission of this review few other species relevant to the subject here described have been reported: a new triple helix (Y. Cui, H.L. Ngo, W. Lin, Chem. Commun. (2003) 1388) and a new interweaved clothlike species formed by pairs of chains, in a ‘two-over/two-under’ fashion (Y.-H. Li, C.-Y. Su, A.M. Goforth, K.D. Shimizu, K.D. Gray, M.D. Smith, H.-C. zur Loye, Chem. Commun. (2003) 1630). Moreover, another theoretical approach to the topology of networks and entangled arrays has also appeared (S.T. Hyde, A.-K. Larsson, T.Di Matteo, S. Ramsden, V. Robins, Aust. J. Chem. 56 (2003) 981).

* Corresponding author. Tel.: +39-02-50314446; fax: +39-02-50314454.
E-mail addresses: gianfranco.ciani@unimi.it (G. Ciani), davide.proserpio@istm.cnr.it (D.M. Proserpio).

0010-8545/$ – see front matter © 2003 Elsevier B.V. All rights reserved.
doi:10.1016/S0010-8545(03)00126-7

1. Introduction

The interest in polymeric coordination networks [1] is rapidly expanding not only for their potential properties as functional solid materials (see e.g. [2]), in host–guest chemistry, ion exchange, catalysis, and for the development of optical, magnetic and electronic devices, but also for their intriguing architectures and topologies. Indeed, many examples have evidenced that structural types and topological features unprecedented in the world of inorganic compounds and minerals can be observed in coordination polymer frameworks. Within the realm of supramolecular chemistry [3], the crystal engineering of coordination polymers represents a relatively recent *area*, whose basic concepts were proposed at the beginning of the nineties by Robson and coworkers [1a,4]. In principle, the network topology could be driven by carefully selecting the coordination geometry of the metal centers and the structure of the organic ligands. However, a variety of weak interactions and subtle factors can play a decisive role in orienting the outcome of the crystallization processes, so that a 'true' engineering of polymeric networks, both from a structural and a functional point of view, still remains a quite difficult challenge. An additional complexity in these systems consists in the frequent finding of supramolecular isomers and polymorphs [5]. Nevertheless, interesting materials have been obtained by means of crystal engineering principles.

The efforts of many groups in these years have produced a *plethora* of polymeric structural motifs. Many of these reports describe rather trivial structures, without proven functional properties, that mainly contribute to increase the already rich structural database of coordination polymers. In a recent article, Sharma [6] has noticed that 'ironically' the major achievement of all this activity consists in 'viewing crystal structures as networks', and has illustrated advantages and limits of this concept. Indeed, we believe that the 'network approach' or topological approach [7,1b] to crystal chemistry is an important achievement. It is a useful tool for the analysis, comparison and design of network structures in that it simplifies complex species to schematized reference nets. It results fundamental in the rationalization of the fascinating but intricate entanglements of multiple motifs that are continuously being reported. A topological investigation is a necessary preliminary work in this field in order to identify packing trends that may allow for the rational design of functional materials.

Only few papers have been up to now specifically devoted to the study of the relationship between properties and the topology of 'interpenetration' in these species, and much work is still necessary along this direction. Interpenetrating nets have been considered as potential super-hard materials [8], and peculiar magnetic and electrical properties have been attributed to extended systems as a consequence of their interpenetration [9,10]. Moreover, interpenetration can also, unexpectedly, enhance the porosity of a network [11] and can produce flexible hosts with high selectivity for guest inclusion [12].

In what follows we will examine this variety of entangled polymeric networks in the attempt to accomplish a 'first level' classification of the different interweaving and interlocking aspects. This review is not intended to be comprehensive in that we have not considered here important classes of interpenetrating networks, that have already been discussed in other detailed reviews [13–15] and, moreover, we have mainly focused our analysis on coordinatively bonded rather than on hydrogen bonded systems. Particular attention has been devoted to characterize in these extended entanglements the *phenomena* of mechanical interlocking typical of molecular structures such as catenanes, rotaxanes, and knots [16,17]. Our re-examination of the network structures has, *inter alia*, evidenced many misinterpretations appeared in the literature and has allowed us to recognize the existence of unexpected and puzzling topological features, like Borromean links.

2. Entanglements in coordination networks

The increasing number of coordination networks reported in the literature offers a rich variety of new structural types that continuously increase our knowledge of these polymers, also called metal-organic frameworks (MOF). Many of these arrays are particularly intriguing because of the presence of independent motifs entangled together in different ways. Besides to species that are nowadays considered relatively common, like inclined interpenetrating square grid 2D layers or *n*-fold interpenetrating diamondoid nets, a number of new types of entanglements have been recently found, that need to be rationalized and classified.

An entangled system is an extended array more complex than its constituents, that is comprised of individual motifs forming, *via* interlocking or interweaving, a periodic architecture infinite in at least one dimension. Most of these species can be considered regularly repeated infinite versions of the finite molecular motifs illustrated in Scheme 1.

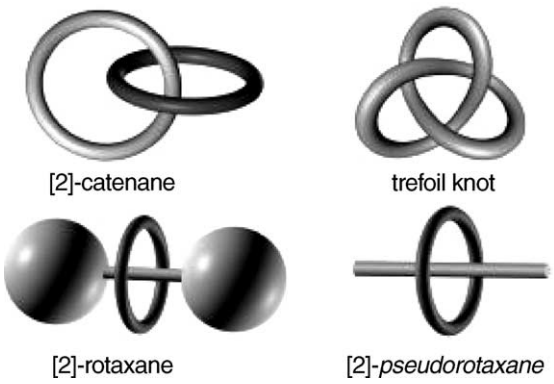

Scheme 1.

The linkages in catenanes, knots and rotaxanes are the subject of many topological investigations [18,19] especially concerning the classification of isomers within complex organic molecules, organic polymers and biopolymers, natural and synthetic forms of DNA and so on [16,17]. Thus, in treating the complexity of entangled coordination polymers, we will try to use concepts derived both from crystal chemistry, that has furnished the bases for the topological classification of inorganic nets, and from the mathematical theory of knots and links.

Before analyzing the different structural classes we will examine some preliminary aspects concerning the topology of entanglements.

2.1. From crystal structures to topological classification

A correct analysis of the crystal structures is fundamental in order to avoid misinterpretations, that can easily occur, about the nature and extent of the entanglements, as we shall see in the next sections. The rationalization of these, often quite complicated, structures implies a sequence of steps leading to the basic nets of linked nodes.

The steps can be summarized as follows: (i) simplification process, (ii) identification and separation of the individual motifs, (iii) topological analysis of these motifs, and (iv) topological analysis of the whole entanglement.

The simplification phase, exemplified by Hoskins and Robson in an early paper on this subject [4], consists in the rather obvious operation of removing all the unnecessary elements that have no topological relevance, thus leaving only the essentials, represented by nodes and links (vertices and edges, respectively, according to the nomenclature of graph theory). For instance, polyatomic nodes (like metal clusters or polyfunctional ligands) can be replaced by their baricentres.

The simplified model must be effectively representative of the connectivity of the real network. In some cases, however, this step leads to structural descriptions that are rather subjective in the selection of both the nodes and, especially, the connections (links) joining the nodes. Alternative rationalizations can be accomplished, that result in motifs of different topology, depending upon the choice of the chemical or/and mechanical bonds considered relevant in the assembly of the architecture.

This is the same kind of problem encountered in the construction of the graph of a molecule (representing the molecular constitutional formula) for the study of its topology. While the identification of the vertex set is straightforward, the relationship of the edges in the graph to the bonds in the molecule is less well defined, and we should establish which bonds in the molecule can be regarded as "topologically significant". Mislow, in his studies on molecular chirality, has also suggested an "edge weighted" complete graph (each atom being bonded to every other atom) in the analysis of isomeric structures, with the weights associated to the "nature and extent of bonding and non-bonding interactions within pairs of atoms". A considerable arbitrariness is inevitably implicit in any graph, and "whether or not a given geometrically chiral molecular model is considered to be also topologically chiral depends on which subset of bonds in the molecule is considered to be topologically significant" [18]. According to the common usage in organic chemistry, Walba had suggested to consider topologically significant only covalent bonds [19], but there is no obvious reason to limit the 'edge set' to these bonds, thus ignoring the whole *area* of supramolecular chemistry.

In coordination networks concurrent chemical forces are often operative, including coordinative bonds, hydrogen bond bridges, secondary bonds involving the anions, aurophilic metal-metal interactions, π-interactions and others. Thus, we are faced with the problem of deciding when a link is a topologically significant link. A current useful practice consists in assuming a level within this hierarchy of forces to be applied in the description of the net. For instance, in $[Zn(4,4'\text{-bipy})_2(H_2O)_2](SiF_6)$ [20] the $Zn(4,4'\text{-bipy})_2$ coordination sublattice can be described as a 3D array comprised of two sets of (4, 4) layers giving inclined interpenetration (see Fig. 1 top). However, the metal atoms on layers of the different inclined sets are connected *via* H_2O–SiF_6–H_2O hydrogen bond bridges involving the Zn-coordinated water molecules. Taking into account also these interactions results in a more complex 3D single 4,8-connected array showing the peculiar feature of self-penetration, as illustrated in Fig. 1 (bottom).

Situations like this are rather common (others will be encountered in the following sections) and both the above descriptions could be considered, for different reasons,

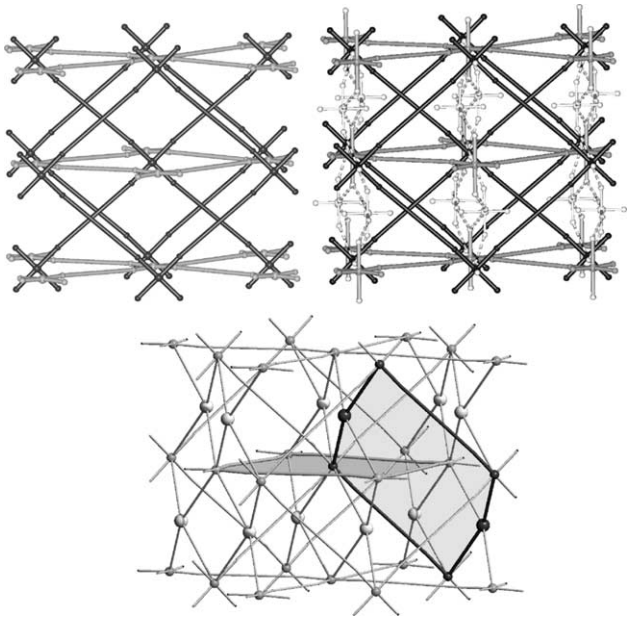

Fig. 1. Schematic views of the inclined interpenetration of the (4, 4) layers in $[Zn(4,4'\text{-bipy})_2(H_2O)_2](SiF_6)$ [20], without (top left) and with (top right) the hydrogen bond bridges, and the resulting unique 3D self-penetrating net (bottom).

valuable for the elucidation of the network topology. Thus, the insertion in a model of additional weaker interactions can have drastic effects like changing the topology of the individual motifs, the type of entanglement or also the dimensionality of the whole array.

Mechanical bonds, as those illustrated in Scheme 1, are responsible for the formation of the majority of the known extended periodic entanglements. In examining polythreaded systems, however, one debatable point concerns the difficult distinction between a rotaxane and a *pseudo*-rotaxane. At the molecular level rotaxanes are characterized by the presence of bulky stoppers on the rods, that must inhibit dethreading, while *pseudo*-rotaxanes can be separated by chromatography or at high temperatures. However also rotaxanes obtained by slippage can have low energy barrier to dethreading, so that the difference with respect to *pseudo*-rotaxanes remains a delicate problem and the boundary is not well-defined [17a]. The extended polymeric analogues of these species present problems of similar nature, with the additional complication that no experiments can be envisaged to differentiate the two situations. Two examples of polythreaded 2D architectures are illustrated in Scheme 2. In both cases, 1D chains (comprised of rings in I and of side arms in II) are threaded into the rings of other 1D motifs. The arrays can be 'disentangled' in a ideal sense only if one judges the rings or the side arms inadequate as stoppers (i.e. if the barriers to dethreading are considered low and the systems are classified as poly*pseudo*-rotaxanes rather than as polyrotaxanes). Considerations about the flexibility of the spacers and/or the rigidity at the nodes could lead to a specific choice, but, perhaps, as in molecular species [17a,21], also in these cases the point remains substantially open.

According to the above comments we could conclude that establishing the topology of these species is not only a formal procedure but rather an interplay between chemistry and mathematical theory. The process of simplification or abstraction that represents the passage from real objects to their idealized models needs chemical considerations. After simplification the problem remains exclusively based on a mathematical ground.

The next step requires that we identify the individual motifs contributing to the entanglement. The separation can be accomplished in a computer-aided process, whose output consists of a set of distinct 'colored' nets [22].

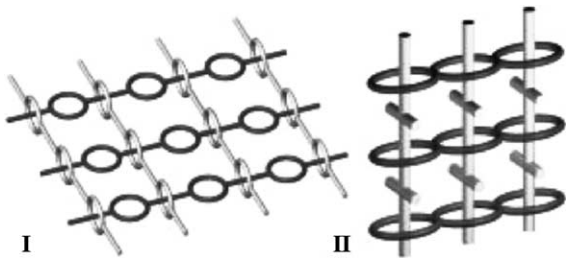

Scheme 2.

The topological classification of the individual component motifs is then carried out according to generally accepted *criteria* adopted in a variety of structural contexts. To this purpose a fundamental contribution is represented by a famous series of articles and books on crystal chemistry published many years ago by Wells [23], who analyzed and classified a great number of nets. He introduced a method for the systematic generation of 3D arrays from 2D nets and described also many hypothetical motifs that were successively discovered within coordination polymers. The studies by Smith on the classification of zeolites and related materials are also valuable [24]. The more recent developments of the theory are largely due to the work of O'Keeffe [25], who has shown that both the enumeration and the topological definition of nets are still difficult open problems. Nevertheless, also a 'partial' topological classification of the nets can result of great utility.

The notation for 2D or 3D nets is based on the analysis of the 'circuits', i.e. the closed paths beginning and ending at each node, characterized by the number q of edges comprised in the loop. Any two edges at a node define an angle, and with p-connected nodes there are $[p(p-1)/2]$ such angles in a 3D net (but only p in a 2D simple layer [25c]), for each of which we can find a large number of different circuits. A p-connected node can be identified by a Schläfli symbol (or *point symbol*) of the type $q_1^a \cdot q_2^b \cdots$ that gives the size (number of edges) of the "shortest circuit" at each angle. Thus, we have for the 2D honeycomb and square-grid nets and for the 3D diamond net, all uninodal (i.e. containing a single type of node), the Schläfli (short) symbols 6^3 [or (6, 3)], 4^4 [or (4, 4)] and 6^6, respectively. Hereinafter, we will adopt for uninodal plane nets the most common symbols (6, 3) or (4, 4).

Unfortunately these symbols are far from being sufficient to unambiguously identify a net, as evidenced, for instance, by the fact that NbO and quartz have the same symbol $6^4 \cdot 8^2$. A modified version of the above notation, the long Schläfli symbol (also "vertex symbol"), is more useful. This requires that instead of the "shortest circuits" we take into account the "shortest rings", being a "ring" an n-membered circuit that represents the shortest possible path connecting *all* the $[n(n-1)/2]$ pairs of nodes belonging to that circuit, without any "short cut" [25a,25b]. Not all the "shortest circuits" are also "shortest rings". The long Schläfli symbol for a p-connected node has a form like $q_{1A} \cdot q_{2B} \cdots q_{pZ}$, where q_1, q_2, ... are the "ring" sizes and A, B, ... are the numbers of "rings" that close at each angle. For diamond the long Schläfli symbol is $(6_2 \cdot 6_2 \cdot 6_2 \cdot 6_2 \cdot 6_2 \cdot 6_2)$. More interestingly, different symbols can be assigned to NbO $(6_2 \cdot 6_2 \cdot 6_2 \cdot 6_2 \cdot 8_2 \cdot 8_2)$ and quartz $[(6_1 \cdot 6_1 \cdot 6_2 \cdot 6_2 \cdot 8_7 \cdot 8_7)$ or better $(6 \cdot 6 \cdot 6_2 \cdot 6_2 \cdot 8_7 \cdot 8_7)]$. The long symbol in PtS (cooperite), that contains 'square-planar' Pt and 'tetrahedral' S nodes with the same short symbol $4^2 \cdot 8^4$, allows also to differentiate the two nodes: Pt $(4 \cdot 4 \cdot 8_2 \cdot 8_2 \cdot 8_8 \cdot 8_8)$ and S $(4 \cdot 4 \cdot 8_7 \cdot 8_7 \cdot 8_7 \cdot 8_7)$. Also the long Schläfli symbols, however, are unable to differentiate, e.g. diamond from lonsdaleite and other parameters,

like the "coordination sequence" [25a,25b], must be considered. Computer programs, as EUTAX [26], could give an essential help in the above analysis.

In conclusion, we have many theoretical tools at our disposal but a general method for an univocal classification of the nets seems still lacking, as we shall see.

Within coordination networks a variety of topological types have been observed, the most frequently found being those reviewed by O'Keeffe et al. [7].

Going on, we are now faced with the problem that is the central subject of this review, i.e. how the different motifs are inter-related. This step consists in attempting a rationalization and classification of the modes of entanglement, i.e. in exploring the topology at a higher level of organization.

2.2. Interpenetration and other entanglements: general aspects and definitions

Among the different types of entangled systems those commonly called 'interpenetrating networks' [13] are nowadays the more numerous and the more extensively studied from a topological point of view. The origin of interpenetration can be ascribed to the presence of large free voids in a single network, though it has been demonstrated that interpenetration does not prevent the possibility of obtaining open porous materials [11,27].

Interpenetrating networks were also known within inorganic chemistry and mineral world. Wells introduced the theme of interpenetrating nets (identical or of two or more kinds) by stating that they "cannot be separated without breaking links" [23b]. At that time (1977) few examples were known: the mineral neptunite, a two-fold interpenetrating net with the α-$ThSi_2$ topology [10^3–b, ($10_2{\cdot}10_4{\cdot}10_4$)] [28], cuprite Cu_2O (one of the first crystal structures determined), some borates and Ice VII, all containing two-fold interpenetrating diamondoid nets, and some others, including also the first examples of well characterized supramolecular assemblies *via* hydrogen bond bridges in β-quinol [29], [two-fold $6{\cdot}10^2$, ($6{\cdot}10_2{\cdot}10_2$)] or *via* coordinative bonds ([Cu(adiponitrile)$_2$](NO_3), six-fold diamondoid [30]).

Since then a great number of structural reports have appeared on interpenetrating coordination polymers, sustained both by coordinative or by hydrogen bonds. The current world records for the degree of interpenetration belong to two recently reported diamondoid networks: within coordination polymers the maximum number of interpenetrating nets (10-fold interpenetration) has been observed in [Ag(ddn)$_2$](NO_3)] (ddn = 1,12-dodecanedinitrile) [31], while a higher number of interpenetrating frames (11-fold interpenetration) has been reported for a hydrogen-bonded structure, with molecules of a tetraphenol as tetrahedral centers and benzoquinone units as rods [32].

Though particular aspects of the topology of interpenetration have been described in a number of papers in the rich literature on coordination polymers and on metal-based supramolecular chemistry, few systematic studies on this subject have been reported. We can mention some analyses of interpenetration in layered structures by Zaworotko [1e], in open porous cubic lattices by Yaghi and coworkers [33] and in diamondoid nets [31,34]. The most important and comprehensive contributions can, indeed, be found in two reviews by Batten and Robson [13,14], that have introduced some basic and commonly accepted concepts and definitions. Of much interest are also the recent highlights by Batten [15], to whom all the researchers in the *area* should be grateful for making available a precious list (recurrently updated) of the entanglement *phenomena* in a web site (http://www.web.chem.monash.edu.au/Department/Staff/Batten/Intptn.htm) [15a].

According to Batten and Robson [13] interpenetrating structures, that "can be disentangled only by breaking internal connections", are characterized by the presence of infinite structurally regular motifs that must contain rings "through which independent components are inextricably entangled".

We have previously observed [35] that, within structures that are consistent with all the conditions described above, different subclasses can be envisaged. A more detailed classification is generally an useful enhancement, so we suggest to consider the distinct subclass of 'polycatenanes', having the peculiar features that all the constituent motifs have lower dimensionality than that of the resulting architectures and that each individual motif is catenated only with the surrounding ones but not with all the others, as a single ring of a chain. Moreover, we think that, in principle, also 0D motifs could be comprised within the possible components. A comparison of the main aspects of this subclass with those that we could think to attribute to interpenetrating networks is given in Table 1.

The features listed in the left column are those observed in the 'classical' interpenetrating networks, like *n*-fold parallely interpenetrating 2D layers or *n*-fold interpenetrating 3D nets. In both interpenetrated and polycatenated species, the individual motifs cannot be separated "without breaking *rings*". In between these two subclasses, however, additional intermediate situations are also possible, like some recently found examples of interpenetrating 3D *plus* 2D frameworks [37].

According to the concepts of chemical topology [18,19] applied to the study of molecular knots and links (catenanes), both these subclasses give nontrivial entanglements, in the sense that the whole arrays can be considered 'topological isomers' of their component motifs (like an *n*-catenane versus the separated *n* rings).

At difference from polycatenated arrays, other entangled systems that will be considered in the next sections, like polyrotaxanes, poly*pseudo*-rotaxanes (or *pseudo*-polyrotaxanes?), interweaved chains and infinite multiple helixes, are all trivial (separable) entanglements in a strict topological sense. Polyrotaxanes (see Section 4.1) deserve a special

Table 1
Interpenetration vs. polycatenation

Interpenetration	Polycatenation
The component motifs are infinitely extended 2D or 3D nets	The motifs can be 0D and 1D (with closed circuits) or 2D, of the same or of different types
The individual motifs have an identical topology[a]	The resulting entangled array is infinite periodic
The number of the entangled motifs is finite	Finite or infinite number of entangled motifs
The resulting dimensionality is the same of the component motifs	The resulting dimensionality is increased
Each motif is interlaced with all the other ones forming the array	Each motif is never interlaced with all the other ones of the array

[a] This is an arbitrary choice and not a strictly necessary condition. Rare examples are known of interpenetrating 3D nets with different topology [36].

comment in that they are currently described as interpenetrating systems, i.e. that cannot be disentangled [13]. This, indeed, relies on metrical (dimensions of the components, geometrical rigidity) or energetical (barriers to dethreading) considerations rather than on topological ones. By analogy with the topological nomenclature for stereoisomers [19] we could suggest different terms for polycatenane and polyrotaxane arrays, *namely* 'Topological' or 'Euclidean' entanglements, respectively. In spite of their trivial nature, rotaxanes are discussed together with catenanes in many reviews on linked systems. Their topological relevance is still debated [19] and studies are known that include also rotaxanes in the realm of topology [38]. We will return to this point in the proper section.

Finally, we must also mention here that the renewed interest for the topological analysis of crystal structures and for the classification and enumeration of networks has produced recently novel approaches, including the characterization of nets based on tilings [39a,39b], on minimal surfaces [39c,39d] and on graphs [39e,39f].

3. Polycatenation

As previously stated, the main feature of polycatenation consists in that the whole catenated array has a higher dimensionality then that of each of the component motifs. These motifs can be, in principle, 0D, 1D or 2D species that must contain closed loops and that are interlocked *via* topological Hopf links [40] (see Scheme 3). Each motif can be catenated with a finite or also with an infinite number of other independent motifs *but not* with all.

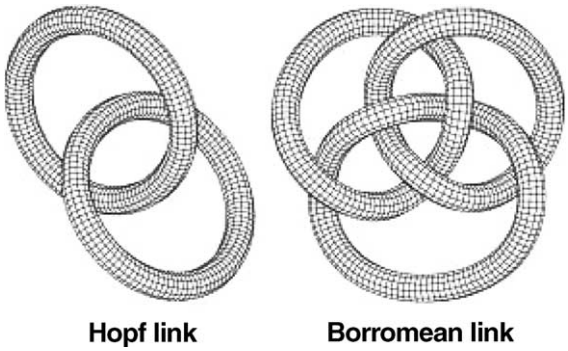

Scheme 3.

In order to classify these entanglements we need to establish in each case: (i) the topology of the individual motifs; (ii) the mode of catenation of these motifs, and (iii) the 'degree of entanglement'.

The mode of catenation concerns the mutual orientation and interrelation of the component motifs.

The degree of entanglement requires more comments. While, for instance, in *n*-fold interpenetrated diamondoid networks we can easily define the degree of interpenetration since they contain a finite number of independent nets, in a polycatenated species we are forced to introduce some different concepts. First of all, we must make a distinction between the cases of finite or infinite interlocking of individual motifs (see, e.g. I, II, V for finite, and III, IV for infinite interlocking, respectively, in Scheme 4). In the first case, we must specify only the number *n* of motifs effectively entangled with each individual motif. In the second case, on the other hand, we should specify the number of rings of other motifs that are interlocked with a single ring of each independent component (in general different values are possible for the different components).

With the need for a shorthand we could tentatively introduce an index of the 'degree of catenation' (Doc), defined by the number *n* of motifs entangled to a single motif for the finite interlocking, or by a symbol of type (*a*/*b*/...) for the infinite one, where *a*, *b*, ... are the numbers of 'external' rings catenated to a single ring in the first, second, ..., motif, in order of increasing value. For instance, we have Doc = 2 for II and V, and Doc = (1/1) for III and IV in Scheme 4. This is of course, as we shall see, a rather rough provisional notation, waiting for a systematic mathematical analysis of the topology of the entanglement *phenomena*.

We must mention here that molecular motifs containing different rings could give inextricable entanglements not only *via* Hopf links. One alternative way involving at least three closed circuits at a time is represented by the Borromean links [41] (see Scheme 3). These are nontrivial links in which three rings are entangled in such a way that any two component rings form a trivial link, i.e. if any one ring is cut the other two are free to separate. Using links of this type infinite 1D, 2D or 3D arrays can be imagined, two of which are illustrated in Fig. 2 (none actually observed) [42]. The

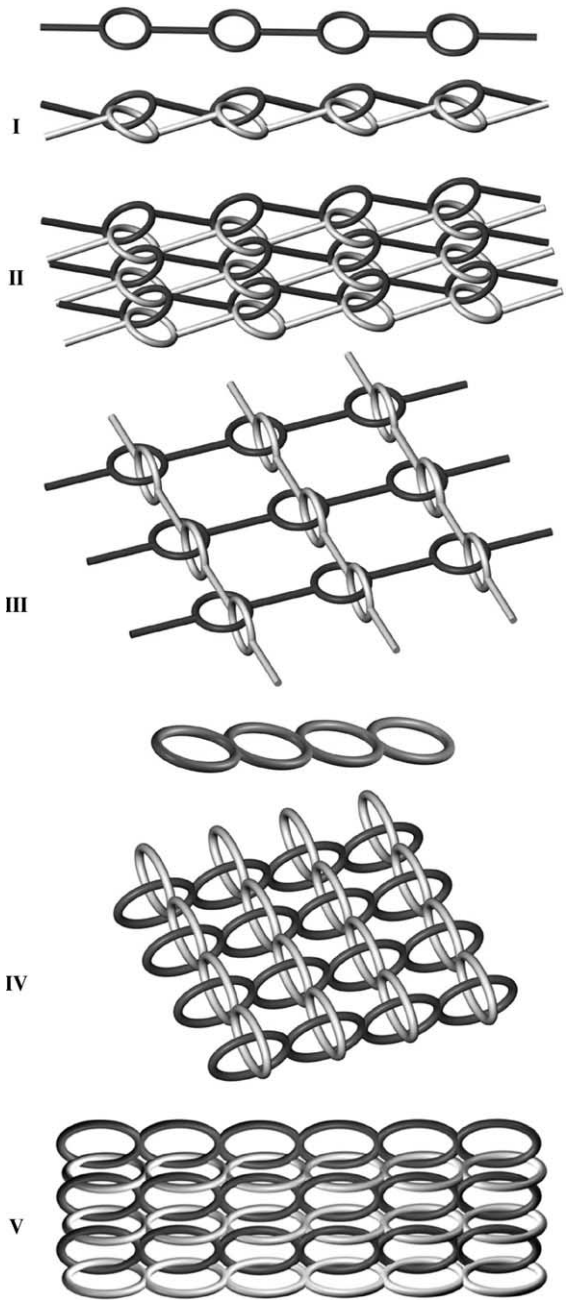

Scheme 4.

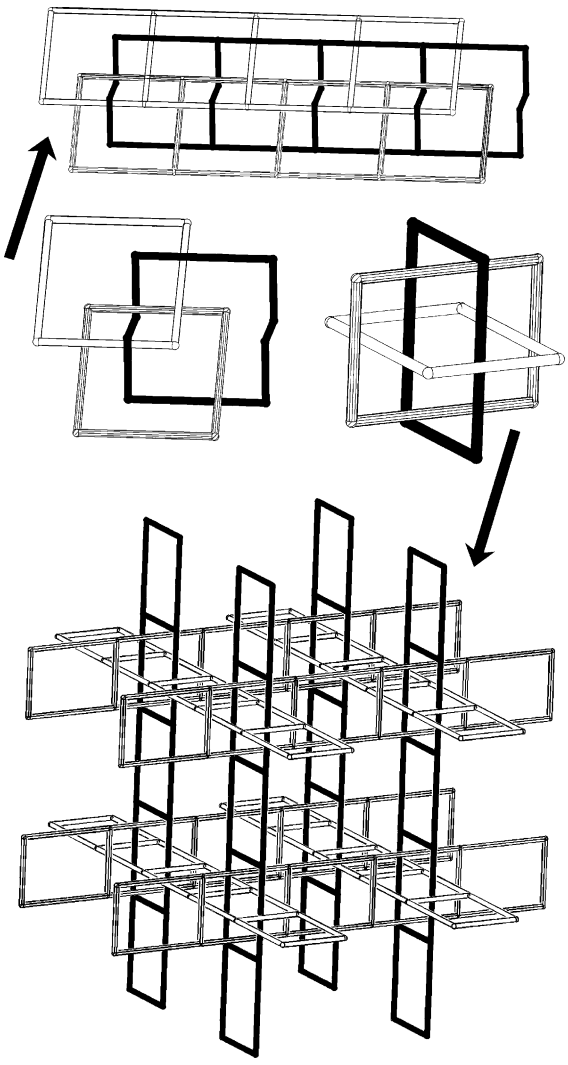

Fig. 2. Extended entanglements *via* Borromean links: (top) 'three Borromean ladders' and (bottom) a 3D 'Borromean array'. The different presentations of the Borromean rings in the two cases are evidenced. The individual motifs (ladders) are not catenated but cannot be disentangled [42].

peculiar and intriguing topological feature of these extended entanglements is that none of the motifs is catenated to the other ones (Doc = 0) but altogether they are not separable. Links like these could appear only mathematical curiosities; indeed we have been able to identify real infinite examples of these interweaving *phenomena*, that will be discussed in Section 3.2.1.

We will describe in this section the different types of known polycatenated species, classified on the basis of increasing dimensionality of the component motifs.

Though finite (0D) motifs, that contain closed circuits, could give, in principle, catenation into infinite periodic arrays, no real example has been as yet characterized. A number of metal-based molecular rings, polygons and cages have been obtained in recent times using the synthetic strategies of coordination chemistry and supramolecular chemistry [43]. These species are potential candidates as building blocks for the construction of extended architectures, as shown by the numerous examples of metal containing n-catenanes and other mechanically linked systems [16,17,44]. Catenation of rings *via* Hopf links could result in polymeric species of different dimensionality, as, infinite 1D polycatenanes or 2D polycatenated layers ("chain mail" like) (see Scheme 5).

Many examples of polycatenated species containing a certain number of molecular rings have been described within complex organic species [17], proteins [45] and synthetic DNA assemblies [46].

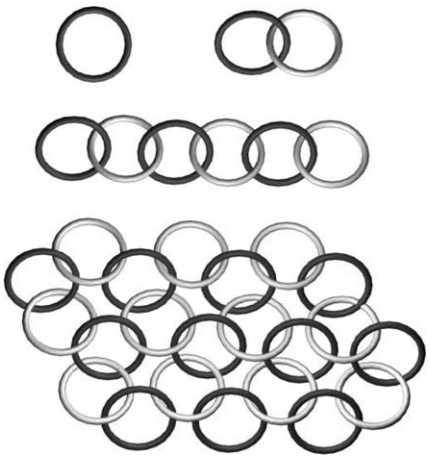

Scheme 5.

3.1. Polycatenated 1D motifs

Different types of 1D polymeric species can be considered suitable to give polycatenation, that include chains of alternating rings and rods, ribbons of rings and ladders. Some possible modes of catenation of 1D chains are illustrated in Scheme 4; three cases of catenated ladders are shown in Scheme 6.

The known real examples are, at present, exclusively based on infinite molecular ladders. Ladders are rather common 1D motifs within coordination polymers, considering the number of reported structures containing non entangled variants of this theme [47]; however, catenation makes the difference.

The catenation of two ladders running in a parallel direction can give the two-fold interpenetrated 1D structure of the type illustrated in Scheme 6 (I) and observed only in the hydrogen bonded network of [1,3,5-$C_6H_3(CH_2COOH)_{1.5}(CH_2COO)_{1.5}](NH_4)_{1.5}$ [48]. The two ladders are interpenetrated at a dihedral angle of 83°. All the other characterized systems are 2D or 3D entanglements.

Only one example has been reported that illustrates the (1D → 2D) catenation. In the complex $[Cu_2(MeCN)_2L_3](PF_6)_2$ [L = 1,4-bis(4-pyridyl)butadiyne] [49a] undulating ladders run in parallel direction and are laterally catenated by two other ladders by each side, thus forming 2D entangled layers (see Fig. 3). The same structure is observed also with the BF_4^- counterion [49b]. Each ladder is penetrated by other four (Doc = 4) and the two inner ladders are themselves catenated. In this case, the tetrahedral Cu(I) centers allow the ladder to undulate, but this type of 'side catenation' can be realized also with planar ladders, disposed as in III of Scheme 6.

Few examples are also known of polycatenated flat ladders that give a 3D architecture (1D → 3D). The inclined mode of catenation and the resulting 3D architectures are similar in all the known cases. Within the species $[M_2(bpethy)_3(NO_3)_4]$ (M = Zn [50a] or Co [50a,50b], bpethy = 1,2-bis (4-pyridyl)ethyne), $[Co_2(bpethe)_3(NO_3)_4]$[bpethe = 1,2-(4-pyridyl)ethene)] [50c] and $[Cu_2(ip)(4,4'\text{-bipy})_2]$ (ip = isophthalate) [50d] the ladders are catenated as in Fig. 4 (top and middle).

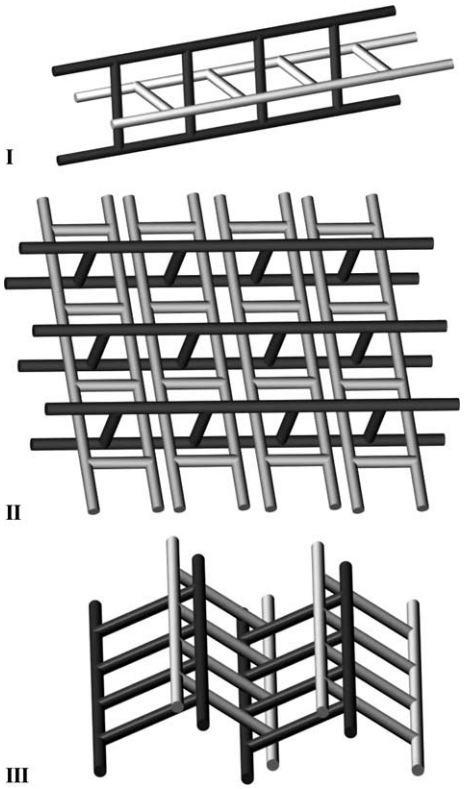

Scheme 6.

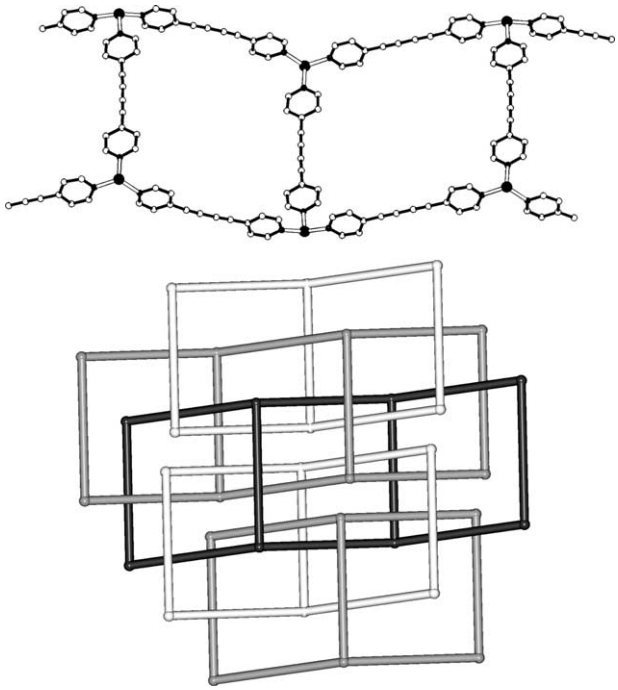

Fig. 3. A single undulated ladder (top) and the (1D → 2D) catenation (bottom) in $[Cu_2(MeCN)_2L_3](PF_6)_2$ [49a].

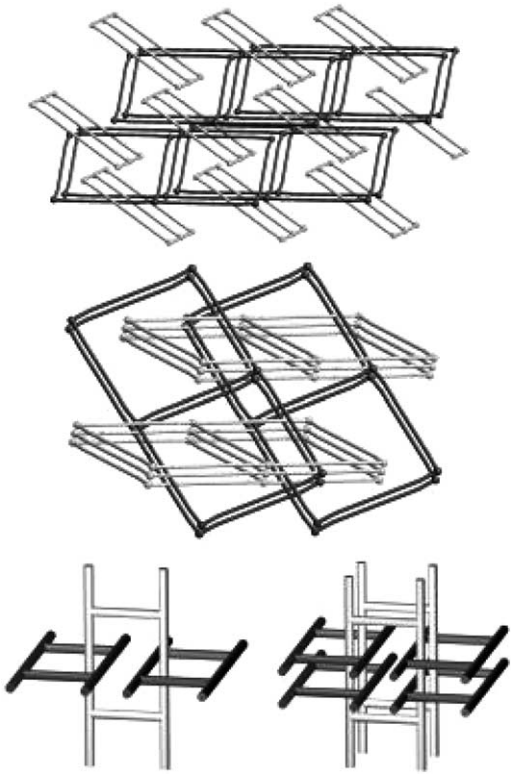

Fig. 4. Polycatenated ladders in the $[M_2(bpethy)_3(NO_3)_4]$ species [50a,b] (top, middle and bottom left) and in $[Cd(L)_{1.5}](NO_3)_2$ [51] (bottom right).

The squares of each ladder are interlocked with two inclined ladders [Doc = (2/2)], as shown in Fig. 4 (bottom left). On the other hand, in $[Cd(L)_{1.5}](NO_3)_2$ [L = 1,4-bis(4-methylenepyridyl)benzene] [51], due to the presence of longer bidentate spacers, each square of a ladder is catenated by four other ladders [Doc = (4/4)] instead of two (see Fig. 4, bottom right).

3.2. Polycatenated 2D motifs

Interlocked 2D layers are well known to belong to two distinct classes, depending on the relative orientations of the planes of the independent motifs. When the planes of all the entangled sheets are parallel the arrays have been described as showing 'parallel interpenetration'; otherwise different sets of sheets are observed (usually two) that cross at a certain angle, giving rise to an overall 3D entangled architecture, in the mode that has been called 'inclined interpenetration' [13].

In the former class, moreover, all the entangled sheets can lie or not on a common average plane. If they lie the resulting array is an *n*-fold interpenetrated 2D structure, with no increase in dimensionality and a finite number of interweaved motifs. These arrays include interpenetrated (6, 3) or (4, 4) layers (and also few cases with more rare topologies) that have already been classified and described in detail [13,52]; they will not be further discussed here. Only the other modes, leading to 3D arrays, i.e. to structures showing an increase of dimensionality with respect to the component motifs (2D → 3D), will be considered.

3.2.1. The 'parallel' interlocking mode

We describe here species that are comprised of independent layers whose average planes are parallel but displaced in a perpendicular direction, thus generating a polycatenated 3D architecture. Interlocking can occur either because the sheets are deeply undulated simple layers or because they are multiple layers, in both cases exhibiting some thickness.

This interlocking mode has been discovered only recently (the first example has been reported in 1997 [53]) but the number of examples is ever growing.

It can be useful for the rationalization of these entanglements to establish also the number of motifs that must be 'removed' in order to separate the whole array into two distinct parts (index of separation, Is). As a chain can be disrupted by breaking one ring so the 'ideal' elimination of a single motif is sufficient to separate the more simple of these 3D entanglements (Is = 1). In frameworks showing higher complexity more motifs must be removed (Is > 1). The same index could be applied to other systems polycatenated in a parallel fashion, like the ladders already illustrated in Fig. 3 (having Is = 2).

Catenated simple layers are relatively less common (see Table 2). Two examples containing (4, 4) layers are known. In $[Cd(dca)_2(bpp)]$ [dca = dicyanamide; bpp = 1,3-bis(4-pyridyl)propane] [54] the four-membered meshes exhibit different types of edges (two are bridged by one bpp ligand and two are bridged by two dca ligands), as shown in Fig. 5 (left). The arc-shaped bpp ligands protrude from both sides of the sheets. Thus each undulated layer results catenated with the two nearest neighboring ones (Doc = 2), that are rotated about the normal axis (i.e. on adjacent layers the 'waves' run in almost perpendicular directions), as illustrated in Fig. 5 (right). A single 'square' of each layer is interlocked with two 'squares', one of the 'upper' and one of the 'lower' layer.

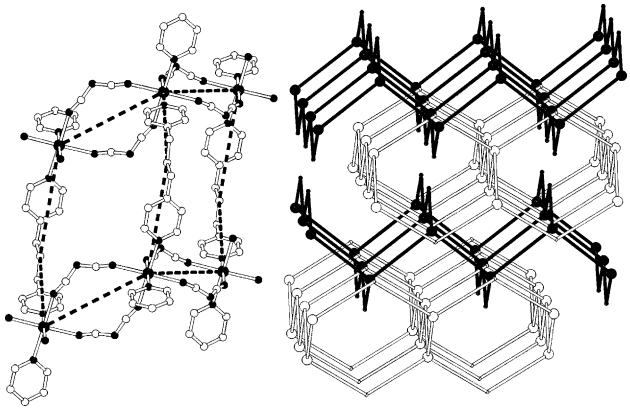

Fig. 5. The four-membered meshes (left) and the polycatenation of the undulated layers (right) in $[Cd(dca)_2(bpp)]$ [54].

Table 2
Parallel interlocking (2D → 3D)

Compound	Layer topology	Mode of catenation	Doc	Reference
Simple layers				
$[Cd(dca)_2(bpp)]$ [dca = dicyanamide; bpp = 1,3-bis(4-pyridyl)propane]	(4, 4)	*ABCD* stacking sequence; *A–C* pair rotated with respect to the *B–D* one; Is = 1	2	[54]
$[Cu_6(CN)_5(trz)]$ (trz = triazolate)	(4, 4)	*AB* stacking sequence; *A* rotated respect to *B*; Is = 1	2	[55]
$[Cu(bpethe)_{1.5}(PPh_3)](PF_6)\cdot 1.5CH_2Cl_2$ [bpethe = 1,2-bis(4-pyridyl)ethene]	(6, 3)	*AB* stacking sequence; Is = 1	2	[56]
$[Cu_3(4,4'\text{-bipy})_2(pydc)_2]\cdot 4H_2O$ (pydc = pyridine-2,4-dicarboxylate)	(6, 3)	Two entangled sets of parallel weavy layers that are 'out-of-phase'; Is = 3	4	[57]
$[AgL](CF_3SO_3)$ [L = 1,3,5-(4-methoxy benzonitrile)-2,4,6-trimethylbenzene]	(6, 3)	Catenation of two-fold parallely interpenetrated layers; Is = 2	3	[58]
$[Ag_2(H_2L)_3](NO_3)_2$ [H_2L = *N*,*N*′-bis-(salicylidene)-1,4- diaminobutane]	(6, 3)	*ABC* stacking sequence; *N*-Borromean links; Is = 1	0	[59]
Compound	Layer type	Mode of catenation	Doc	Reference
Multiple layers[a]				
$[Zn_2(tp)(4,4'\text{-bipy})(V_2O_6)]$ (tp = terephthalate)	Double-level sheets of (4, 4) layers; cut of α-Po; thick = 11.3 Å	*AB* stacking sequence; Is = 1	2	[60]
$[Cu_4(tp)_3(4,4'\text{-bipy})_2]$ (tp = terephthalate)	Double-level sheets of (4, 4) layers; cut of α-Po; thick = 11.1 Å	*AA* stacking sequence; Is = 1	2	[61]
$[Cd(in)_2(bpe)_{1/2}(H_2O)]$ [in = isonicotinate; bpe = 1,2-bis(4-pyridyl) ethane]	Double-level sheets of (4, 4) layers; cut of α-Po; thick = 18.7 Å	*AA* stacking sequence; Is = 1	2	[62]
$[Cu_3(bpethe)(in)_6(H_2O)_2]$ [bpethe = 1,2-bis(4-pyridyl)ethylene; in = isonicotinato]	Triple-level sheets; cut of $CdSO_4$; thick = 22.8 Å	*AA* stacking sequence; Is = 1	2	[63]
$[(ZnL)(4,4'\text{-bipy})]\cdot x$Solv (L = 5,10,15,20-tetrakis(4-hydroxyphenyl) porphyrinato; Solv = nitrobenzene)	Complex three-level layers, with coordinative and hydrogen bonds; thick = 31.7 Å	*AB* stacking sequence; Is = 1	2	[64]
$[Ag(sebn)_2](SbF_6)$, $[Ag(sebn)_2](CF_3SO_3)$ (sebn = sebaconitrile)	Self-penetrating four-level sheets; $(6\cdot6\cdot6\cdot6_2\cdot6_2\cdot6_2)$, thick = 31.6 Å	*AA* stacking sequence; Is = 1	2	[65]
$[Ag_3(L)_2](PF_6)_3\cdot 1.6F\cdot 0.5C_6H_6\cdot 2CH_2Cl_2$ [L = tetrakis(4-cyanophenyl) silane]	Double-level sheets of (6, 3) layers; cut of diamond; thick = 22.8 Å	*AA* stacking sequence; Is = 2	4	[53]
$[Cu_4(dca)_4(4,4'\text{-bipy})_3(MeCN)_2]$ [dca = dicyanamide]	Double-level sheets of (6, 3) layers; cut of diamond; thick = 23.6 Å	*AA* stacking sequence; Is = 2	4	[66]
$[Co_5(bpe)_9(H_2O)_8(SO_4)_4](SO_4)\cdot 14H_2O$ [bpe = 1,2-bis(4-pyridyl)ethane]	Five-level chiral layers; cut of 'dense' net; thick = 54.6 Å	*ABC* stacking sequence; Is = 2	4	[67]
$[Ag(bpe)](L)_{0.5}]\cdot H_2O$ [bpe =1,2-bis(4-pyridyl)ethane; L = 4,4′-biphenyldicarboxylate]	Bilayers of $8^2\cdot 10$ topology; thick = 17.9 Å	Two entangled sets of catenated *AB* bilayers; Is = 2	2	[68]

[a] The parameter thick is defined as the height of each layer evaluated from the outmost non-hydrogen atoms.

Also in $[Cu_6(CN)_5(trz)]$ (trz = triazolate) [55], exhibiting a complicated structure, highly undulated layers are present, comprised of large 36-membered $\{Cu_{14}(CN)_{10}(trz)_4\}$ rings that can be described in terms of (4,4) topology. The sheets give parallel (2D → 3D) catenation, recognized as such by Batten [15a]. Like in the previous polymer the adjacent sheets are rotated about the normal axis. In this case, however, each of the shortest (4, 4) circuits is interlocked with twelve others, six from the upper and six from the lower layer. Short interlayer Cu · · · Cu contacts, down to ca. 2.7 Å, are also present, that have been neglected in the above analysis.

An example of (2D → 3D) polycatenation of undulated (6, 3) layers is represented by $[Cu(bpethe)_{1.5}(PPh_3)](PF_6)\cdot 1.5CH_2Cl_2$ [bpethe = 1,2-bis(4-pyridyl)ethene] [56]. The Cu(I) centers are tetrahedral and form with the bpethe

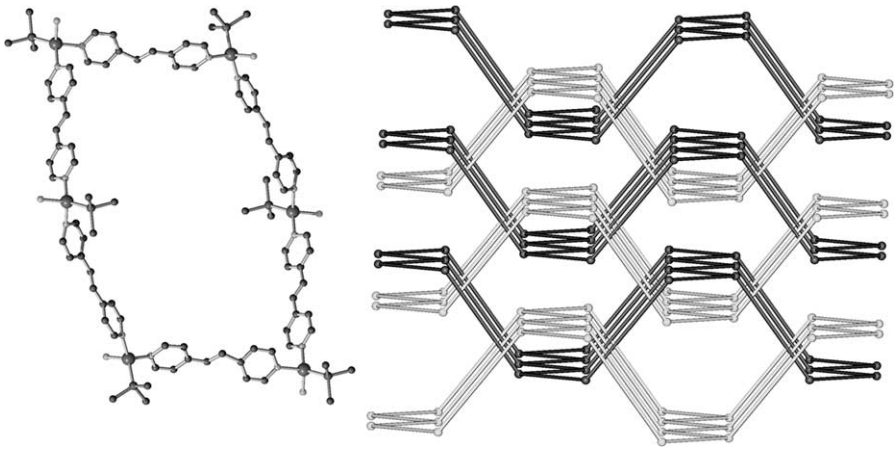

Fig. 6. A 6-membered ring (left) and the catenation of layers (right) in $[Cu(bpethe)_{1.5}(PPh_3)](PF_6)\cdot 1.5CH_2Cl_2$ [56].

ligands 6-membered rings in the chair conformation (see Fig. 6). Each 2D puckered layer, of the black-P type, is catenated by two others ('above' and 'below').

A more complex example of the same type has been reported very recently. In $[Cu_3(4,4'\text{-bipy})_2(pydc)_2]\cdot 4H_2O$ (pydc = pyridine-2,4-dicarboxylate) [57] highly undulated (6,3) layers, ca. 13.6 Å thick, form two different sets. Each set is comprised of parallel non catenated wavy layers and the two sets are displaced (out-of-phase waves) in such a way to give an unique 3D polycatenated array (see Fig. 7), with each window of a layer catenated by four layers of the other set (Doc = 4 and Is = 3).

Though our interest is focused on coordination networks, we must cite here an exceptional example of this polycatenated class, obtained from the self-assembly of organic molecules *via* hydrogen bond bridges. Glidewell and coworkers have reported that 1,1,1-tris(4-hydroxyphenyl)-ethane and 4,4′-bipyridyl, interacting *via* O–H···N hydrogen bonds, form a 2:3 adduct comprised of puckered 2D nets of very large hexagonal meshes [69]. Its peculiar topological feature consists in that the (6,3) layers give parallel (2D → 2D) five-fold interpenetration and that these entangled layers are (2D → 3D) polycatenated into a unique 3D array (see Fig. 8). Each layer results interlinked with ten others, i.e. four sharing the same average plane, *plus* three out of the five 'above' and three out of the five 'below'. Thus, Is = 5 and Doc = 10.

We have recently observed the same unusual topological type, implying both parallel (2D → 2D) interpenetration and parallel (2D → 3D) catenation of the interpenetrated

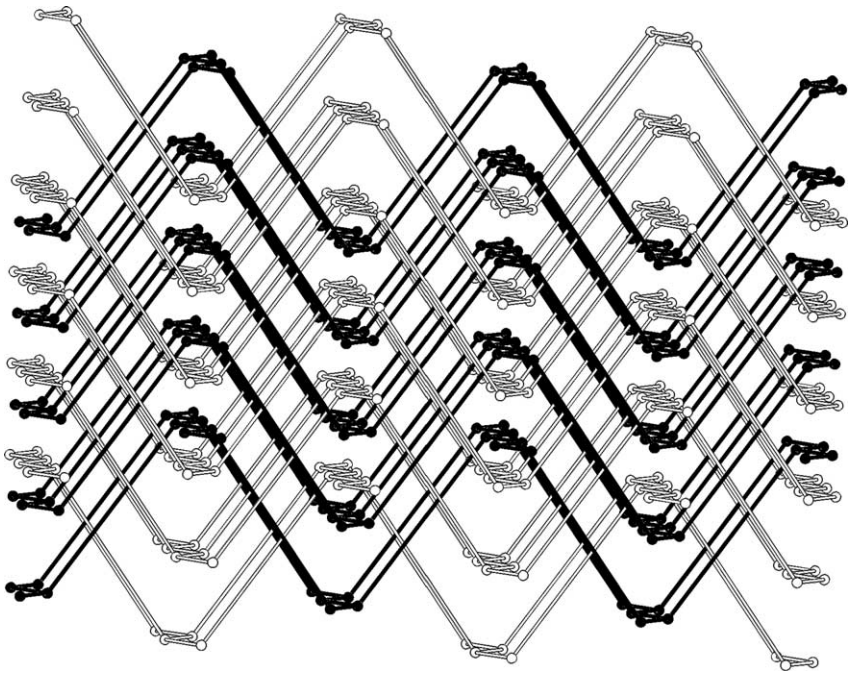

Fig. 7. Schematic view of the polycatenation in $[Cu_3(4,4'\text{-bipy})_2(pydc)_2]\cdot 4H_2O$ [57]. Two sets of layers (see text) are evidenced.

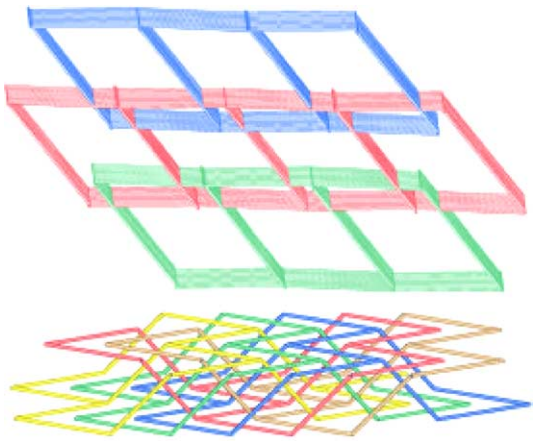

Fig. 8. Schematic view of the whole polycatenated array (top) and of the five-fold interpenetrated 2D layers (bottom) in the hydrogen bonded organic net of [69].

motifs, in the coordination polymer $[AgL](CF_3SO_3)$ [L = 1,3,5-(4-methoxybenzonitrile)-2,4,6-trimethylbenzene] [58]. This species contains (6, 3) layers of hexagonal meshes, with alternating triconnected Ag(I) centers and tridentate ligands. The undulated layers (black-P type) are associated in pairs to give parallely interpenetrated sheets that are catenated to the two adjacent ('upper' and 'lower') sheets. In the resulting 3D array (see Fig. 9) each sheet is interlinked with three others, i.e. one on the same average plane, *plus* one of the two interpenetrated 'above' and one of the two interpenetrated 'below' layers.

Particularly fascinating are the structures of two isomorphous polymeric complexes reported by Chen and coworkers [59] in which bis-monodentate phenol groups of a Schiff base ligand serve as bridges, *namely* $[Ag_2(H_2L)_3](NO_3)_2$ and $[Ag_2(H_2L)_3](ClO_4)_2$ [H_2L = *N*,*N*′-bis(salicylidene)-1,4-di-aminobutane]. These species are good examples illustrating one point raised in Section 2.1. They are comprised of highly undulated (6,3) layers, with six-membered rings of 3-connected silver centers (see Fig. 10(a)). The silver atoms exhibit interlayer unsupported Ag···Ag interactions of 2.934(2) and 2.946(2) Å in the two species. Different topologies can be envisaged depending on which links are included in the topological model. Taking into account these Ag···Ag contacts a single 3D array results, that can be described as a 4-connected self-penetrating species (see later, Section 5), or even as an overall 6-connected α-Po net, whose nodes are represented by the Ag_2 units (according to the description proposed by the authors). On the other hand, and much more interestingly, if the Ag···Ag interactions are neglected, the array appears like a polycatenated (2D → 3D) system, as previously noticed [15a,59], that is shown in Fig. 10(b). Each layer seems catenated by two others (one 'above' and one 'below'). However, a more careful examination leads to the exceptional finding that the adjacent layers are not catenated but are interlinked *via* Borromean links. This is

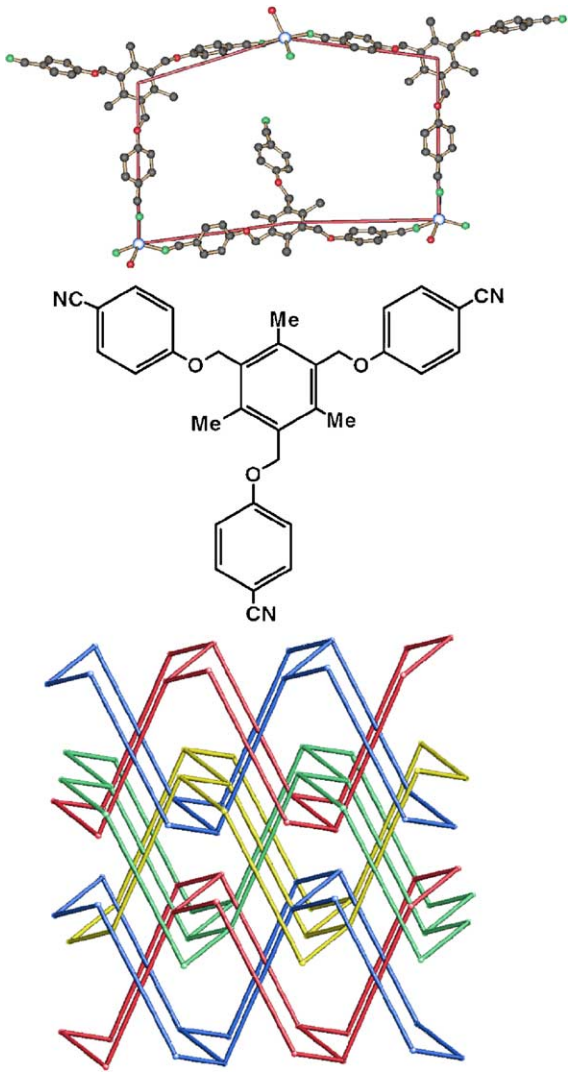

Fig. 9. Polycatenation of the two-fold interpenetrated (6, 3) layers in $[AgL](CF_3SO_3)$ [58]. A single ring and the tridentate ligand are also shown.

evident on considering three hexagonal rings from three different adjacent layers (Fig. 10(c)) that are entangled as the three Borromean rings of Scheme 3, in which no two individual rings are interlocked.

What stated for three rings can be extended to the whole array, that represents an infinite case of n-Borromean links (Fig. 10(d)). This chain of rings is such that no one ring is catenated to other ones (Doc = 0) but cannot be separated. Theoretical examples of *n*-Borromean links have been described by Mislow [41a]; for instance, the chain illustrated in Fig. 11(a) represents an entangled array that can be completely separated into the component rings by cutting only one ring, a property that is called 'Brunnian' [41,70]. Obviously, three Borromean rings must have this property. The species here described, like the chain in Fig. 11(b), does not show the Brunnian property, i.e. the cut of one ring separates the chain into two halves but leaves all the other rings inextricably entangled.

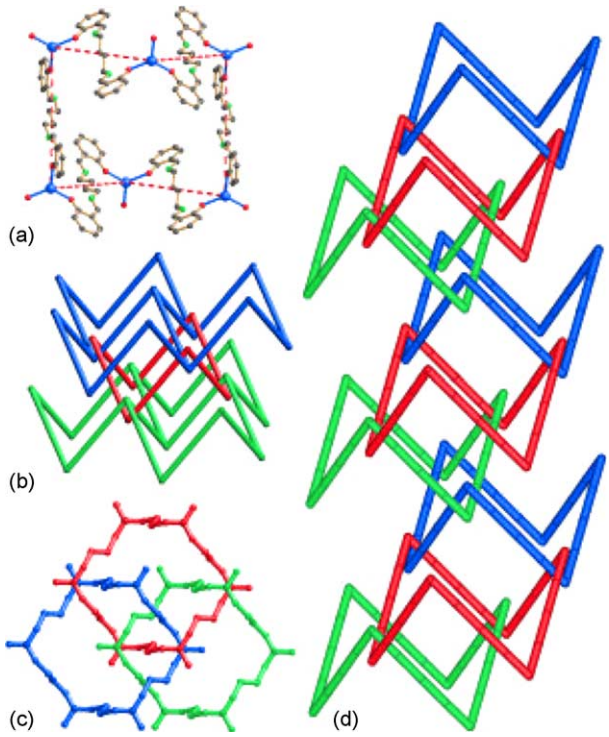

Fig. 10. The 'Borromean net' in $[Ag_2(H_2L)_3](NO_3)_2$ [59]: (a) a six-membered ring, (b) the entanglement of the stacking layers, (c) three rings from three adjacent layers, linked as the Borromean rings in Scheme 3, (d) the infinite chain of *n*-Borromean links.

Chemists since the early sixties have considered the realization of Borromean links in molecular form as a synthetic goal of great interest [17a,42,71]. The unique case previously known was constructed with DNA nanotechnology by Seeman in 1997 [72]. This is, to our knowledge, the first characterization of such an entanglement in an infinite chemical species. After this finding, however, we were encouraged to look for other cases with the same links. In the recent literature, we have so found another 3D 'Borromean' array with an identical entanglement topology, *namely* $[Ag_2L_3(OH)](ClO_4)\cdot 2.5H_2O$ [L = *N*, *N*′-bis(3-pyridinecarboxamide)-1,6-hexane] [73]. Moreover, as a natural extension, we have also examined in detail the examples of three-fold parallely 'interpenetrated' sheets listed by Batten [15a]. We have thus discovered a new class of (2D → 2D) 'Borromean layers'. Three species have been identified, all comprised of three-fold entangled (6, 3)

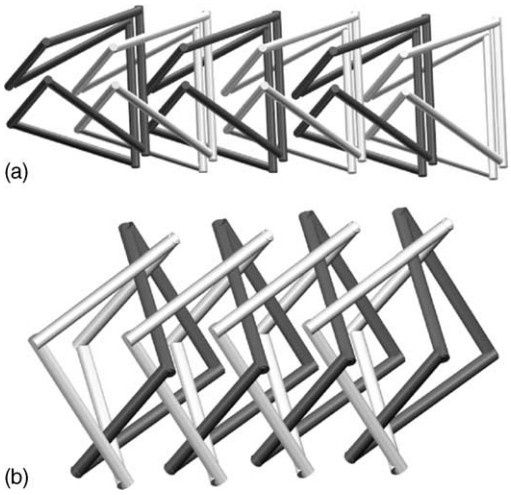

Fig. 11. Extended examples of *n*-Brunnian (a) and *n*-Borromean (b) links [42].

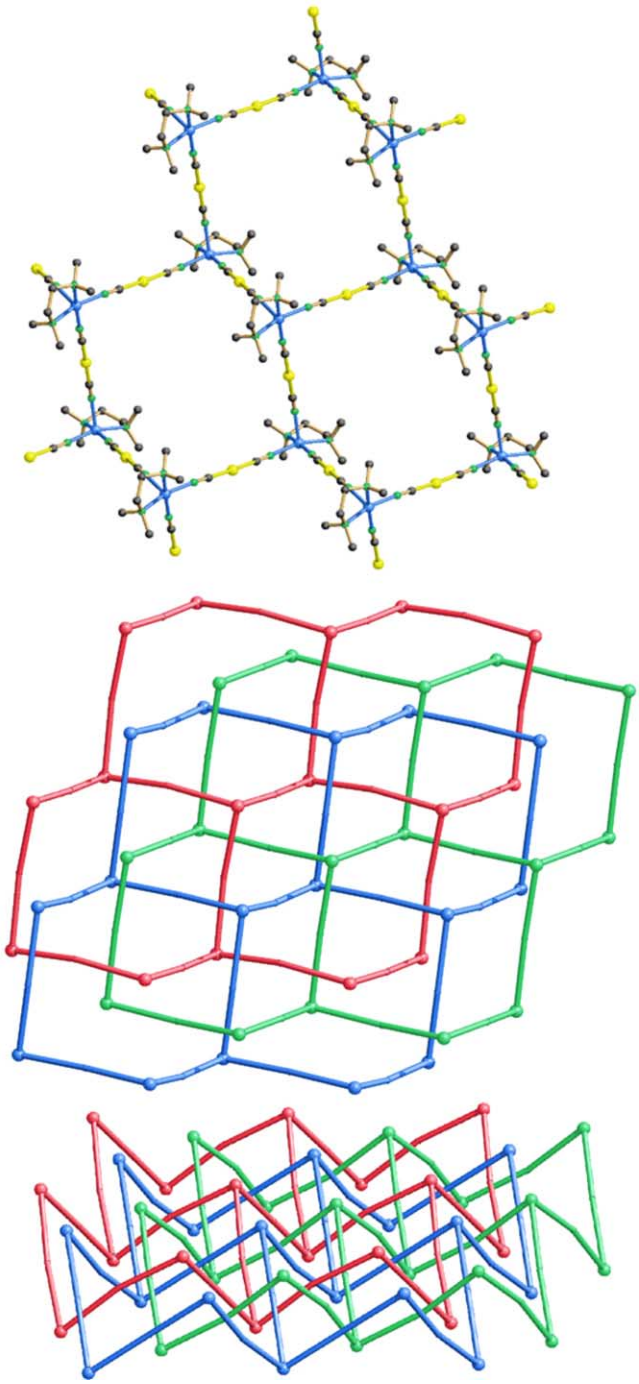

Fig. 12. A single layer (top) and two schematic views of the Borromean links (middle and bottom) in $[Cu_2(tmeda)_2\{Au(CN)_2\}_3]$ (ClO_4) [74].

layers that are neither interpenetrated nor catenated (i.e. do not contain Hopf links) but exhibit Borromean links, which were previously unrecognized as such.

In $[Cu_2(tmeda)_2\{Au(CN)_2\}_3](ClO_4)$ [tmeda = *N*,*N*,*N*′,*N*′-tetramethylethylendiamine] [74], the structure contains (6, 3) undulated layers, with $Cu(tmeda)^{2+}$ units as nodes linked by $Au(CN)_2^-$ linear complexes (see Fig. 12, top). Three such layers are entangled *via* Borromean links, as schematically shown in Fig. 12 (middle and bottom). One can easily realize this point observing that the blue net is completely located above the red one, the green net above the blue one, but the red net lies above the green one. This is a general *criterion* for Borromean links involving three parallel motifs at a time. Aurophilic Au···Au inter-layer contacts are observed in the central plane, ranging in the interval 3.40–3.60 Å.

The same topological entanglement has been found also in $[\{Ni(cyclam)\}_3(TCPEB)]_2\cdot 6C_5H_5N\cdot 4H_2O$ [TCPEB = 1, 3,5-tris(2-(4-carboxyphenyl)-1-ethynyl)benzene] [75], containing rather flat (6, 3) layers, with the trigonal tridentate ligands as nodes and the Ni(cyclam) units acting as spacers.

The third species is a framework belonging to the realm of supramolecular chemistry: in [K(K·2·2·2)]I(1,8-diiodoperfluorooctane)$_{1.5}$ (K·2·2·2 = 4,7,13,16,21,24-hexaoxa-1,10-diazabicyclo[8,8,8]-hexacosane) [76] strong halogen bonding $I^-\cdots I$ between naked iodide ions and the diiodoperfluoroalkanes generates 2D layers of (6, 3) topology, having the I^- anions as nodes. Three such layers give Borromean links as in the two above cases. Though the authors classify this system as a case of three-fold parallel interpenetration, they have noticed that "two of the nets are not interpenetrating as they can be separated without any bond breakage. It is only the addition of the third net that ties them all together in the observed structure". Note that all these Borromean arrays must have Doc = 0 and Is = 1. At difference from the 3D Borromean arrays previously described, these 2D entanglements must be obviously of the Brunnian type.

The second class of polycatenated (2D → 3D) systems contains multi-level layers with a certain thickness. Examples containing individual 2D motifs of increasing complexity and of variated 'height', as well as with a different number of interlocked components, have been characterized (see Table 2).

Three of these species are comprised of two-level sheets that are catenated with the two adjacent ones. The individual motifs can be described as a cut of the α-polonium net.

$[Zn_2(tp)(4,4'\text{-bipy})(V_2O_6)]$ (tp = terephthalate) [60] contains tetravanadate-pillared double-layered sheets built up from polymeric cationic $[Zn_2(tp)(4,4'\text{-bipy})]$ layers of (4, 4) topology linked by $V_4O_{12}^{4-}$ anions. Each double sheet is bicatenated in a parallel fashion by two other ('upper' and 'lower') sheets that pass through the 'channels' of the first sheet. A similar system is present in $[Cu_4(tp)_3(4,4'\text{-bipy})_2]$ (tp = terephthalate), that has the peculiarity of containing mixed-valence $[Cu_2]^{3+}$ subunits [61].

A single 'box' unit of the polymeric $[Cd(in)_2(bpe)_{1/2}(H_2O)]$ [in = isonicotinate; bpe = 1,2-bis(4-pyridyl)ethane] [62] is shown in Fig. 13, together with a schematic view of the catenation of the double sheets.

Also $[Cu_3(bpethe)(in)_6(H_2O)_2]$ [bpethe = 1,2-bis(4-pyridyl) ethylene, in = isonicotinate] [63] presents the same type of polycatenation but, at difference from the above species, the individual motifs are triple-level sheets. These layers can be described as a piece of the $CdSO_4$ type net.

Catenated complex layers have been reported by Goldberg and coworkers; they have described the induced assembly of [5,10,15,20-tetrakis(4-hydroxyphenyl)porphyrinato]zinc (ZnL) by a combination of axial coordination through bridging 4,4′-bipyridyl and of lateral hydrogen bonding, to give the networked species $[(ZnL)(4,4'\text{-bipy})]\cdot x$Solv (Solv = nitrobenzene) [64]. Individual thick layers (schematically shown in Fig. 14, bottom), comprised of three levels, are catenated to produce a 3D array (Fig. 14, top).

Within polycatenated (2D → 3D) species having Doc = 2 a quite different 2D structural motif is that found for the two species $[Ag(sebn)_2](SbF_6)$ and $[Ag(sebn)_2](CF_3SO_3)$

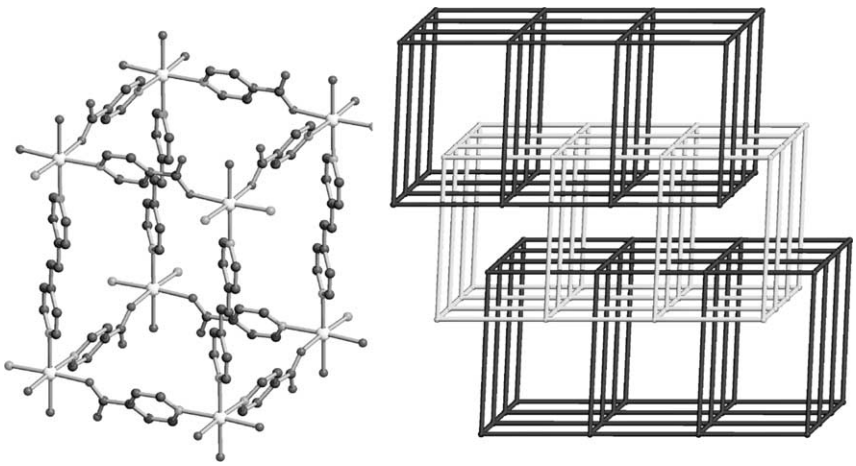

Fig. 13. A single box (left) and the catenation of the double layers (right) in $[Cd(in)_2(bpe)_{1/2}(H_2O)]$ [62].

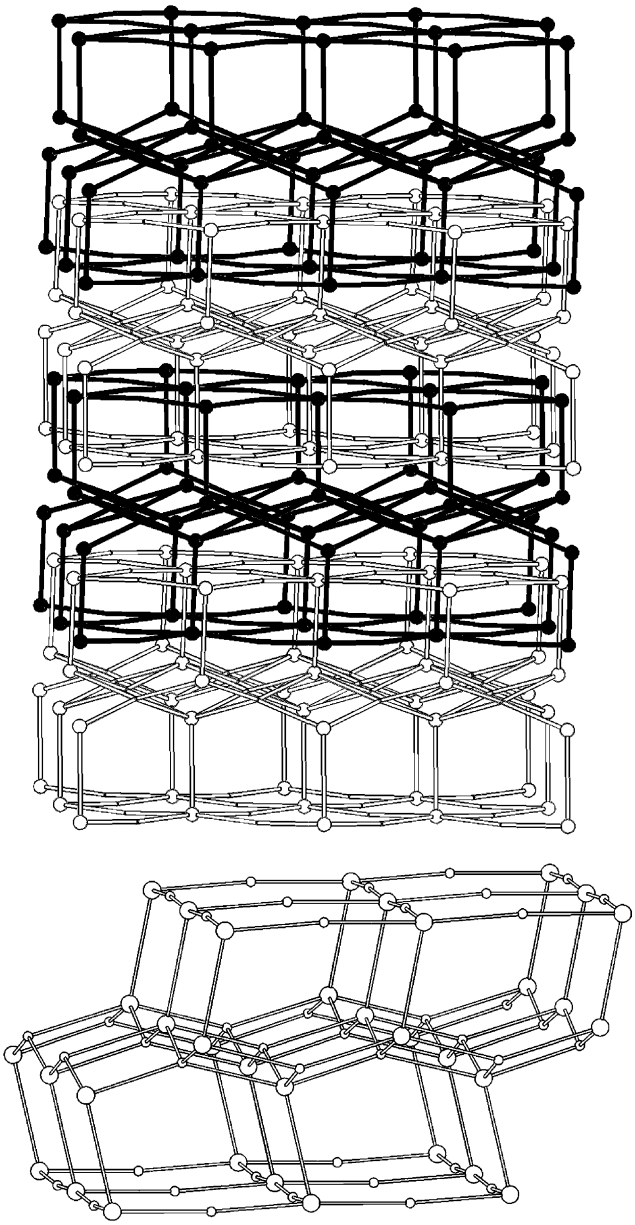

Fig. 14. The polycatenation (top) of the complex layers (bottom) in a Zn-porphyrinato network [64].

[sebn = sebaconitrile, (1,10-decanedinitrile)] [65], which are isomorphous in spite of the different nature of the anions. The 2D complex layers are based on distorted tetrahedral silver(I) centers disposed on four different levels. These layers are intertwined by simple translation in such a way that each one is catenated by the two adjacent identical motifs (the 'upper' and the 'lower' ones), as schematically illustrated in Fig. 15 (top), and exhibits also some interdigitation with the second nearest neighboring sheets.

Due to the structural complexity, when we reported these results we overwieved a feature of great relevance. Re-examination of the 2D layers (see Fig. 15) has now revealed that these are uninodal self-penetrating nets (see Section 5). All the shortest circuits at each metal center

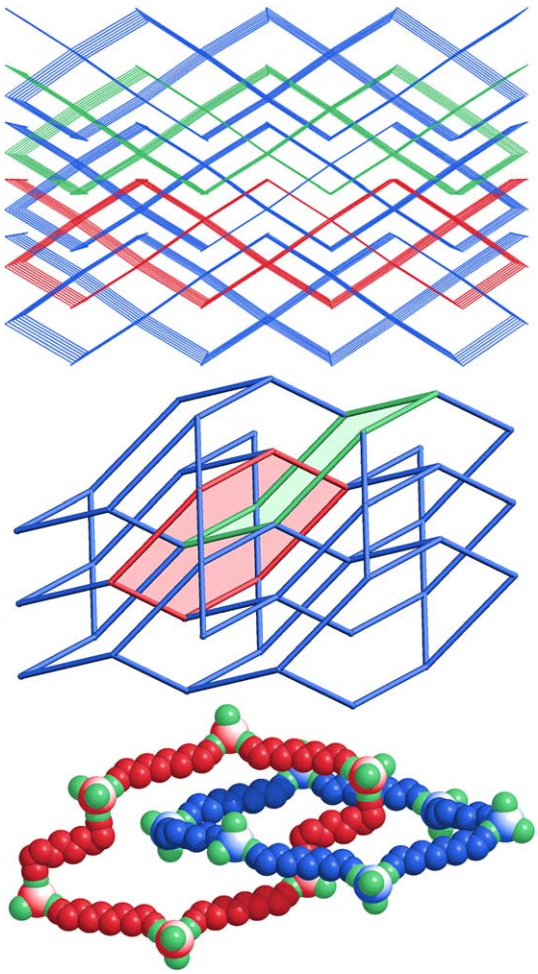

Fig. 15. The polycatenated (2D → 3D) network in $[Ag(sebn)_2]X$ [65] (top). An individual self-penetrated layer (middle) and the detail of the catenation of two six-membered rings in the layer (bottom) are also shown.

are 6-gons and the short topological symbol of the net is 6^6 (long Schläfli symbol $6{\cdot}6{\cdot}6{\cdot}6_2{\cdot}6_2{\cdot}6_2$). In spite of the presence of two different types of silver ions in these layers (the *internal* ones and the *surface* ones), all the centers exhibit an identical topology. Self-penetrating 2D nets are a rarity but the contemporary presence of self-penetration and polycatenation *phenomena* is exceptional. A noteworthy consequence is that the shortest six-membered rings (Fig. 15, bottom) are catenated by rings of the same size not only "internal" but also "external" to the layer.

The first polycatenated (2D → 3D) network was reported few years ago by Liu and Tilley [53]. This polymer, $[Ag_3(L)_2](PF_6)_3{\cdot}1.6THF{\cdot}0.5C_6H_6{\cdot}2CH_2Cl_2$ [L = tetrakis(4-cyanophenyl)silane], contains individual 2D motifs that consist of two stacked 3-connected layers, with six-membered rings of alternating Ag and Si centers, in the chair conformation, which are cross-linked *via* $Si(C_6H_4CN)$-Ag-$(NCC_6H_4)Si$ synthons (Ag in digonal coordination). The 2D motif represents a cut of diamond. These sheets exhibit an *AA* stacking sequence and the entanglement is such that each double sheet is catenated by

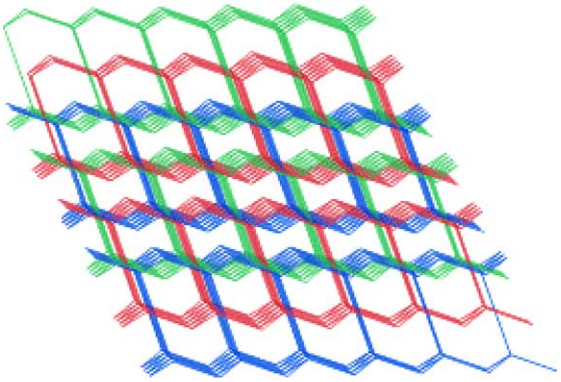

Fig. 16. Schematic view of the polycatenated network in $[Ag_3(L)_2](PF_6)_3 \cdot 1.6THF \cdot 0.5C_6H_6 \cdot 2CH_2Cl_2$ [53].

four others in non coincident planes (two 'upper' and two 'lower', Doc = 4), as shown in Fig. 16.

The two sheets lying deeper inside are interlocked between themselves. At difference from the other species of this class above described, two sheets must be 'removed' to break the catenation (Is = 2). The same type of entanglement above described is observed also in the polymer $[Cu_4(dca)_4(4,4'\text{-bipy})_3(MeCN)_2]$ (dca = dicyanamide) [66].

The structure of $[Co_5(bpe)_9(H_2O)_8(SO_4)_4](SO_4) \cdot 14H_2O$ [bpe = 1,2-bis (4-pyridyl)ethane] [67] shows the presence of multiple layers containing five parallel levels of 1D linear polymers (stacking sequence *ABCAB*) connected along the normal direction *via* five-metals helical motifs (see Fig. 17), all exhibiting homochirality, thus resulting in a chiral multilayer. This motif can be described as a five layers section of the chiral 3D 4-connected framework named by O'Keeffe the 'dense' net [25a,25b]. Two other sets of quintuple layers are generated by a 3_1 symmetry axis; the three sets (stacking sequence *ABC*) are entangled in such a way that each layer is catenated not only by the two nearest neighboring ('upper' and 'lower') layers but also by the two second nearest neighboring ones, as illustrated in Fig. 17. Thus, each layer is entangled with other four, to give a fascinating polycatenated array.

A recently reported network of this class exhibits quite unusual and puzzling topological features. The polymeric species $[Ag(bpe)(L)_{0.5}] \cdot H_2O$ [bpe =1,2-bis(4-pyridyl)ethane; L = 4,4′-biphenyldicarboxylate] [68] is comprised of catenated 2D bilayers of a $8^2.10$ topology (see Fig. 18), similar to that previously observed in non-entangled structures [77].

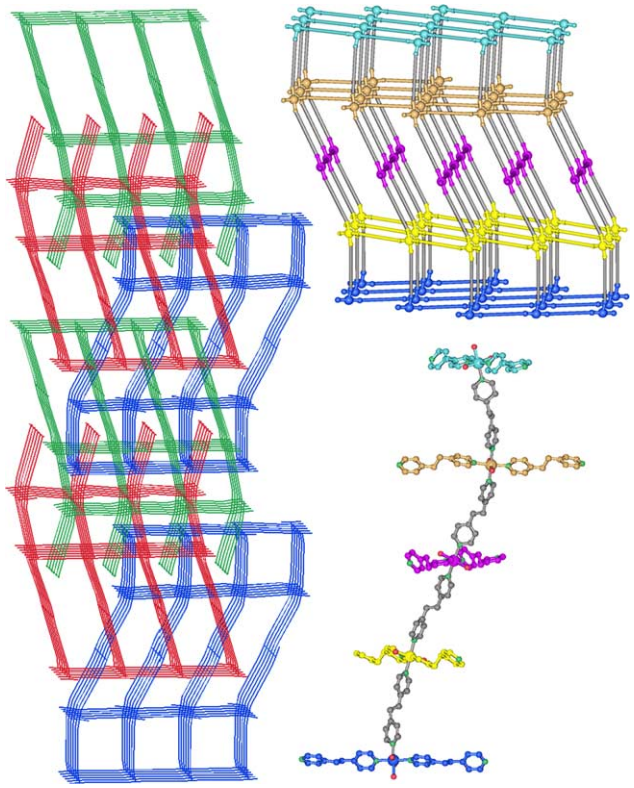

Fig. 17. The polycatenated network (left) comprised of individual five-deck layers (top right) in $[Co_5(bpe)_9(H_2O)_8(SO_4)_4](SO_4) \cdot 14H_2O$ [67]. The 1D linear polymers on the five levels are connected along the normal direction *via* five-metals helical motifs (bottom right).

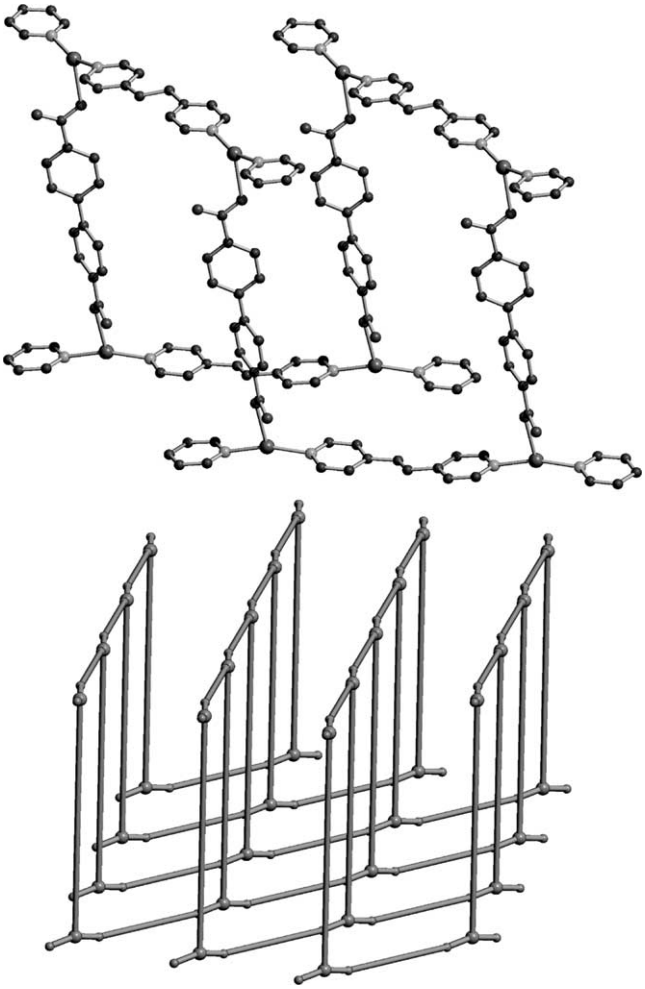

Fig. 18. A single 'cell' and the individual bilayer in $[Ag(bpe)(L)_{0.5}] \cdot H_2O$ [68].

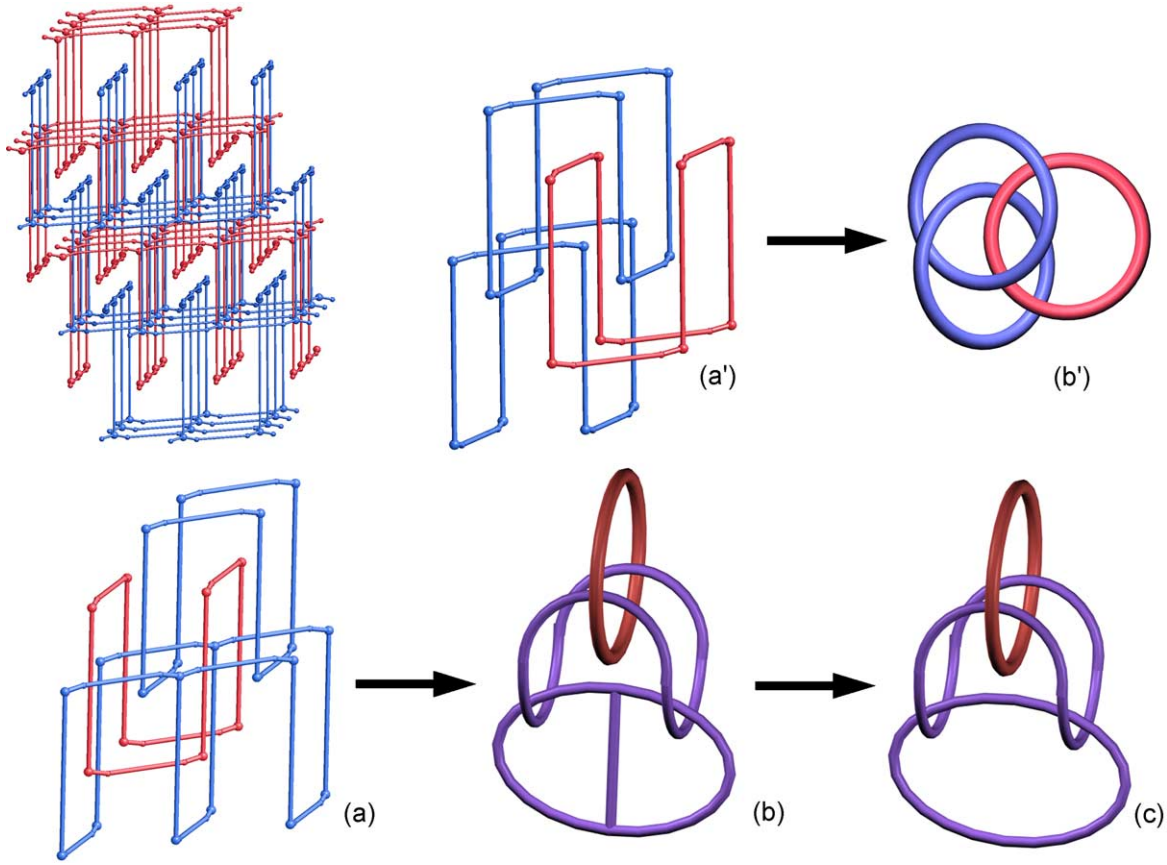

Fig. 19. The entangled layers in $[Ag(bpe)(L)_{0.5}]\cdot H_2O$ [68] (top left). The three adjacent 'cells' (a′) are equivalent to the three entangled rings (b′) corresponding to two catenated rings (blue) + one free ring (red). The fundamental entanglement (a) in the network corresponds to the nontrivial linkage (b), which, in turn, is related to the Borromean links (c).

At first glance the structure seems another case of parallel catenation involving thick layers, like those previously described. Each sheet was erroneously described by the authors as interlocked by four adjacent ones (two 'upper' and two 'lower'). The entanglement is illustrated in Fig. 19 (top left) and is comprised of two sets of polycatenated layers (in blue and red) with each 2D motif interlocked only with the two nearest neighboring ones of the same set (Doc = 2). Quite surprisingly none motif of one set is catenated by the motifs of the other set, and the closest layers belonging to different sets are simply interdigitated in pairs, in the tongue-and-groove fashion [77]. In a sequence of 'cells' (eight-membered loops) along the direction of catenation only those of the same color are interlocked. Two blue and one red adjacent such 'cells' are shown in Fig. 19(a′) and display the same entanglement of the three (*pseudo*-Borromean [41b]) rings in Fig. 19(b′), i.e. an assembly of two catenated *plus* one free rings. But which is the nature of the linkage between the two sets? This can be clearly seen in Fig. 19 (bottom): the elemental link between them (a) is equivalent to the nontrivial entanglement (b), in which the catenation of the blue rings prevents the disentanglement of the (non-catenated) red one; the way in which this entanglement can be transformed into Borromean links (c) is also shown.

Note that our considerations are entirely of topological nature. This means that the closed loops can undergo 'ideal' continuous deformations (like rubber rings), without taking into account metrical factors (dimensions of the components, geometrical rigidity) or energetical factors (barriers to deformation), that do not belong to the realm of topology [18,40].

3.2.2. *The 'inclined' interlocking mode*

There are numerous examples of this class of polycatenated frameworks [13], the majority of which consists of two identical sets of 2D parallel layers, of (6, 3) or (4, 4) topology, spanning two different stacking directions. In these species, we have an increase of dimensionality (2D → 3D) and each individual layer is catenated with an infinite number of other inclined layers but, obviously, not with all the frames contained in the 3D array.

In the topological analysis of this class different ways of interlocking of the two independent sets have been envisaged for both types of sheets [13,52]. For (4, 4) layers three possible arrangements have been suggested, called parallel–parallel (p–p), parallel–diagonal (p–d) and diagonal–diagonal (d–d), depending on how the networks orient and penetrate through each other, as illustrated in Fig. 20 [1e,52].

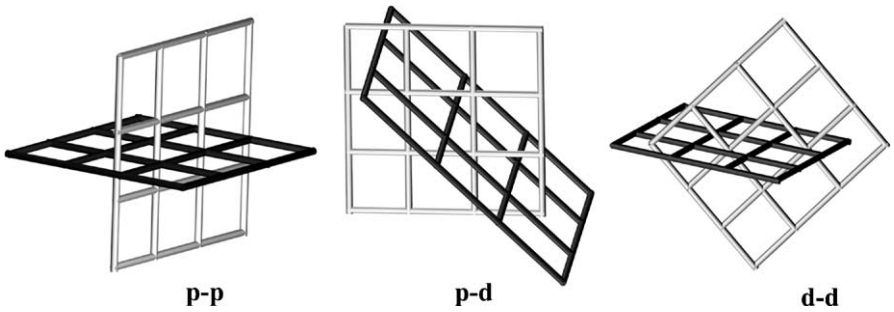

Fig. 20. The possible modes of catenation of inclined (4, 4) layers.

The oldest structural reports on coordination polymers belonging to this class described the members of the family $[M(4,4'\text{-bipy})_2(H_2O)_2](SiF_6)$ (M = Zn, Cu, Cd) [20], involving (4, 4) entangled layers with the (d–d) disposition. The structures of these species, with Doc = (1/1), have already been discussed (see Section 2.1, and Fig. 1).

One of the first examples within coordination networks exhibiting an inclined catenation of (6,3) layers was a Cu(I) polymer reported by Zaworotko and coworkers, *namely* $[Cu_2(pyz)_3](SiF_6)$, (pyz = pyrazine) [78], schematically illustrated in Fig. 21.

A noteworthy species, that can be considered both as polycatenated or as polythreaded (see later, Section 4), was described by Whang and Kim [79a], *namely* $[Ag_2(H_2L)_3\cdot(\text{cucurbituril})_3](NO_3)_8\cdot 40H_2O$ [L = N,N′-bis(4-pyridylmethyl)-1,4-diaminobutane]. Cucurbituril beads are threaded on the rods of 2D layers of six-membered rings of silver centers. The rings with rotaxane edges, display a chair conformation. The (6, 3) sheets give inclined interweaving (see Fig. 22) and each ring is interlocked with two distinct inclined layers [Doc = (2/2)].

Systematic enumerations of these entangled species have already appeared in previous reviews [13–15,52]. In more recent years, a great number of such systems have been reported in the literature, containing both (6, 3) layers [80] or (4, 4) ones [81]. Among these reports it is worth mentioning a paper by Plater et al. [82] that describes two interesting species: in $[Cd(NO_3)_2(L)_2]$ [L = 1,6-bis(4-pyridyl)hexane] (4, 4) layers oriented in the diagonal-diagonal mode give high catenation [Doc = (3/3)] and in $[Cd(SO_4)(bpp)_3]$ (bpp = 1,3-bis(4-pyridyl)propane) the unusual interlocking of tessellated layers of 6-gons and 4-gons is observed (Schläfli symbol: $[(4\cdot6\cdot4\cdot6),(4_2\cdot6)^2]$ [25c]). The hexagonal windows are catenated by four inclined layers while the square ones only by two. The topology of this latter species clearly shows how difficult could be to find a generally applicable notation.

We will no further discuss here about these species but rather, in the following part, we prefer to deal with some cases that show peculiar features or remarkable differences from the other members of this class. Unusual situations can be due to the presence of:

(i) topologically different layers;
(ii) more than two stacks;
(iii) cross-linking of the 2D layers to give an unique 3D array;
(iv) additional polymeric motifs threaded through the catenated array;
(v) inclined interweaving of 2D layers of particular nature.

All the above features are, indeed, quite rare.

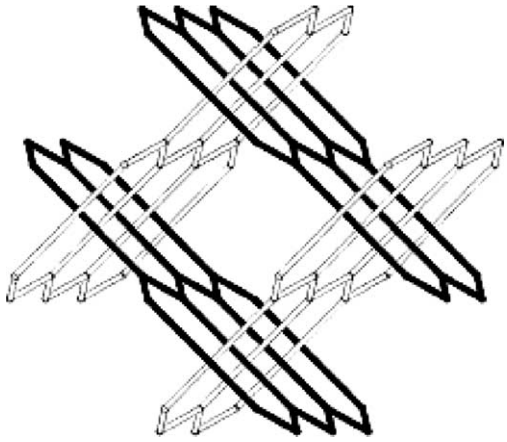

Fig. 21. The inclined catenation of the (6, 3) layers in $[Cu_2(pyz)_3](SiF_6)$ [78].

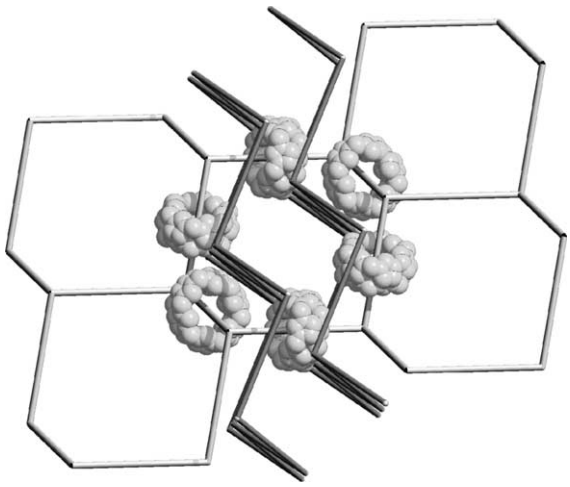

Fig. 22. Inclined interlocking in $[Ag_2(H_2L)_3\cdot(\text{cucurbituril})_3](NO_3)_8\cdot 40H_2O$ [79a]. The cucurbituril beads are shown only in the central ring.

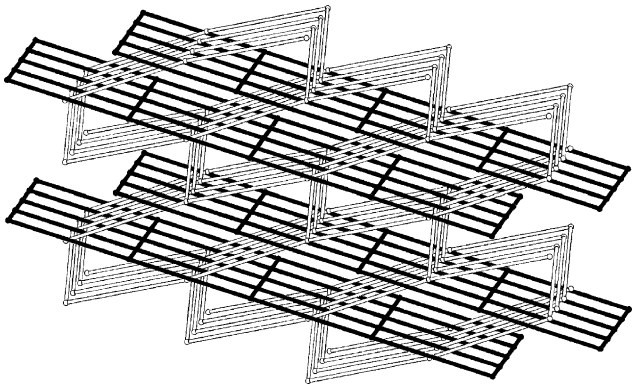

Fig. 23. Inclined catenation in $[Ni(azpy)_2(NO_3)_2]_2[Ni_2(azpy)_3(NO_3)_4]\cdot 4CH_2Cl_2$ [83].

Case (i). Only one coordination network has been reported, to our knowledge, that contains entangled 2D layers of different topology. In $[Ni(azpy)_2(NO_3)_2]_2[Ni_2(azpy)_3(NO_3)_4]\cdot 4CH_2Cl_2$ [azpy = *trans*-4,4′-azobis(pyridine)] [83] there are two types of sheets, i.e. layers of almost regular squares [(4,4) topology] and brick-wall layers [(6, 3) topology] in the ratio 2:1. The inclined catenation occurs at an angle of ca. 45°, as shown in Fig. 23. While each square of the former layers is catenated by a single layer of the other type, the rectangular windows of the brick-wall sheets are interlocked with two square grids [Doc = (1/2)].

Another example is worth of mention in this concern. Zaworotko and coworkers have described a family of compounds with composition $[M(4,4'\text{-bipy})_2(NO_3)_2]\cdot n$(aromatic guest) (M = Co, Ni) [52,84] that contain coordination layers of (4, 4) topology. The aromatic guest molecules form extended sheets sustained by non covalent bonds, i.e. by edge-to-face interactions, and in the case of $[M(4,4'\text{-bipy})_2(NO_3)_2]\cdot 3$(naphthalene) [84] the naphthalene sublattice can be described as consisting of hexagonal (6,3) layers. Interestingly, the two sets are interlocked in an inclined fashion.

Case (ii). Four networks are presently known that contain more than two sets of differently oriented layers. The possible existence of a 3D architecture built up by three mutually perpendicular interlocking sets of sheets was anticipated by Batten and Robson prior of any structure report [13].

The first species reported was a network sustained by hydrogen-bond bridges, $[Pt(HL)_2L_2]\cdot 2H_2O$ (HL = isonicotinic acid) [85], containing three sets of (4, 4) sheets stacking in three ‘perpendicular’ directions (see Fig. 24, left).

The second example, $[Fe(bpb)_2(NCS)_2]\cdot 0.5$MeOH [bpb = 1,4-bis(4-pyridyl)butadiyne] [86], is a 3D network entirely based on coordinative bonds, similar to the previous one in that it also contains three sets of (4,4) layers stacking again in three ‘perpendicular’ directions (see Fig. 25).

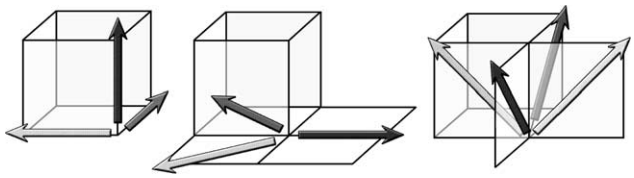

Fig. 24. The stacking directions of the independent sets of layers in the known species containing more than two sets.

Extending the terminology used for inclined interweaving of two stacks of (4, 4) layers we observe that the penetration mode within each pair of sets is of the diagonal-diagonal type (overall: diagonal–diagonal–diagonal or d–d–d), and that each square window of one of the nets is catenated by three other nets, while the square windows of the other two nets are catenated by five different nets [Doc = (3/5/5)]. It is worth noting that the interlocking mode hypothesized by Batten and Robson for three sets of (4, 4) layers [13] was different from that here described.

The third species is a quite noteworthy coordination network, *namely* $[Co_2(azpy)_3(NO_3)_4]\cdot Me_2CO\cdot 3H_2O$ (azpy = 4,4′-azopyridine) [87], whose entanglement was rather overviewed by the authors. It contains four different set of (6, 3) sheets (brick-wall pattern) that stack along four crystallographic directions (Fig. 24, right) and are interlocked as shown in Fig. 26. All the hexagonal windows of a layer are catenated by three other nets, one from each of the different sets [Doc = (3/3/3/3)].

We have recently obtained a fourth example of this class with an unprecedented topology. Compound $[Ni_6(bpe)_{10}(H_2O)_{16}](SO_4)_6\cdot xH_2O$ [bpe = 1,2-bis(4-pyridyl)ethane] [88]

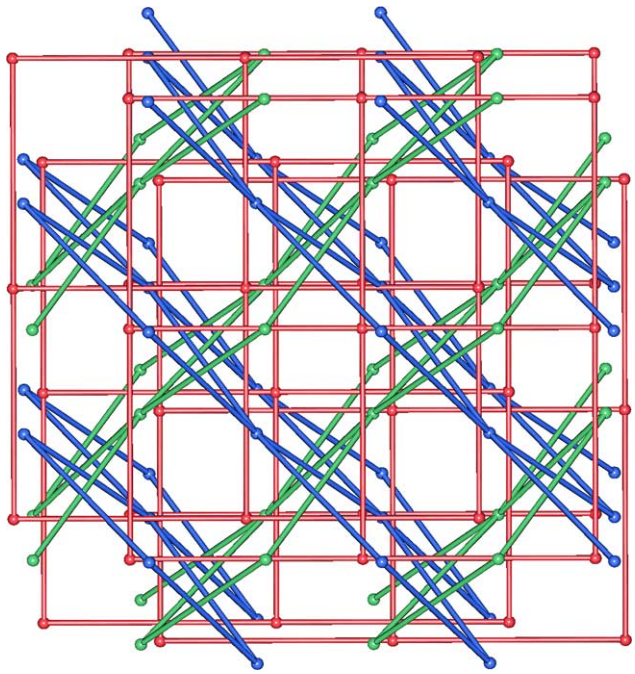

Fig. 25. Schematic view of the polycatenated nets in $[Fe(bpb)_2(NCS)_2]\cdot 0.5$MeOH [86].

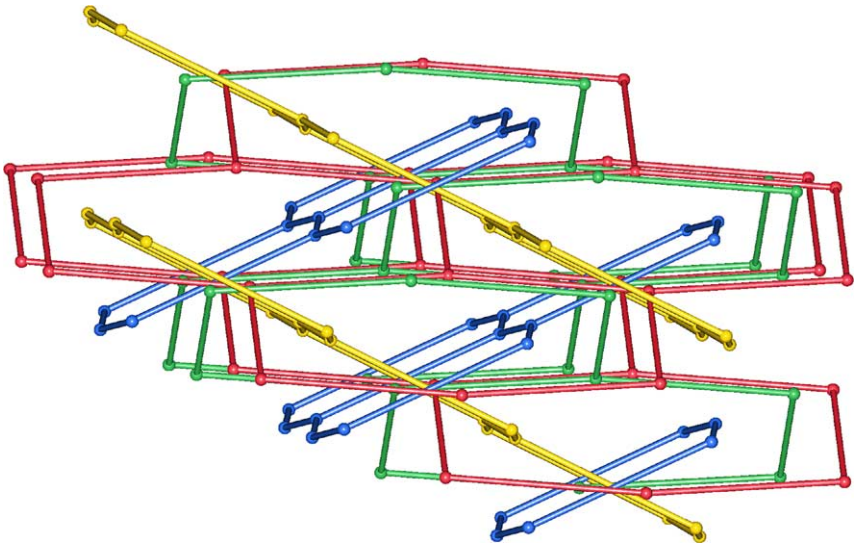

Fig. 26. Interlocking of the four sets of (6, 3) sheets in $[Co_2(azpy)_3(NO_3)_4]\cdot Me_2CO\cdot 3H_2O$ [87].

contains three distinct sets of (4, 4) layers that span three different spatial orientations and give inclined mutual penetration (Fig. 27).

The layers belong to two different types, with rectangular (A) and square (B) meshes, in the ratio 2:1. The three sets are parallel to the same crystallographic axis and display a relative rotation about this axis of ca. 120°. This species is unique in that the three stackings occur along three coplanar directions (see Fig. 24, middle). The interlocking mode can be described as parallel–parallel–parallel (p–p–p). Each rectangular window of the A layers is catenated by two inclined layers of the same type A and by two layers of type B, while a square window of the B layers is catenated by one A layer of each of the two sets [Doc = (2/4/4)].

Case (iii). Cross-linking of two distinct sets of 2D layers that give inclined interlocking results in an unique overall 3D self-penetrating network (this point will be discussed in more detail later, see Section 5.2). Cross-linking can be due to weak interactions, like hydrogen bond bridges, π–π interactions or secondary bonds to the anions. The case of $[Zn(4,4'\text{-bipy})_2(H_2O)_2](SiF_6)$ has already been discussed (see Section 2.1 and Fig. 1).

Case (iv). In compound $[Cu(bpe)_2][Cu(bpe)(H_2O)_2(SO_4)_2]\cdot 2H_2O$ [bpe = 1,2-bis(4-pyridyl)ethane] [89] two sets of (4, 4) layers, of composition $[Cu(bpe)_2]^{2+}$, give inclined catenation [p–p, Doc = (1/1)] and, moreover, 1D chains –Cu–bpe–Cu–bpe– are threaded through the channels of the entangled 3D array, as shown in Fig. 28. Taking into account the weak axial coordination of the SO_4^{2-}anions bound to the Cu atoms of the chains on the copper centers in the sheets, an unique 3D network can be alternatively

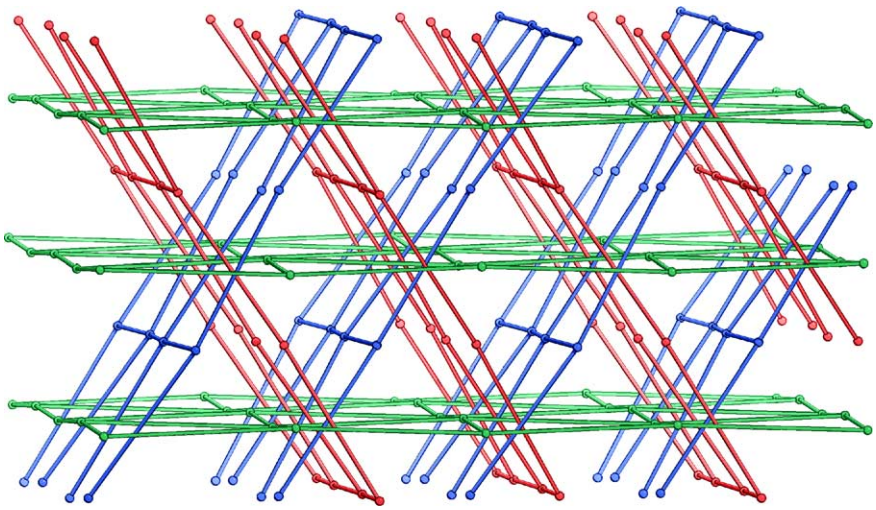

Fig. 27. View of the interlocking of the three sets of layers that stack along three coplanar directions in $[Ni_6(bpe)_{10}(H_2O)_{16}](SO_4)_6\cdot xH_2O$ [88].

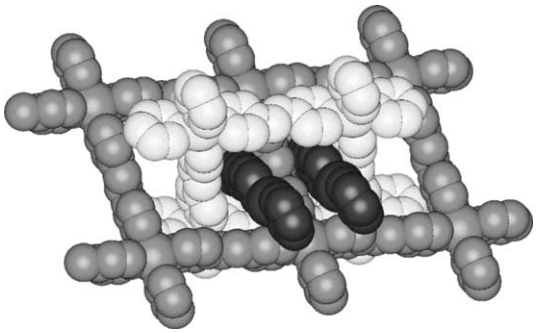

Fig. 28. The 1D chains (black) threading the two sets of interlocked square grid layers (white and gray) in $[Cu(bpe)_2][Cu(bpe)(H_2O)_2(SO_4)_2]\cdot 2H_2O$ [89].

envisaged. This species could be also considered in the context of the polythreading *phenomena* (see Section 4.2).

Case (v). Batten and Robson [13] have described the interesting structure of the species $[M_2(OH)(bpb)_4](BF_4)_3\cdot H_2O\cdot C_2H_5OH$ [M = Cd, Cu, bpb = 1,4-bis(4-pyridyl)butadyine] [90], containing a 3D network generated by the inclined interlocking of two sets of doubled-up square grid sheets, joined together *via* μ-OH bridges. No other case of 'thick' layers giving this type of entanglement, instead of the parallel mode, has been as yet characterized.

Another exceptional polycatenated complex has been obtained by Moore and coworkers [91]. The structure of $[AgL_2](SbF_6)$ (L = 3-cyanophenyl-4-cyanobenzoate) consists of 2D undulated layers of (4, 4) topology that show two-fold parallel interpenetration of common type (see Fig. 29, top). The noteworthy topological feature of this compound is that the interpenetrated layers show two differently oriented sets that give inclined interlocking, resulting in an overall 3D network (schematically illustrated in Fig. 29, bottom). The inclined catenation is of the (d–d) type (Fig. 20). This is another unique species, because of the simultaneous presence of parallel interpenetration and inclined interlocking.

3.3. Polycatenation involving motifs of different dimensionality

A wide-ranging variety of hypothetical polycatenated species based on motifs having different dimensionality could be envisaged, e.g. (0D + 1D), (0D + 2D) or (1D + 2D). Few cases are illustrated in Scheme 7.

The known examples are true rarities, but, given the explosive growth of the structure reports in this *area*, very likely other species will be found in the near future.

The structure of $[Cu_5(bpp)_8(SO_4)_4(EtOH)(H_2O)_5](SO_4)\cdot EtOH\cdot 25.5H_2O$ [bpp = 1,3-bis(4-pyridyl)propane] [35] shows the presence of two different and independent polymeric motifs packed together: one consists of ribbons of

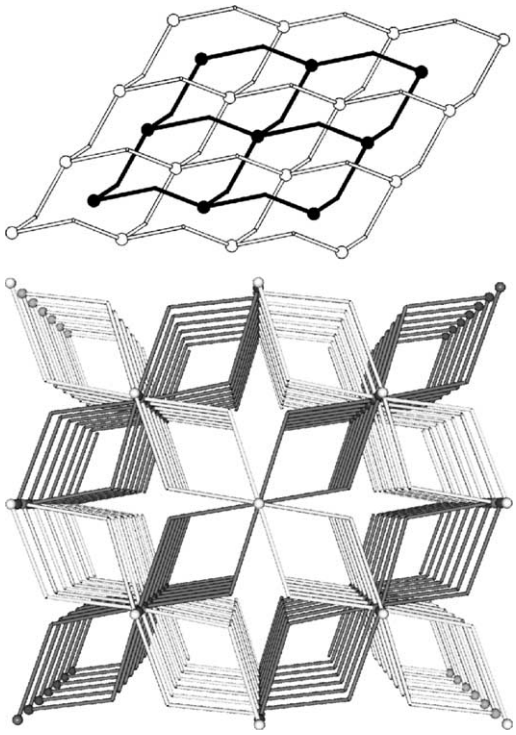

Fig. 29. A view of the parallel two-fold interpenetration (top) and of the inclined catenation of the two-fold interpenetrated layers (bottom) in the $[AgL_2](SbF_6)$ species [91].

48-membered cycles and the other of 2D tessellated sheets of (4, 4) topology (see Fig. 30). The layers stack with an *ABCD* sequence and the ribbons and the layers are entangled to give an unique 3D polycatenated array. Each ring of the ribbons locks two adjacent layers and each 'square' of the layers is catenated by two rings belonging to different ribbons.

Another species with a similar topology has been briefly mentioned in a review [92] but never published: in $[Fe(btb)_2(NCS)_2]$ [btb = 1,2-bis-(1,2,4-triazol-1-yl)-butane] (4, 4) sheets and 1D chains of rings have been described to give polycatenation at an inclined angle.

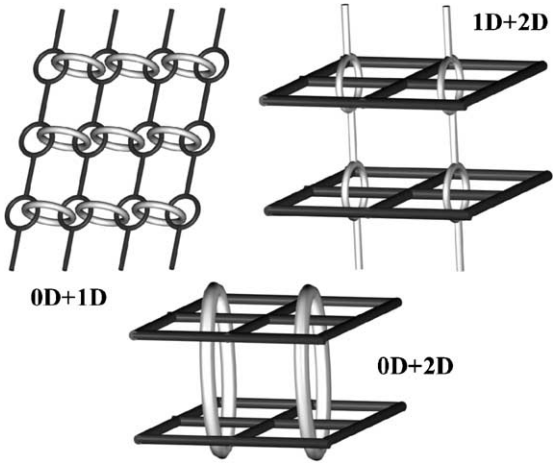

Scheme 7.

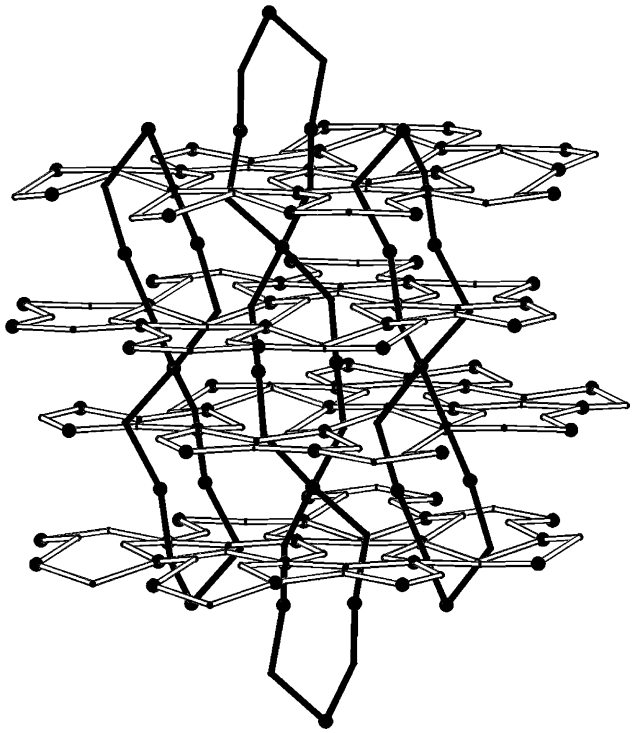

Fig. 30. Polycatenation of the two different motifs in $[Cu_5(bpp)_8(SO_4)_4(EtOH)(H_2O)_5](SO_4)\cdot EtOH\cdot 25.5H_2O$ [35].

4. Polythreading

The great number of structural data that are nowadays available on metal-based polymeric species has evidenced other types of infinite entanglements. Polythreaded systems can be considered as extended periodic analogues of the molecular rotaxanes or *pseudo*-rotaxanes (see Scheme 1). Distinct motifs can be entangled *via* rotaxane-like mechanical links and this implies the presence of closed loops as well as of elements that can thread the loops. These two types of moieties may belong to the same unit or may be separately supplied by motifs having different structures. The constituent motifs could be, in principle, 0D species, 1D polymers or arrays of higher dimensionality. The resulting array can show the same or an increased dimensionality with respect to that of the polythreaded units (see Schemes 8 and 9, that illustrate examples of the rotaxane and *pseudo*-rotaxane type).

Known examples involving 0D motifs, i.e. molecular 'beads' (cucurbituril molecules), threaded by coordination polymers of different topology have been described by Kim and coworkers [79] (see Section 3.2.2, Fig. 22). These include 1D poly*pseudo*-rotaxanes (see I in Scheme 9), with linear [79b], zigzag [79b,79c] or helical [79b,79d] polymeric chains, as well as 2D polyrotaxanes [79b] and a noteworthy 3D polyrotaxane network with the α-Po topology [79e]. Note, however, that in the polymers containing beads interlaced with closed loops the topologically significant links are Hopf links (catenation).

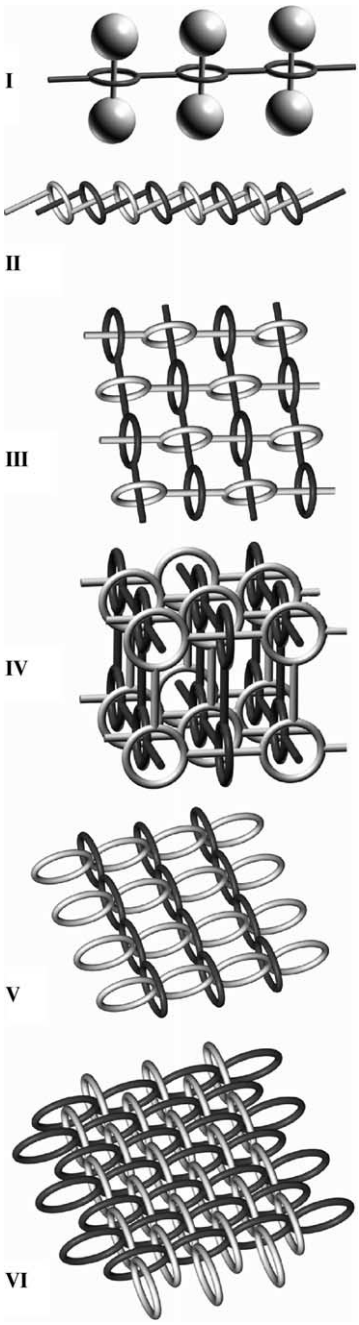

Scheme 8.

As we have already observed, not only poly*pseudo*-rotaxanes but also polyrotaxanes are trivial topological entanglements. By means of 'ideal' continuous deformations we could separate the components of any finite portion of a polyrotaxane, like those in Scheme 8. However, we are used to consider coordination polymers as infinite entities (this is an idealization, that, in some way, parallels the concept of 'perfect crystal' within crystallography). Including this additional 'boundary condition' a different topological description could result for these interweaving systems, but this is at present an almost completely unexplored *area* of chemical topology [39e].

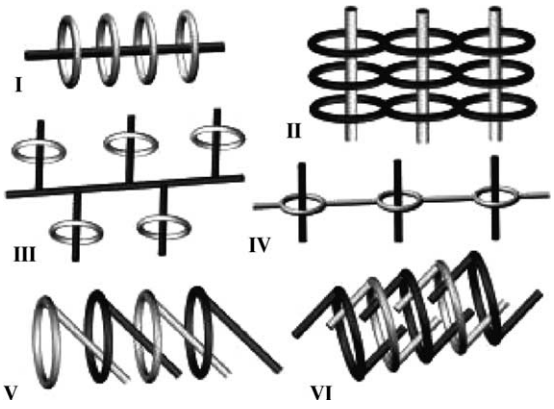

Scheme 9.

We have suggested the term 'Euclidean entanglements' for polyrotaxanes, meaning that only the presence of geometrical or energetical constrains (non topological) can prevent the separation of the individual motifs. In this concern we are faced with the problem of establishing case by case the nature of the linkages, i.e. rotaxane or *pseudo*-rotaxane like (see Section 2.1).

We can differentiate into two classes the known polythreaded examples on the basis of the 'ideal' possibility to extricate (or less) the components. When the different motifs 'cannot be disentangled' without breaking links the system can be described as belonging to the class of polyrotaxanes.

The second class contains motifs that are threaded by chains or strings which, in principle, can be slipped off. These species can be described as infinite periodic poly*pseudo*-rotaxanes and display a type of entanglement that is neither topological nor Euclidean. Furthermore, the threading elements can be of two types: infinite chains or finite components. These two situations will be examined separately.

4.1. Extended systems that 'cannot be disentangled'

Many examples belonging to this class have been reported only very recently. The already mentioned 1D chain motif comprised of alternating rings and rods, potentially useful for polycatenation (see Scheme 4), is particularly suitable for polythreading since it contains both the elements needed in a rotaxane-like mechanical linkage. Chains of this type have been found to give both (1D → 1D) and (1D → 2D) polythreaded arrays. In the former case, a pair of such entangled chains run in a parallel direction, while in the second case two distinct sets of chains exhibit two 'inclined' directions of propagation.

Two quite fascinating examples of (1D → 1D) polythreaded species have been reported in 2001 by the groups of Stang [93] and Puddephatt [94]. These polymers exhibit some common features: (i) both are comprised of 1D chains of alternating rings and rods sustained by

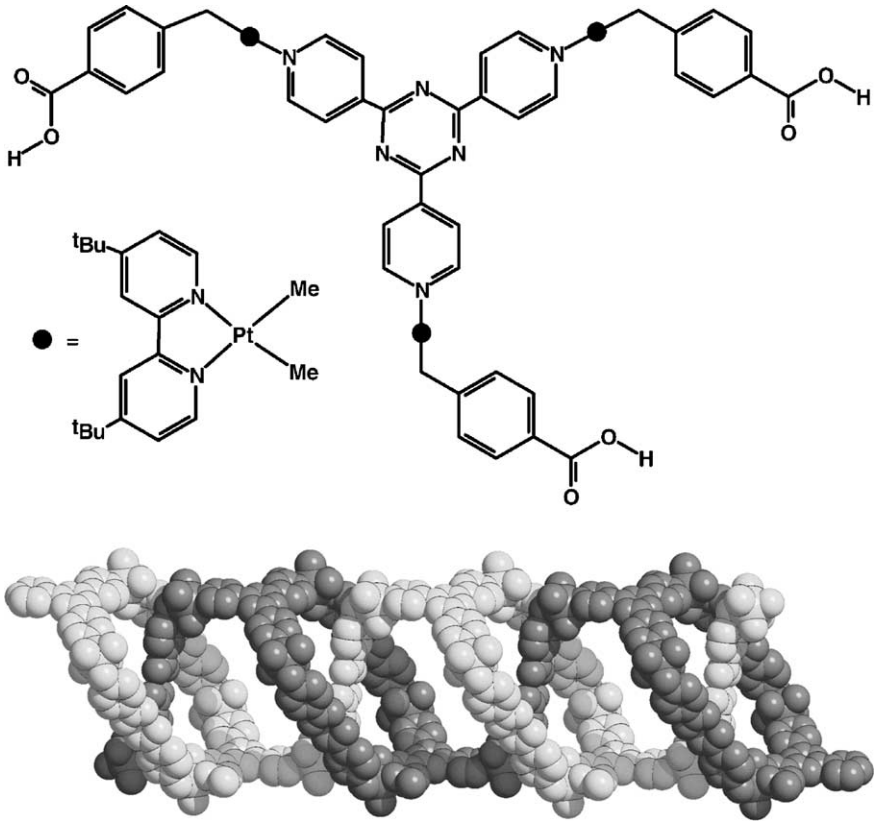

Fig. 31. The building block and the 1D polyrotaxane of [94].

concomitant coordinative and hydrogen bonds, (ii) both contain organometallic centers, (iii) in both cases pairs of chains are entangled, with the same topology, as II in Scheme 8, without increase of the dimensionality.

In the first of these two species, *namely* $[(C_5Me_5)RhL_3](OTf)_2$ (L = isonicotinamide) [93], the building blocks consist of $(C_5Me_5)Rh^{2+}$ centers, bearing three isonicotinamide groups bonded to the metal through the ring nitrogen atoms, that are joined together *via* hydrogen bonds involving the amide functionalities. The resulting strands are interwoven in pairs to give an infinite 1D polyrotaxane. Each strand is offset from the other by ca. 11 Å. Further amide-amide hydrogen bonds between neighboring strands link the entangled chains into a 3D architecture.

The second complex contains building blocks of composition $[\{(HO_2CC_6H_4CH_2)(Bu_2bipy)Me_2Pt\}_3(tpt)]^{3+}$ [Bu_2-bipy = 4,4′-di-*tert*-butyl-2,2′-bipyridine, tpt = tris(4-pyridyl)triazine, counterions = PF_6^-] (see Fig. 31, top) that possess three carboxylic acid functional groups designed to take part in intermolecular hydrogen bonding [94]. These units give self-assembly into chains of rings and rods *via* $-(COOH)_2$ synthons (O···O 2.60–2.70 Å). These polymeric chains are entangled in pairs, as in the previous species, to form a polyrotaxane, illustrated in Fig. 31.

Two cases of (1D → 2D) polythreaded species are also known. The fascinating coordination polymer $[Ag_2(bix)_3](NO_3)_2$ [bix = 1,4-bis(imidazol-1-ylmethyl)benzene], reported by Robson and coworkers [95], is a 2D polyrotaxane formed by 1D chains of rings and rods that give polythreading as shown in III of Scheme 8.

The second species, obtained by Suslick and coworkers from freebase 5,10,15,20-*tetrakis*-(4-carboxyphenyl)porphyrin with Ca(II) ions, contains infinite 1D bands of porphyrin units joined *via* coordination to calcium ions [96]. Each Ca^{2+} ion interacts with two carboxylates from two adjacent porphyrins and each porphyrin is connected to four metal ion. These bonds generate polymeric species similar to those observed in the 1D complex $[(HgBr_2)_2(H_2tpyp)]$ [97]. The chains of rings propagate into two inclined directions giving a polythreaded 2D array illustrated in Fig. 32. Though the component 1D structural motifs are much different from those of the $[Ag_2(bix)_3](NO_3)_2$ species above described, the topology of the entanglement (see also VI versus III in Scheme 8) is essentially the same.

A remarkable structure recently reported must also be discussed in this concern. Compound $[Cu_2(bpa)_2(phen)_2(H_2O)]_2{\cdot}2H_2O$ [bpa = biphenyl-4,4′-dicarboxylate, phen = 1,10-phenanthroline] [98] contains molecular rhombi, with $[Cu(phen)]^{2+}$ units as corners and bpa^{2-} anions as edges, to form large open rhombic cavities. The phen ligands, extended outward of the rhombi, play an important role in the self-assembly *via* aromatic π-interactions leading to higher dimensionality. The two phen ligands at the acute angle sites of each rhombus interact with the same moieties of two lateral rhombic units, forming a chain of rings by means of π–π stacking interactions (face-to-face distance

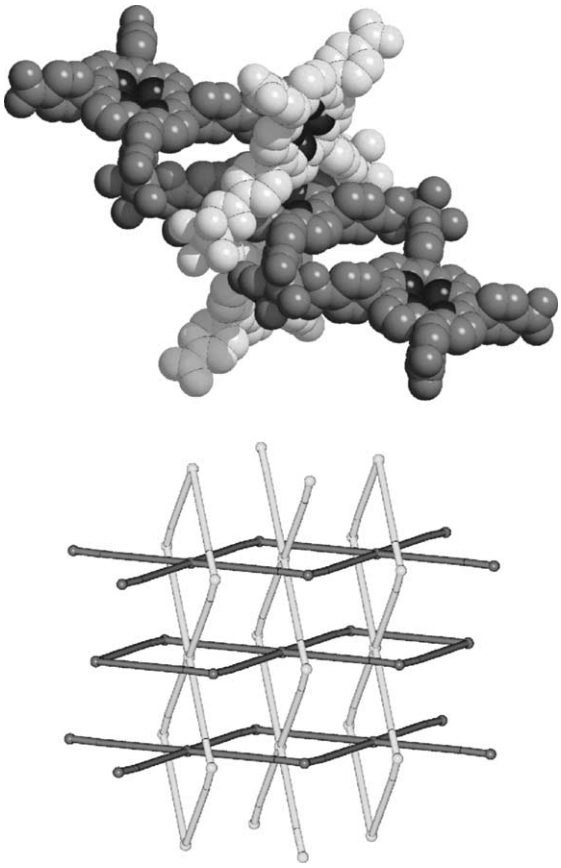

Fig. 32. The 2D polyrotaxane species from Ca(II) and 5,10,15,20-*tetrakis*-(4-carboxyphenyl)porphyrin [96].

3.46 Å). These interactions occur inside the rhombic cavities of other rhombic units that form analogous chains running with an included orientation. This generates a 2D polyrotaxane architecture (see Fig. 33) with the same topology of the polymer in Fig. 32.

Curiously, the polyrotaxane layers are further connected between them into a 3D network *via* similar π–π stacking interactions involving the phen ligands at the obtuse angle sites of the rhombi. The topology of the resulting array is similar to that of IV in Scheme 8.

A completely different example of a polythreaded structure is present in compound $[CuL_3(H_2O)_2(NO_3)_2][CuL_2(H_2O)(NO_3)]_2(NO_3)_2{\cdot}EtOH$ [L=1,6-bis[(4-pyridyl)-hexane], reported by Plater and coworkers [99]. In this species, two different kinds of infinite 1D chains are present, i.e. single stranded 1D chains $[CuL_3(H_2O)_2(NO_3)_2]$ (A), in which one of the bis(4-pyridyl) spacers acts as bridging while the other two are mono-coordinated dangling ligands, and chains of rings $[CuL_2(H_2O)(NO_3)]$ (B), in which the metal centers are doubly bridged by the ligands forming 30-membered Cu_2L_2 rings. The two motifs (A and B), exhibiting a 1:2 ratio, are entangled to give 2D layers, illustrated in Fig. 34. The A chains are threaded into the rings of the B ribbons, in such a way that each Cu–L–Cu segment penetrates two loops in two adjacent ribbons. Neighboring

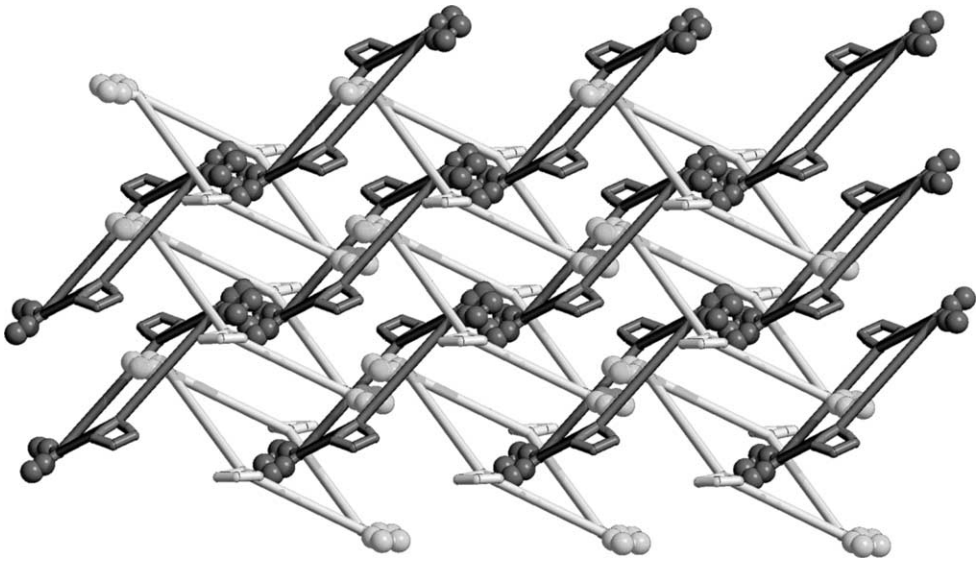

Fig. 33. A 2D polyrotaxane layer sustained by π–π interactions in $[Cu_2(bpa)_2(phen)_2(H_2O)]_2{\cdot}2H_2O$ [98].

A chains show a relative displacement. From the topological point of view this Euclidean entanglement (see Section 2.1 and II in Scheme 2) can be described as a polyrotaxane or as a poly*pseudo*-rotaxane depending on the ability of the side arms on the A chains to work as stoppers that can prevent the extrusion of these motifs. A similar ambiguity is present also in the hypothetical species V in Scheme 8.

Two noteworthy 'older' cases of (2D → 2D) polythreading must also be mentioned here (see Scheme 10), both representing unusual modes of parallel interpenetration of 2D sheets, that were described by Batten and Robson as examples having both polyrotaxane and polycatenane character [13]. Compound $[Zn(bix)_2](NO_3)_2{\cdot}4.5H_2O$ [bix = bis(imidazole)xylene] [100] contains 2D layers of (6, 3) topology, with two edges of the hexagonal meshes that are doubly bridged by the bix ligands producing $Zn_2(bix)_2$ loops. Two such layers give parallel interpenetration (I in Scheme 10) because the loops in one layer are threaded by rods of the other layer and vice versa. The two-fold sheets can also be described as formed by interconnected parallel 1D polyrotaxane chains like those previously described (see II in Scheme 8). The polyrotaxane nature of this species is evident but only the presence of catenated rings makes nontrivial the topology of the entanglement.

Similar considerations apply to the entanglement in $[Mn(p\text{-XBP4})_3](ClO_4)_2$ [*p*-XBP4 = *N*,*N*′-*p*-phenylenedimethylenebis(pyridin-4-one)] [101]. The main difference consists in that the layers here can be described as having the (4, 4) topology (see II in Scheme 10).

4.2. Entangled arrays containing 'separable' motifs

Numerous examples are now known that contain 1D polymers threaded into the rings belonging to other motifs of different nature. These extended architectures can be considered as infinite poly*pseudo*-rotaxanes (see Scheme 11). One case has already been discussed (see Section 3.2.2, Fig. 28).

Parallel threading of 1D chains into undulated 2D (4, 4) sheets is observed in $[La(NO_3)_4(H_2O)(bpe)][bpeH]$

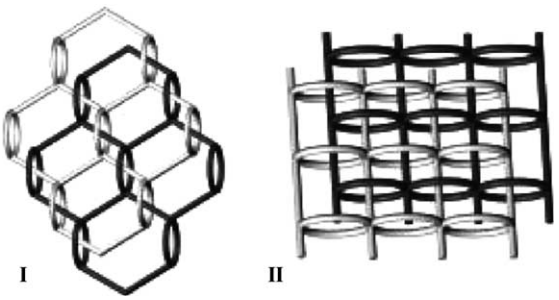

Scheme 10.

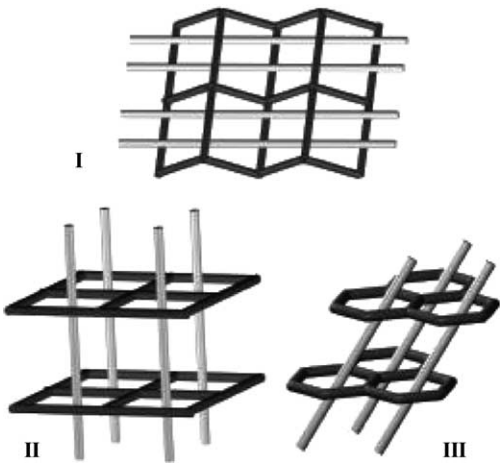

Scheme 11.

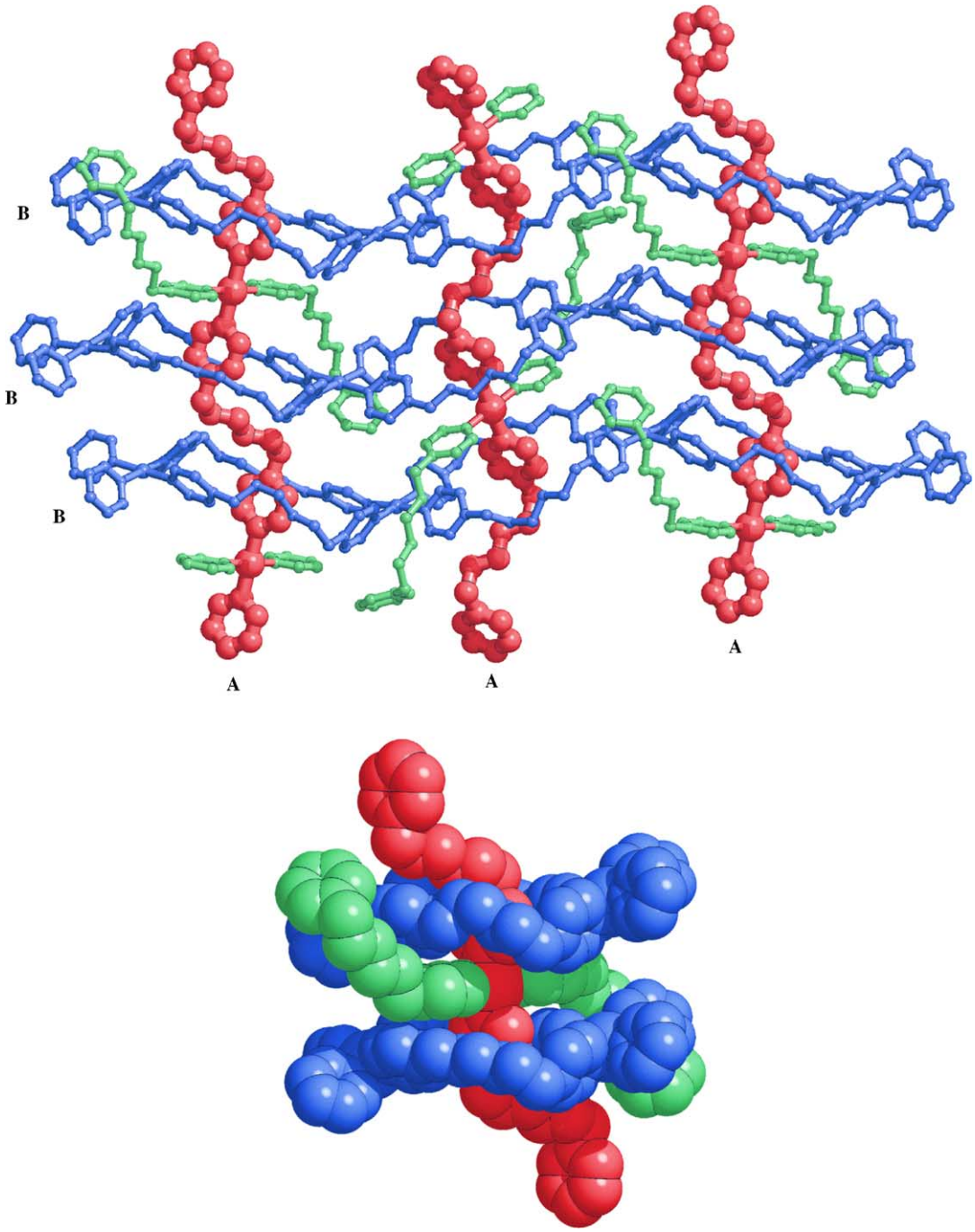

Fig. 34. Polythreading of 1D chains (red) with side arms (green) into the ribbons of rings (blue) in the complex of [99].

[bpe = 1,2-bis(4-pyridyl)ethane] [102], giving an architecture described as 'molecular Chinese blinds'. The La^{3+} ions are complexed by four bidentate NO_3^- anions, two bridging bpe ligands, and one water molecule to give anionic parallel 1D coordination polymers. Hydrogen bond bridges involving coordinated water molecules and nitrate anions belonging to metal ions of adjacent chains lead to the formation of a corrugated sheet structure with channels running in the layer. Each channel is threaded by two linear 1D hydrogen bonded cationic chains of protonated ligand molecules $-bpeH^+-bpeH^+-bpeH^+$, thus resulting in a poly*pseudo*-rotaxane array (see Scheme 11, I).

An interesting 3D poly*pseudo*-rotaxane architecture with 1D polymeric chains penetrating 2D (6, 3) sheets has been observed in $[Ag(bpp)][Ag_2(bpp)_2(ox)](NO_3)$ [bpp = 1,3-bis-(4-pyridyl)propane, ox = oxalate] [103]. Each layer, of composition $[Ag_2(bpp)_2(ox)]$, consists of Ag atoms connected by bpp bridges and bis-chelated ox^{2-} bridges that form hexagonal meshes. Adjacent sheets are stacked in an offset fashion so that the original large hexagonal cavities

within each layer are divided into two halves. The polymeric $[Ag(bpp)]^+$ chains contain metal atoms in linear coordination geometry and penetrate the 2D sheets at an inclined angle (as in III of Scheme 11) to generate the whole 3D array. Two 1D chains pass through each hexagonal window.

More interesting are the two following networks. Compound $[Cu(L)(solv)(NO_3)_2][Cu(L)_{1.5}(NO_3)_2]\cdot 2solv$ (L = 1,4-bis[(4′-pyridylethynyl)benzene], solv = EtOH or MeOH) [104] contains a 3D coordination polymer with a novel structural motif consisting of stacks of infinite ladders penetrated by bundles of 1D chains. The ladders, of composition $[Cu(L)_{1.5}(NO_3)_2]$, run in a parallel direction and stack in a 'terraced' fashion, with a separation of 6.1 Å and a lateral offset of 1/2 the ladder width. The 1D chains, $[Cu(L)(solv)(NO_3)_2]$, contain five-coordinate copper atoms, with two bis-(4-pyridyl) spacers in *trans* positions. The stacking sequence of the ladders generates rectangular channels that are occupied by the 1D chains (two in each channel), as shown in Fig. 35. The chains, therefore, thread the square openings in groups of four.

Reacting the long spacer ligand 4,4′-bis(4-pyridyl)biphenyl (L) with $Cd(NO_3)_2$ Biradha and Fujita have recently succeeded in crystallizing three types of coordination polymers together with guest molecules in one crystal. This surprising species contains 2D layers of (4,4) topology with grids of 20 Å × 20 Å, $[Cd(L)_2(NO_3)_2]$ (A), double linear chains bridged by nitrate anions into ladders, $[Cd_4(L)_4(NO_3)_6(MeOH)_6]^{2+}$ (B), and linear chains $[Cd(L)(NO_3)_3]^-$ (C), for a total composition $[(A)(B)(C)](NO_3)\cdot 2(mesitylene)\cdot 3MeOH$ [105]. The layers A stack on each other with a large interlayer separation of 10.9 Å in an offset fashion, forming channels of section ca. 10 Å × 20 Å. The ladders B are fitted into the channels to form a 3D poly*pseudo*-rotaxane arrangement (Fig. 36). Two ladders thread each square window. The linear chains C are packed between the 2D layers A, making an angle of 90° with polymers B.

4.3. Polythreading with finite components

Another type of entanglement can derive from the repeated threading of elements of finite length through closed loops affording *pseudo*-rotaxane like interactions. Many different situations can be envisaged, depending on the nature of the motifs and on which are the finite components. Some hypothetical examples are illustrated in Scheme 9. In any case, the resulting overall architecture should be an infinite periodic array.

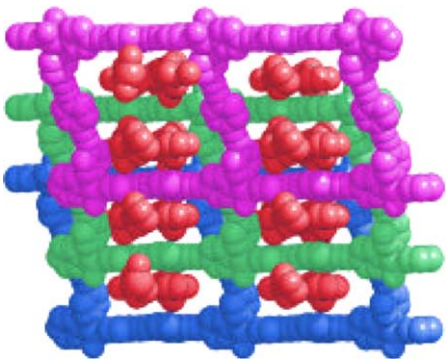

Fig. 35. Infinite ladders penetrated by 1D chains in $[Cu(L)(solv)(NO_3)_2][Cu(L)_{1.5}(NO_3)_2]\cdot 2solv$ [104].

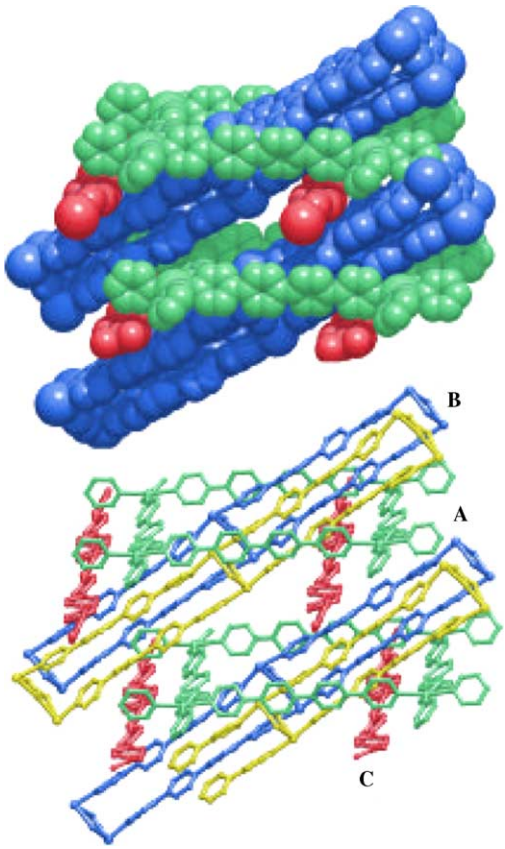

Fig. 36. The 'three in one' structure of [105], with the square grid layers (A) in green, the ladders (B) in blue and yellow and the 1D chains (C) in red.

Extended structures involving 0D motifs can be, in principle, formed by rings with side arms, as in V and VI of Scheme 9. Such molecular modules are self-complementary units, which can self-assemble to give supramolecular oligomeric or polymeric species. Systems like V were called "supramolecular daisy chains" [17b].

Compound $[Co_2(L)_4(NO_3)_4]\cdot(Me_2CO)_2$ [L = 4,4′-bis-(pyridin-4ylmethoxy)biphenyl] [106] contains distinct molecules that consist of 42-membered Cu_2L_2 molecular rings with two additional terminally bonded L ligands, one on each metal (see Fig. 37). The supramolecular organization of these rings with pendages gives 1D parallel columns resembling the chain VI of Scheme 9; however, the dangling ligands of the two adjacent units do not really penetrate the rings but are simply interdigitated on the ring surface.

We are aware of two cases of this class containing infinite motifs, i.e. molecular ladders with side arms (sometimes called molecular "railroads" [47d]).

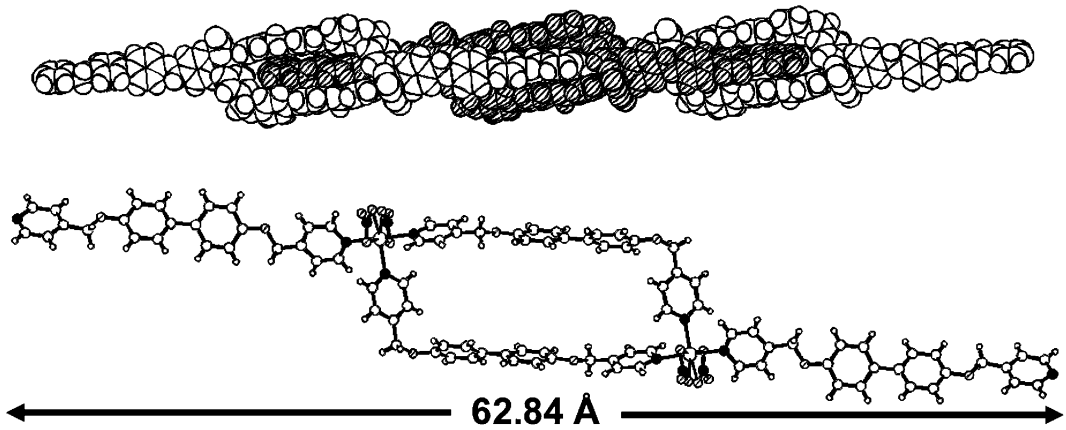

Fig. 37. The columnar organization of the molecular motifs in $[Co_2(L)_4(NO_3)_4]\cdot(Me_2CO)_2$ [106].

The first of these species, $[Ag_2(bpethy)_5](BF_4)_2$ [bpethy = 1,2-bis(4-pyridyl)ethyne] [107], is comprised of ladder-like polymers bearing as extensions by both sides of each rung two additional terminal dangling bpethy molecules, disposed in a mutual *anti* orientation with respect to the ladder plane. All the ladders run in the same direction and are closely and parallely disposed on planes, with an inclination of ca. 22°. The terminal bpethy ligands of each ladder are threaded into the squares of the adjacent ladders, in a "mutual polythreading". The length of the ligands is such that the threading involves not only the first but also to the second nearest neighboring ladders. Each square is therefore penetrated by four bpethy molecules, two entering by one side and two by the opposite one, as shown in Fig. 38, thus resulting in a supramolecular 2D entanglement involving five polymeric units at a time. The threading is stabilized by π–π stacking and weak attractive CH–π interactions.

Polythreaded molecular ladders with dangling arms are present also in the polymeric complex $[M_2(4,4'\text{-bipy})_3(H_2O)(phba)_2](NO_3)_2\cdot 4H_2O$ (M = Cu, Co, phba = 4-hydroxybenzoate), reported by Chen and coworkers [108]. At variance

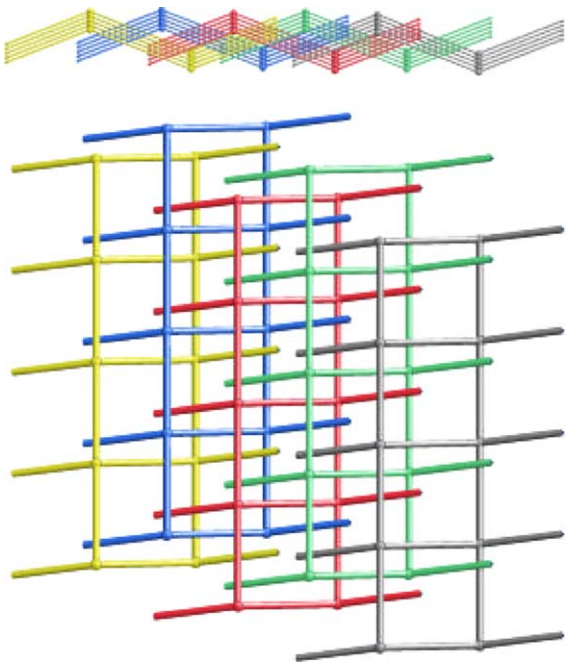

Fig. 38. Two schematic views of the polythreading in the ladder polymers of $[Ag_2(bpethy)_5](BF_4)_2$ [107].

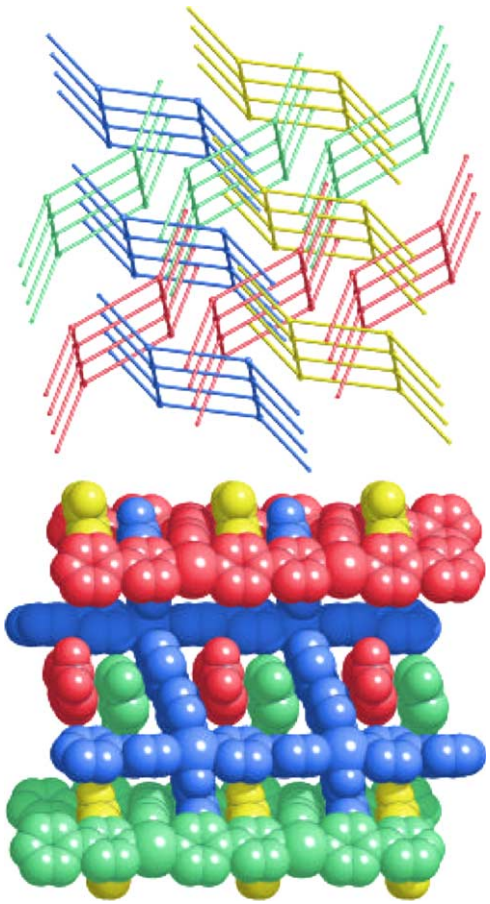

Fig. 39. The 3D polythreaded network in $[M_2(4,4'\text{-bipy})_3(H_2O)(phba)_2](NO_3)_2\cdot 4H_2O$ [108].

from the previous species the ladders have rails and rungs (4,4′-bipy) of different nature with respect to the lateral arms (phba). The dangling ligands are again bent out of the ladder planes and are threaded into the $[M_4(4,4'\text{-bipy})_4]$ squares of adjacent ladders, with each square penetrated oppositely by two phba lateral arms that belong to two different polymers (see Fig. 39). All the ladder motifs run parallel but their planes show two different orientations thus resulting in an overall 3D polythreaded array. The aromatic rings of phba penetrated into the same square are parallel to each other, giving significant π–π interactions between them and with the 4,4′-bipy ligands on the square edges. The decreased number of side arms penetrating each square in this complex when compared with the $[Ag_2(bpethy)_5](BF_4)_2$ species clearly derives from the shorter length of the spacer ligands.

5. Polyknotting (self-penetrating networks)

Among the new types of entanglements in polymeric architectures the *phenomenon* of polyknotting has attracted much attention in recent times. Molecular knots are complex molecular architectures of fascinating topology (see Scheme 1) [18,19]. Their synthesis has been a challenge for a long time until the preparation in 1989 of a molecular trefoil knot by Dietrich-Buchecker and Sauvage [16e].

The extended periodic equivalent of a molecular knot can be described as a polyknotted network. These species are single nets that exhibit the peculiar feature of containing rings through which pass other components of the same network. In more detail, we must refer to the topological classification of nets, represented by their Schläfli symbols (see Section 2.1); if one of the 'shortest rings' is catenated by other 'shortest rings' of the same net we can speak of a true case of self-penetration. This is a necessary condition to be accomplished, since, otherwise, catenated rings or knots can be always found in any kind of network, provided that sufficiently long circuits are considered. For instance, a trefoil knot can be envisaged in an α-Po single network, as that illustrated in Fig. 40, involving 24 nodes of the frame. (We have built this trefoil knot rather naïvely. However, successively, we have discovered on a web site: http://www.amsci.org/ that the subject has a theoretical basis in the topological theory of 'square knots', i.e. knots constructed by joining the nodes in a cubic lattice. The smallest possible closed path in a cubic lattice is a square with $n = 4$, while the smallest nontrivial knot is a trefoil 24 units long (just like that in Fig. 40). This knot (and others of the same length) was proved minimal in 1993 by Yuanan Diao, see [109].)

Different terms have been employed for this type of self-entangled networks. Batten and Robson [14] have underlined the relationship of these species with molecular knots but they have preferred to classify these entanglements as self-penetrating or self-catenating nets. Champness and coworkers have used the term 'polyknotted coordination polymers' [110]. Also the term '*intra*penetrating networks' has been employed [111]. All are equally valid in this context.

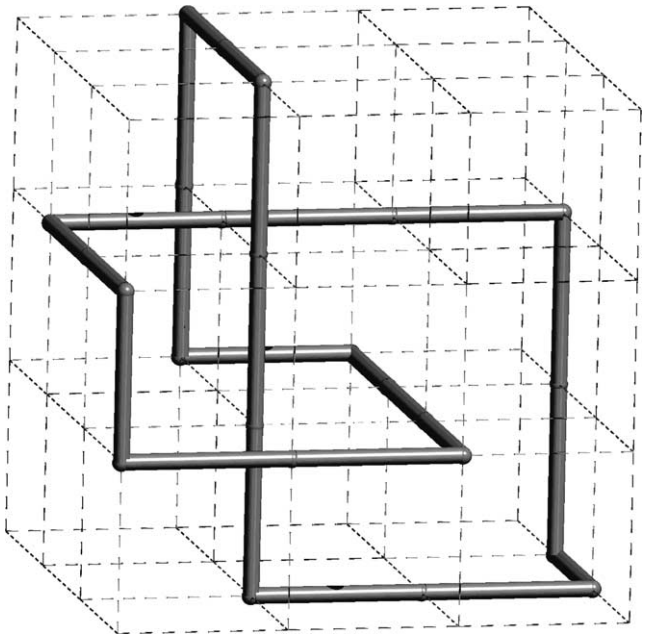

Fig. 40. A trefoil knot obtained connecting nodes in a single 3D network of the α-polonium type.

This unusual topological feature was previously observed also in simple mineral/inorganic frameworks, as in *coesite* (see later for an example of this topology), a high-pressure polymorph of silica, recognized by O'Keeffe to be 'unique among nets found in nature in that it contains 8-circuits that are linked as in a chain' [25b]. Batten has also mentioned the structure of Ice IV as an example of self-penetrating net [15a] (see also [112]).

For classification purposes, we have arbitrarily considered two types of networks, depending on the nature of linkages rather than on topological differences. One class consists of self-penetrating nets entirely sustained by the coordinative bonds of the spacer ligands (of equal or different nature). In the second class, the frames can be considered derived from polycatenated sets of independent coordination polymers that are cross-linked *via* node-to-node bridges of different types, like counterion bridges, hydrogen bond bridges, π interactions, aurophilic metal-to-metal linkages or other weak interactions.

5.1. Self-penetrating networks exclusively based on coordinative bonds

The number of networks showing the feature of self-penetration is much increased in the last few years. These are usually 3D nets but, in principle, also 1D and 2D self-penetrating entanglements are likely to occur, especially when favored by the presence of long flexible ligands. Indeed, we have already described an example of a 2D

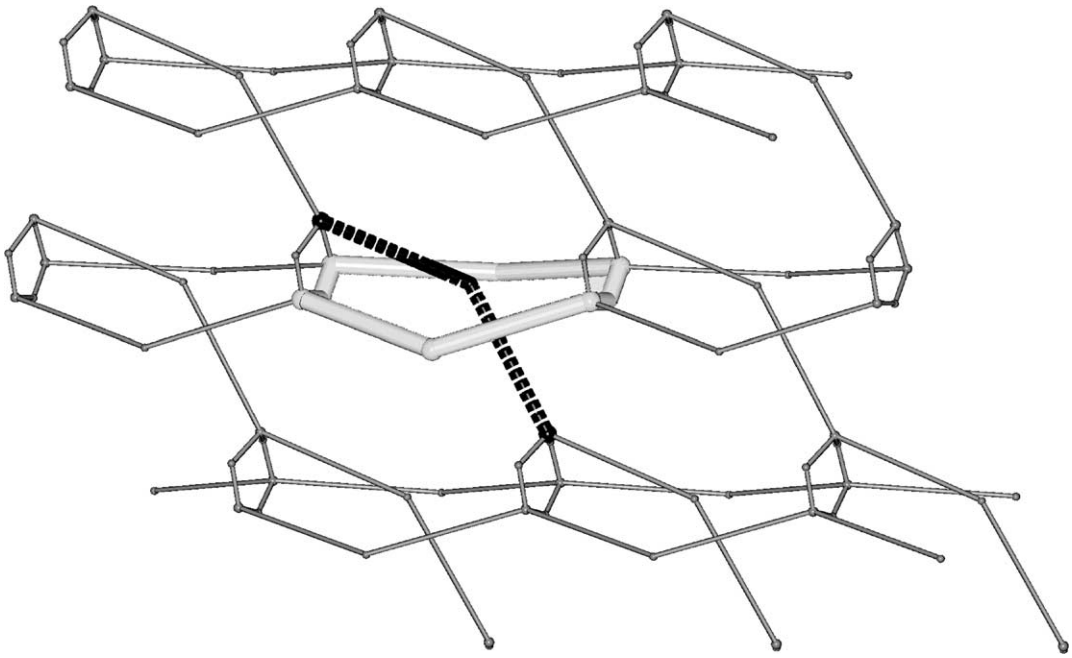

Fig. 41. A schematic view of the self-penetrating 2D net of $[Zn_3(OH)_3(bpp)_3][NO_3]_3{\cdot}8.67H_2O$ [113].

polyknotted species (also polycatenated) in $[Ag(sebn)_2]X$ (see Section 3.2.1 and Fig. 15).

To our knowledge, only one other case of 2D self-penetration is, at present, known. The polymer $[Zn_3(OH)_3(bpp)_3][NO_3]_3{\cdot}8.67H_2O$ [bpp = 1,3-bis(4-pyridyl)propane], reported by Plater et al. [113], consists of topologically complex sheets formed by small six-membered $Zn_3(\mu\text{-}OH)_3$ rings and bpp ligands that join these rings. Each Zn atom is bonded to two bpp ligands. The $Zn_3(\mu\text{-}OH)_3$ hexagons are thus connected by two bpp spacers into 1D ribbons of large 28-membered loops. The ribbons, in turn, are joined into 2D sheets by the third bpp ligand that threads the rings, as schematically illustrated in Fig. 41.

The first examples of 3D self-penetrating frameworks within coordination polymers were described by Robson and coworkers [114]. In the species $[Cd(CN)_2L]$ [L = pyrazine or 1,4-bis(4-pyridyl)butadiene] the $Cd(CN)_2$ sublattices form (4, 4) undulated layers that are joined in a criss-cross fashion by the L spacers. Catenated hexagonal chair-like circuits are observed in the interlayer connections (see Fig. 42). The short Schläfli symbols of these 6-connected nets are $4^8{\cdot}6^6{\cdot}8$ for L = pyrazine, and $4^4{\cdot}6^{10}{\cdot}8$ for L = 1,4-bis(4-pyridyl)butadiene, respectively, so that the requirements for self-penetration are fulfilled, since the catenated 6-rings are shortest rings.

A different self-penetrated system is observed in a related compound, $[Cd(CN)_2(4,4'\text{-bipy})_{0.5}]$ [115]. This illustrates how polyknotting can be attained starting from a certain network by connecting with an additional bidentate ligand pairs of suitable facing nodes. Here the $Cd(CN)_2$ sublattice forms a diamondoid net (6^6 topology) and the 4,4′-bipy ligands join two Cd atoms belonging to two adjacent adamantane-like cages, thus threading an hexagonal window (see Fig. 43). The resulting array is a 5-connected self-penetrating network of 6^{10} topology.

Perhaps one of the most fascinating examples in this family, that has renewed the interest for the topology of self-penetration, is represented by $[Ni(tpt)(NO_3)_2]$ (tpt = tri-4-pyridyl-1,3,5-triazine) [116]. This contains a remarkable 3-connected chiral single network of 12^3 topology (long symbol $12_4{\cdot}12_7{\cdot}12_7$), illustrated in Fig. 44, that was previously enumerated by Wells [23b] but never found in real species. Within uninodal 3-connected nets this is special in that it contains relatively 'large' shortest rings (12-gons), the largest *n*-gons considered by Wells, and exhibits self-entanglement, in the sense that 1/3 of the shortest rings of one center have other such circuits, referred to a different center, passing through them. In the real coordination network the 3-connected nodes are represented by alternating trigonal tpt ligands and T-shaped Ni^{2+} centers in equal number. Interestingly the authors suggest that future findings of networks containing *n*-gons with $n > 12$ as shortest rings should probably evidence other similar self-penetration *phenomena*.

The same 12^3 topology has been attributed to another coordination network, $[CoL(H_2O)_2]$ (L = 2,2′-bipyridine-4,4′-dicarboxylate), in spite of the presence of quite different building blocks [117]. This topological classification seems, however, a rather delicate problem, that depends on the choices in the simplification leading to the idealized net. The authors have considered both the cobalt centers and the multimodal chelating L ligands as distinct 3-connected nodes (for the ligand an 'arbitrary inside point' was selected). Very probably in this case a more realistic

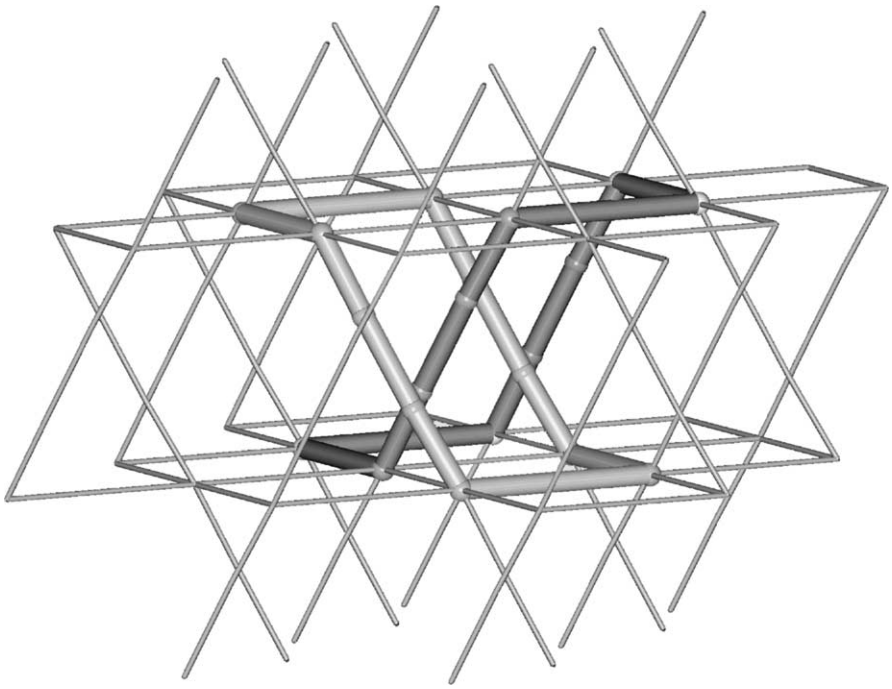

Fig. 42. Self-penetration in $[Cd(CN)_2(pyrazine)]$ [114].

rationalization consists in considering the whole complex $[CoL(H_2O)_2]$ as a single 4-connected node. This gives an overall net of quartz-like topology $6^4{\cdot}8^2$, $(6{\cdot}6{\cdot}6_2{\cdot}6_2{\cdot}8_7{\cdot}8_7)$. Indeed, a major feature that was neglected by the authors is that the network, whichever the topological description, is two-fold interpenetrated.

Self-penetration has been described as a structural compromise between single networks and interpenetration, a feature well illustrated by the structures of the [M(dca)(tcm)] species [M = Co, Ni, Cu, dca = dicyanamide, tcm = tricyanomethanide] [111]. These contain single, self-penetrating networks which are closely related to the binodal net of rutile [they have the same Schläfli short symbol $(4^2{\cdot}6^{10}{\cdot}8^3)(4{\cdot}6^2)$, but not the same long symbol and coordination sequence]. The networks are, indeed, a compromise between the two-fold interpenetrated rutile-like nets of $[M(tcm)_2]$ and the single rutile-like network of α-$[M(dca)_2]$ [15a,111]. There are three types of shortest rings, i.e. four-, six- and eight-membered circuits; the self-penetration involves six-membered rings.

As already mentioned, the high-pressure form of silica named *coesite* (the densest known form of silica) contains an unique self-penetrating 4-connected binodal net, exhibiting a complex $(4^2{\cdot}6^3{\cdot}8)(4^2{\cdot}6{\cdot}8^2{\cdot}9)$ topology. One of the most intriguing features of coordination network chemistry is its ability to produce rare and even only hypothetical structural motifs, given the correct building blocks. Moreover, the models are reproduced on a larger scale. This is, *inter alia*, the case of $[Ag(2\text{-ethpyz})_2](SbF_6)$ (2-ethpyz = 2-ethylpyrazine) that shows the topology of *coesite* (schematically illustrated in Fig. 45), exhibiting self-catenated 8-membered rings [118].

Another example of polyknotting was found in $[Cu(bpe)_2(SO_4)]{\cdot}5H_2O$ [bpe = 1,2-bis(4-pyridyl)ethane] [118]. This is a nanoporous polymer based on 4-connected copper(II) centers forming a $[Cu(bpe)_2]$ 3D binodal network with the complex unprecedented $(6^4{\cdot}8^2)(6{\cdot}8^5)$ topology. All the shortest rings (six- and eight-membered) are self-catenated. The self-penetration of two chains of rectangular six-membered circuits is shown in Fig. 46.

We have recently reported the structure of $[Ag_8(Zntpyp)_7(H_2O)_2](NO_3)_8{\cdot}x$Solv [Zntpyp = Zn(II)-5,10,15,20-tetra(4-pyridyl)porphyrinate] [119] that contains a complex 3D tetragonal open network (Fig. 47, top) with large free voids (55% of the cell volume). It is comprised of 2D layers, of composition $[Ag_4(Zntpyp)_3(H_2O)]^{4+}$, that are disposed all parallel to the tetragonal axis in two sets of pairs spanning mutually perpendicular directions. These pairs of layers, containing large windows, interpenetrate in an inclined fashion, as shown in Fig. 47, bottom. The layers, however, are not independent but are interconnected by perpendicular Zntpyp units, to give an unique 3D self-penetrating network.

Other recent examples of self-penetrating nets are listed by Batten in his web site (see ref. [15a]).

5.2. Self-penetration by cross-linking of polycatenated motifs

Some coordination polymers exhibit notable structures containing independent polycatenated motifs that are joined by bridging counterions or *via* supramolecular weak interactions, thus resulting in an unique self-penetrating net. We have already encountered examples of this

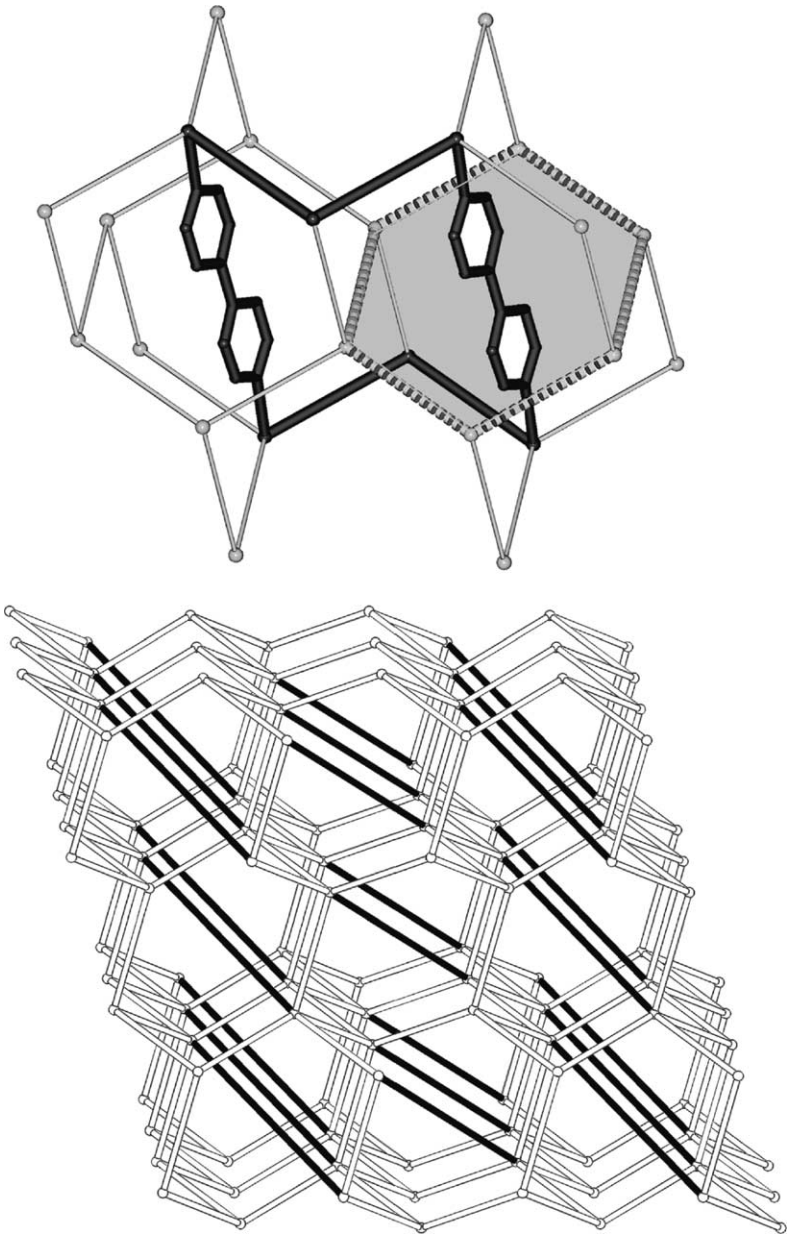

Fig. 43. Catenated rings (top) and schematic network (bottom) in the 5-connected self-penetrated $[Cd(CN)_2(4,4'\text{-bipy})_{0.5}]$ [115].

type that, however, have been described in an alternative way, as in the case of the entangled Borromean species $[Ag_2(H_2L)_3](NO_3)_2$ and $[Ag_2(H_2L)_3](ClO_4)_2$ [H_2L = *N*,*N*′-bis(salicylidene)-1,4-di-aminobutane] [59] (see the discussion in Section 3.2.1 and Fig. 10). An analysis of the self-penetrating net of this species (obtained by including also the Ag···Ag interactions in the model) reveals the surprising feature that the short and long Schläfli symbols, as well as the coordination sequence up the 10th neighbors, are identical to those of diamond [25a]. In spite of the evident differences, it seems that we are unable, at present, to assign a distinct topological classification to the two nets.

A beautiful example of this class has been observed in $[Cd_2(4,4'\text{-pytz})_3(\mu\text{-}NO_3)(NO_3)_3](MeOH)$ [4,4′-pytz = 3,6-bis(pyridin-4-yl)-1,2,4,5-tetrazine] [110]. The structure consists of molecular ladders that give inclined catenation forming a 3D array (see Fig. 48). Each square of a ladder is perpendicularly penetrated by two other ladders. Significantly, the ladders of the two perpendicular sets are cross-linked by $\mu\text{-}NO_3^-$ anions bridging the Cd(II) centers. As a consequence all the ladders are linked together, resulting in the formation of a single 3D polymer, that the authors describe as a ‘polyknot’.

In $[Cu(dca)_2(4,4'\text{-bipy})]\cdot H_2O$ (dca = dicyanamide) [120] the structure consists of two sets of parallel 2D sheets interlocking at an inclined angle of 65°. The layers are comprised of rectangular meshes, with two edges bridged by dca ligands *via* nitrile nitrogen atoms and two edges bridged by

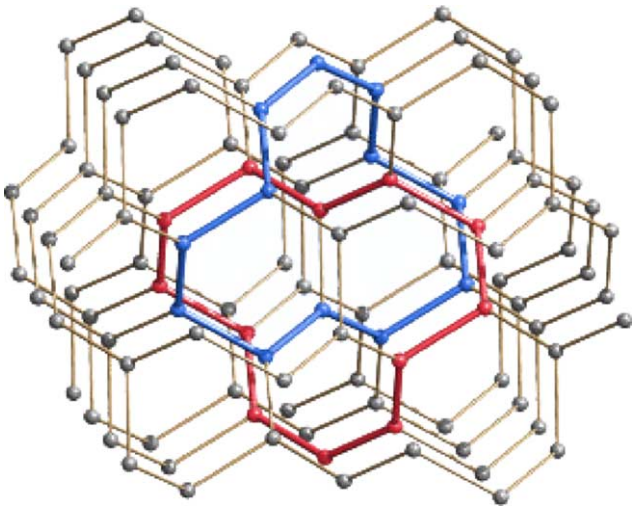

Fig. 44. The 12^3 self-penetrated net in $[Ni(tpt)(NO_3)_2]$ [116]; two catenated 12-gons (in red and blue) are evidenced.

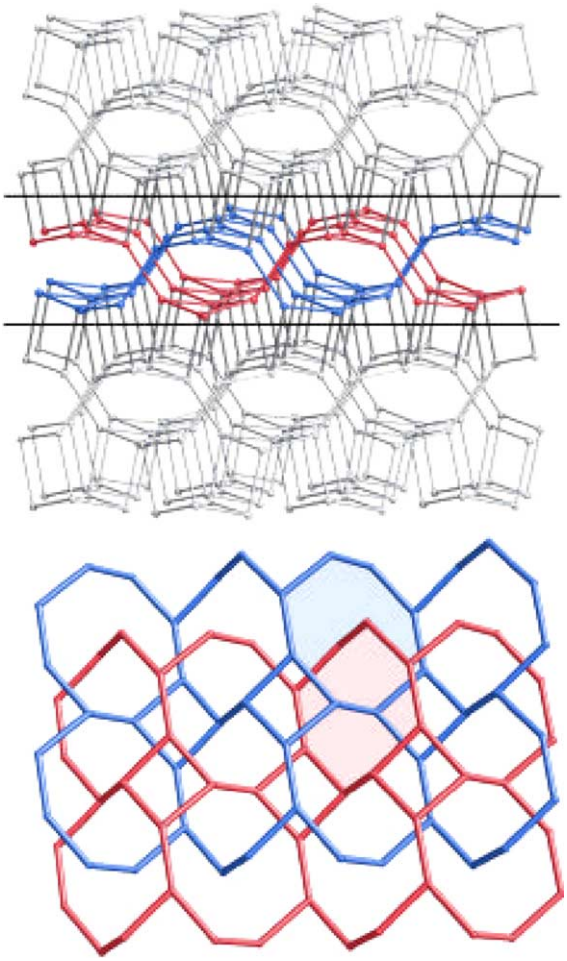

Fig. 45. The coesite-like network (top) and a cut of the net showing two self-penetrated layers (bottom) in $[Ag(2\text{-ethpyz})_2](SbF_6)$ [118].

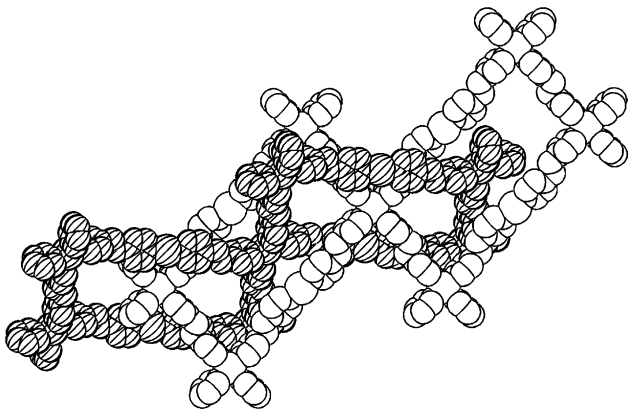

Fig. 46. A detail of the self-penetrating net in $[Cu(bpe)_2(SO_4)]\cdot 5H_2O$ [118].

4,4′-bipy ligands. The other dca ligands attached to each Cu atom are monodentate, *via* a nitrile nitrogen, and furthermore give long Cu-N(amide) bonds (2.87 Å) with the copper atoms on the layers of the inclined set. The polycatenated sheets are thus cross-linked into a single self-penetrating net.

The classification of these species as self-penetrating nets has been carried out on a rather intuitive basis. Adopting a more rigorous point of view should imply to assign for any case the correct Schläfli symbol to the overall net and then to verify that self-catenation involves the shortest rings, according to the definition given above. This is not always the case.

As an example we have analyzed in more detail the notable species $(R\text{-rad}^+)_2M_2[Cu(opba)]_3(DMSO)_2\cdot 2H_2O$ [R-rad$^+$ = 2-(4-N-*alkyl*pyridinium)-4,4,5,5-tetramethylimidazoline-1-oxyl-3-oxide; opba = *o*-phenylene-bis(oxamato); R = Me, Et, Pr, Bu, M = Mn, Co, Ni], exhibiting interesting magnetic properties [121]. If we neglect the R-rad$^+$ radical cations the array can be described [13] as two sets of (6, 3) layers giving inclined interweaving, Doc = (1/1), as shown in Fig. 49 (top). However, the cations form weak bonds with the copper atoms, bridging the two sets of layers. The resulting unique net is (3,4)-connected and quite complicated (see Fig. 49, bottom), with Schläfli symbol $(6^2\cdot 7^2\cdot 10^2)(6^2\cdot 7^4)(6\cdot 7^2)$, and the self-catenated circuits are not ‘shortest rings’.

6. Entangled arrays of polymeric chains

Polymeric chains assembled using metal centers and spacer ligands, both rigid or flexible, represent the most simple and common structural motif within coordination polymers. The packing of 1D polymers usually occurs with parallel orientation of all the chains; less commonly they can span two different directions on alternate layers. Independent chains can be sometimes connected into pairs or into extended 2D or 3D arrays by means of weak supramolecular interactions. Quite rare are, on the other

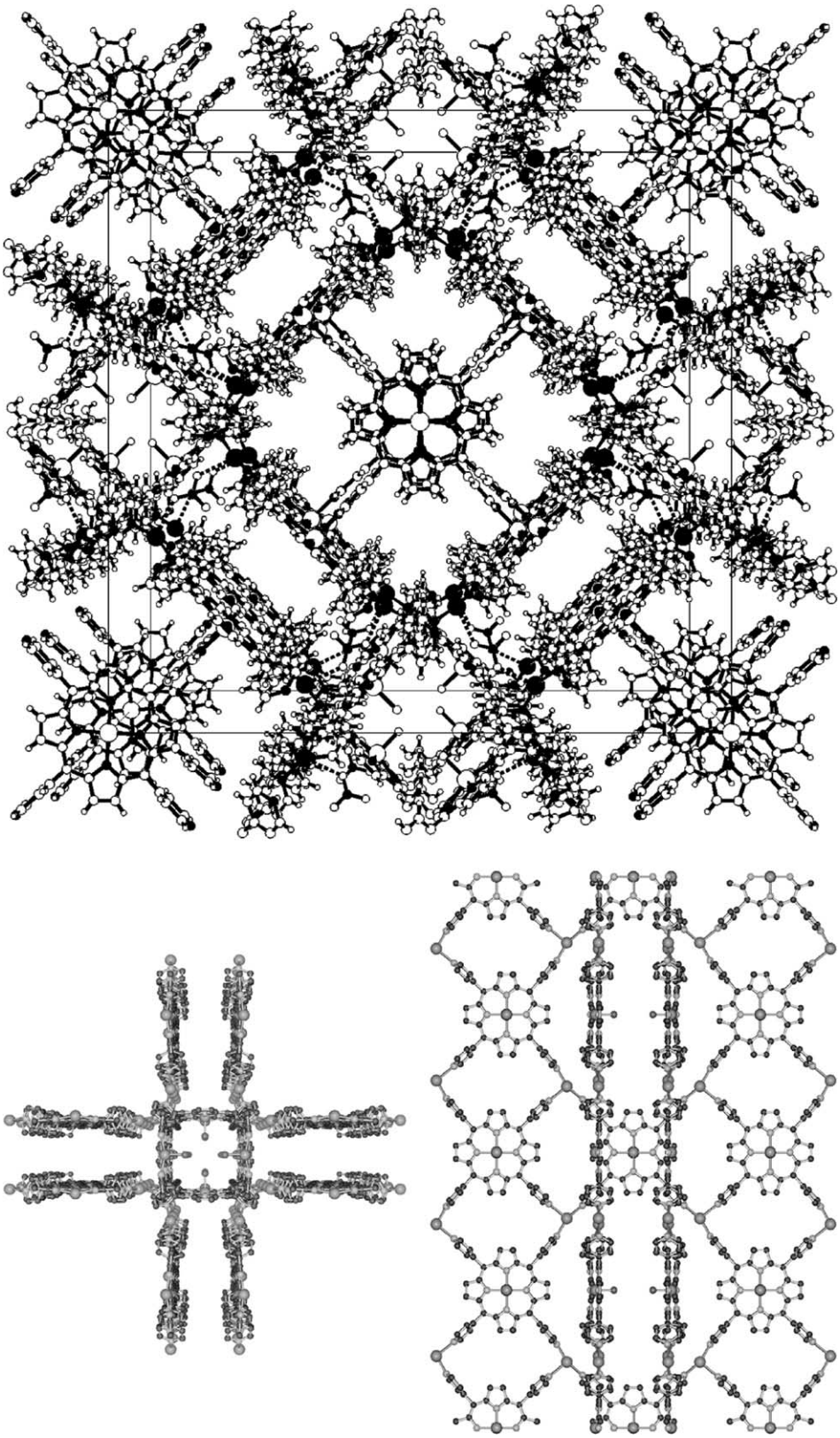

Fig. 47. The whole network (top) and two views of the inclined interlocking of two crossing pairs of layers (bottom) in $[Ag_8(Zntpyp)_7(H_2O)_2](NO_3)_8$ [119].

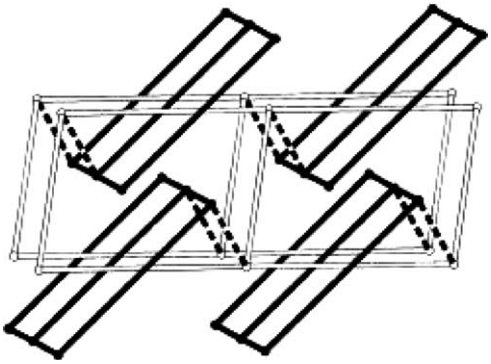

Fig. 48. Schematic view of the self-interpenetration in [Cd_2-(4,4′-pytz)$_3$(μ-NO_3)(NO_3)$_3$](MeOH) [110] due to cross-linking of polycatenated ladders.

hand, other types of associations of the chains resulting in entangled systems of unusual topologies. Two possible ways (out of an innumerable variety) of 2D entaglements are illustrated in Scheme 12.

Both motifs in Scheme 12, i.e. chains woven like woof and weft threads in a cloth (top) and chickenwire like (bottom), have been observed within real species. More complex 3D entanglements could also be, in principle, considered. Furthermore, infinite multiple helixes represent another fascinating mode of 1D association, few examples of which have been discovered within coordination polymers. In all these types of trivial entanglements the individual chains can be 'ideally' separated by slipping off, without the need of breaking links.

6.1. 2D and 3D entanglements of 1D chain polymers

The first example of a 2D entangled layer of woof and weft threads was reported in 1995 by Balch and coworkers, *namely* [$(AuI)_2$(μ-dpph)] [dpph = bis(diphenylphosphino)-hexane] [122]. This species contains dinuclear complexes

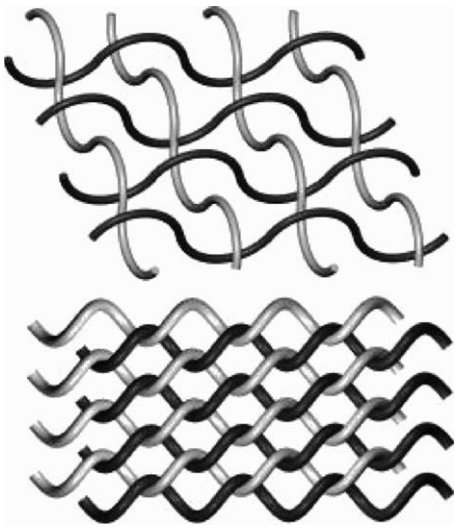

Scheme 12.

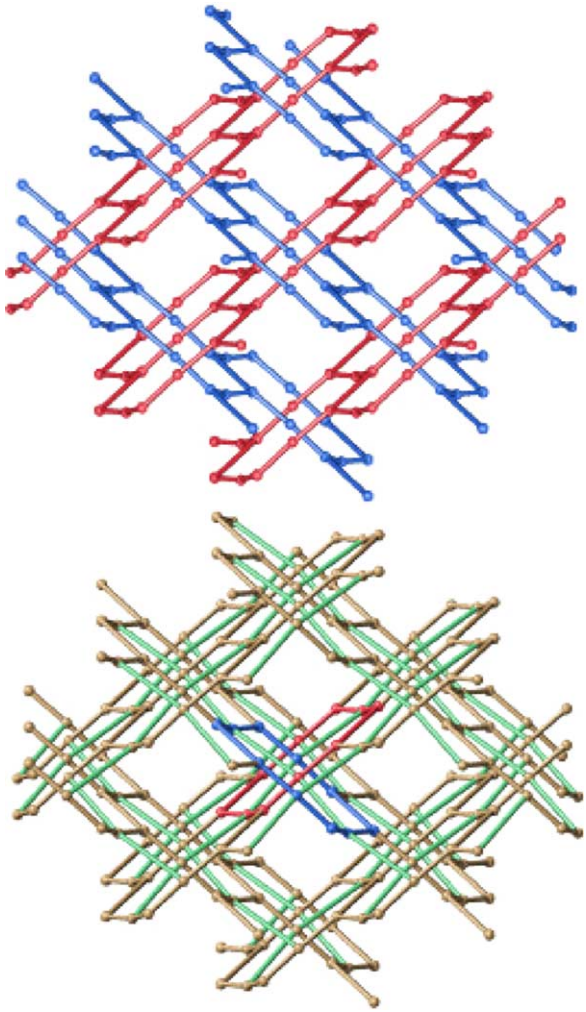

Fig. 49. Schematic view of the inclined interlocking of the two sets of (6, 3) layers in the species reported in [121] (top), and the unique 3D net obtained by taking into account the R-rad$^+$ bridging cations (extra green links) (bottom).

in which two Au(I)-I moieties are linked by a long chain diphosphine. The units are joined into infinite chains *via* aurophilic Au···Au contacts (3.12 Å long). The chains, showing sinusoidal shape, run in two inclined directions and are woven as in Scheme 12 (top).

While in the above gold(I) compound the polymeric chains are formed by means of weak supramolecular interactions, the first case of the same type of 2D organization fully sustained by coordinative bonds was observed in the polymer [Cu(2,2′-bipy)(azpy)(H_2O)](NO_3)$_2$·H_2O [azpy = *trans*-4,4′-azobis(pyridine)] [123]. This is comprised of zigzag chain polymers, with a period of ca. 19 Å, in which Cu(2,2′-bipy)$^{2+}$ molecular corners are joined by *cis*-coordinated azpy spacers. There are two distinct directions of chain propagation, generating warp-and-woof 2D sheets illustrated in Fig. 50.

Also the complex [Ag_2L_2(μ-PO_2F_2)](PF_6) [L = 1-(isocyanidomethyl)-1H-benzotriazole] [124] shows the same entanglement of 1D wavy –Ag–L–Ag–L– chains. In this

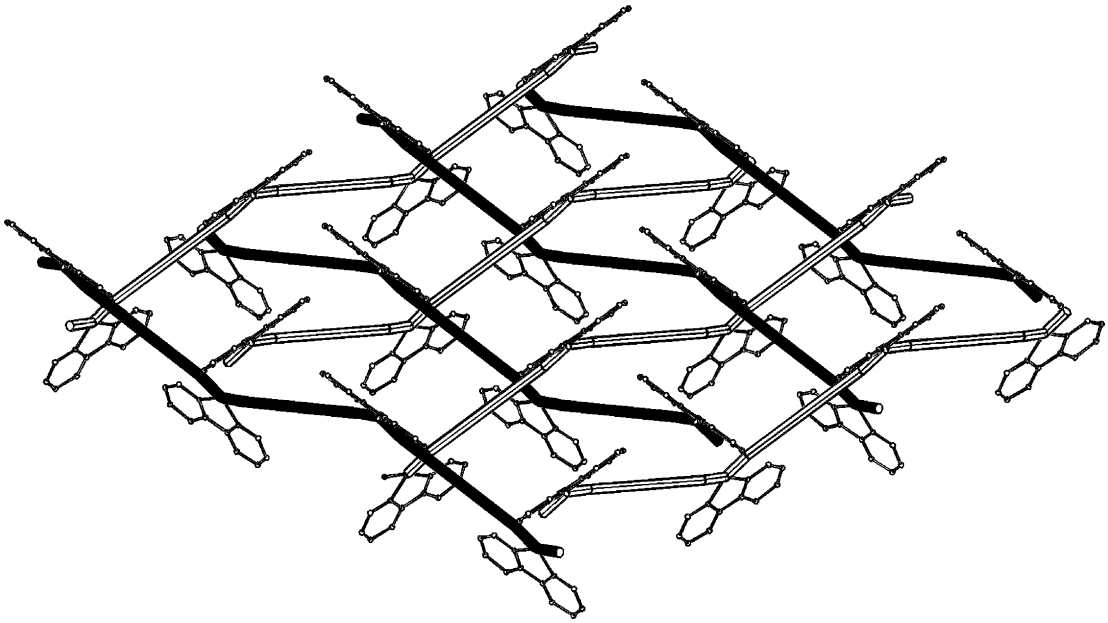

Fig. 50. The warp-and-woof like 2D layer in $[Cu(2,2'\text{-bipy})(azpy)(H_2O)](NO_3)_2{\cdot}H_2O$ [123].

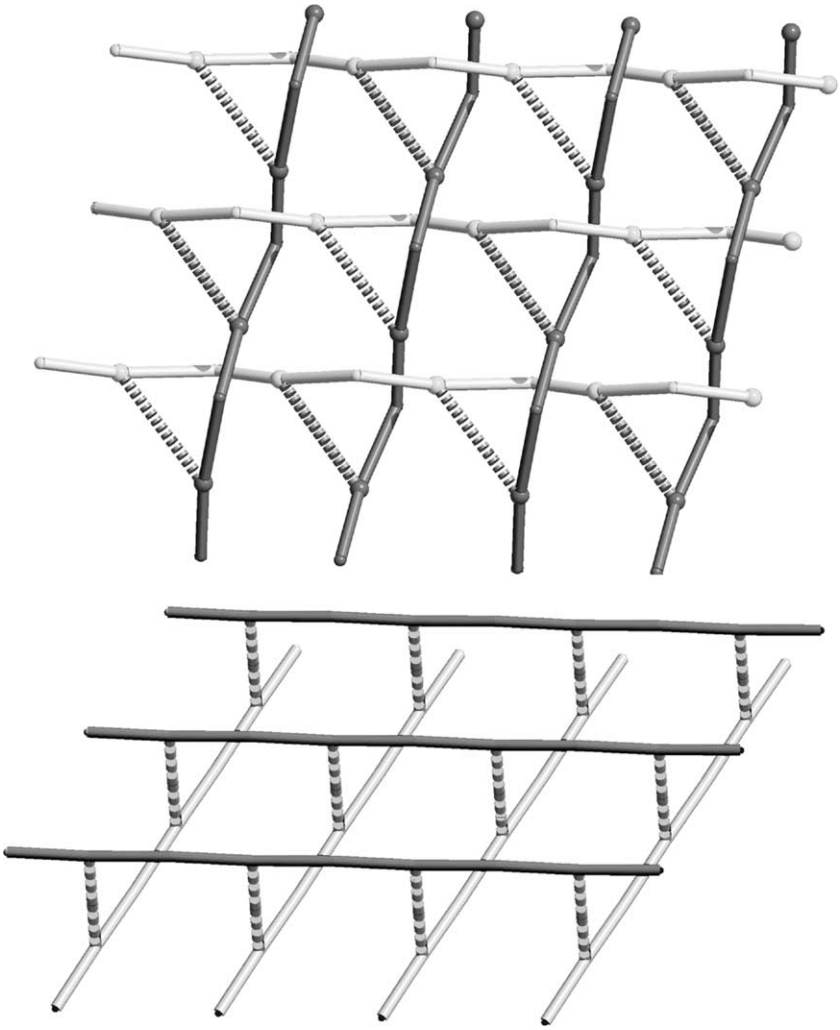

Fig. 51. Comparison of the 2D layer in $[Ag_2L_2(\mu\text{-}PO_2F_2)](PF_6)$ [124] (top) with the more common $8^2{\cdot}10$ net (bottom).

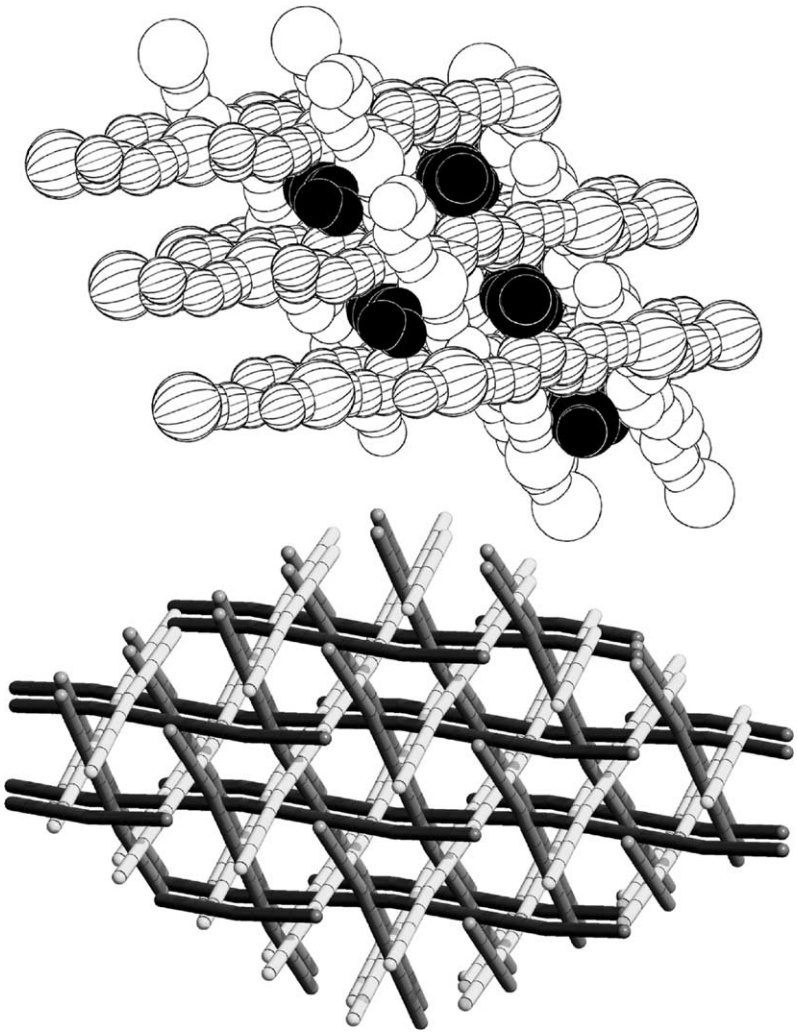

Fig. 52. The entanglement of the 1D polymeric chains spanning three directions in [Ag(sebn)](AsF_6) [65].

case, however, the woven chains are cross-linked *via* bridging $PO_2F_2^-$ anions, each connecting silver atoms of two different polymers (see Fig. 51, top). The resulting array is a single 2D net of uncommon topology. Curiously, it has the same Schläfli symbol [short $8^2{\cdot}10$ and long $(8_2{\cdot}8_2{\cdot}\infty)$], as well as the same coordination sequence of the more usual 2D layer shown in Fig. 51 (bottom). Again (see also Section 5.2) we find a case of two clearly different nets that are not discriminated using the common topological indices. New theoretical approaches should be investigated to classify the complex entities encountered in the *area* of entangled coordination polymers.

A single example of the chickenwire type (Scheme 12, bottom) is known, in an inorganic polymer. Kanatzidis and coworkers have reported the structure of NaAuS [125], containing –Au–S–Au–S– chains that trace 'Figure Eight' as they propagate. These chains are interwoven into chickenwire like layers.

A case of unusual 3D entanglement of 1D polymers is observed in [Ag(sebn)](AsF_6) [sebn = sebaconitrile (1,10-decanedinitrile)] [65], with the Ag(I) atoms linked by the dinitrile molecules into polymeric chains of period 32.8 Å. The peculiar structural feature consists in the unique self-organization of the chains, which extend in three non coplanar directions (related by three-fold crystallographic axes), as schematized in Fig. 52. Other structures are known that contain 1D chains spanning three different directions, as [Ag(pytz)](NO_3) [pytz = 3,6-di(4-pyridyl)-1,2,4,5-tetrazine] [126], but in this case all the polymers extend on parallel layers. [Ag(sebn)](AsF_6) differs from all the other 1D species in that there is no plane that can separate the whole array into two half parts without breaking bonds, and only on slipping off the chains this 3D arrangement can be disentangled.

6.2. *Infinite multiple helixes*

It is worth considering here another class of braided chain polymers resulting in 1D infinite interwoven aggregates; multiple helixes are rare in inorganic and coordination chemistry, and mainly contain digonal silver centers.

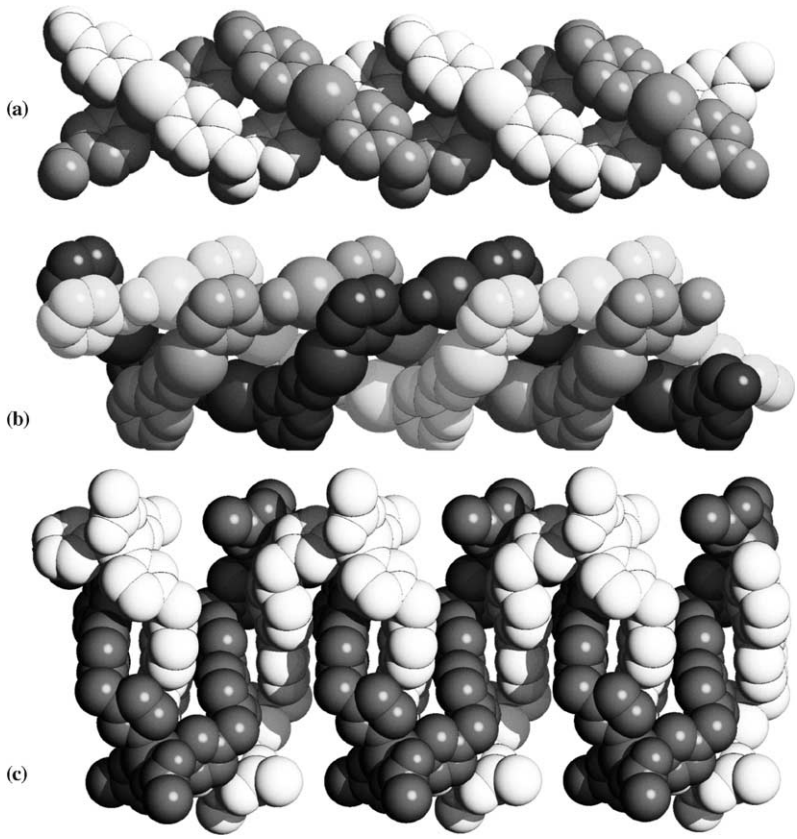

Fig. 53. Views of: (a) the double helix in [Ag(bpp)](CF_3SO_3) [129], (b) the triple helix in [Ag(3-amp)](ClO_4) [134] and (c) the two 'entwined snakes' in [Zn(bimb)$(OAc)_2$]·$6H_2O$ [136].

The first example of a double helix within coordination polymers was probably that described by Dance et al. in the silver-thiolate complex [Ag($SCEt_2Me$)] [127]. This is comprised of chains with sequences of 8 independent alternated Ag^+ cations and SR^- anions that form 4_1 helixes interwoven in pairs. The two independent strands interact only through Ag···Ag contacts of 2.89 Å, that were considered repulsive in nature by the authors.

A very similar species was discovered by Bau in the structural study of the antiarthritic drug Myochrisine [128]. In this compound, of composition $Na_2Cs[Au_2(LH)(L)]$ (L^{3-} = thiomalate), the main gold-sulfur backbone consists of two interweaved spirals, of approximate four-fold helical symmetry. The –Au–S–Au–S– chains are linear at Au and bent at S. New examples were obtained using longer molecular spacers joining the metal centers, as in the case of [Ag(bpp)](CF_3SO_3) [bpp = 1,3-bis(4-pyridyl)propane] [129]. The cationic 1D chains –Ag–bpp–Ag–bpp– form 2_1 helixes of period 21.1 Å entangled in pairs (see Fig. 53a). As the two spirals of DNA are connected by hydrogen bond bridges, in this species the two strands are bridged by weak Ag···Ag aurophilic (d^{10}–d^{10}) interactions of 3.09 Å. In correspondence with these Ag···Ag contacts the two helixes show a remarkable compression, normal to the helical axis. Also the complex [Ag(SalGly)]·$0.33H_2O$ [SalGly = a-*N*-(*o*-hydroxybenzyl)glycinate] [130] contains an infinite double helix, with the peculiarity of having 3_1 helical symmetry.

The 1:1 adduct of $AgPF_6$ with a complex ligand of the CHIRAGEN family consists of chirally predetermined infinite double 6_2 helixes of high symmetry [131]. No interactions are observed between the two helical strands. The pitch of the helix, i.e. the distance between equivalent atoms generated by one full rotation of the six-fold screw axis, is ca. 34.2 Å.

In [Cu(oba)(phen)] [oba = 4,4′-oxybis(benzoate), phen = 1,10-phenanthroline] [132] Cu(phen) units are joined by the bridging dicarboxylates into helical chains that interwave into infinite double helixes.

Other double stranded infinite helixes have been recently obtained using Ag^+ cations and long flexible ligands with two pyridyl groups interconnected by a tetra- or hexa-ethylene glycol fragment [133].

To our knowledge, the first example of a triple helical entanglement has been observed in [Ag(3-amp)](ClO_4) (3-amp = 3-aminomethylpyridine) [134]. The three independent chains exhibit 2_1 helical symmetry with a period of ca. 26 Å (see Fig. 53b). Interestingly, the helixes form tunnels 4 Å wide that contain one-half of the anions inside.

Enantiomerically pure triple stranded infinite helixes have been recently obtained by Hosseini and coworkers from the self-assembly of a bis-monodentate tecton based

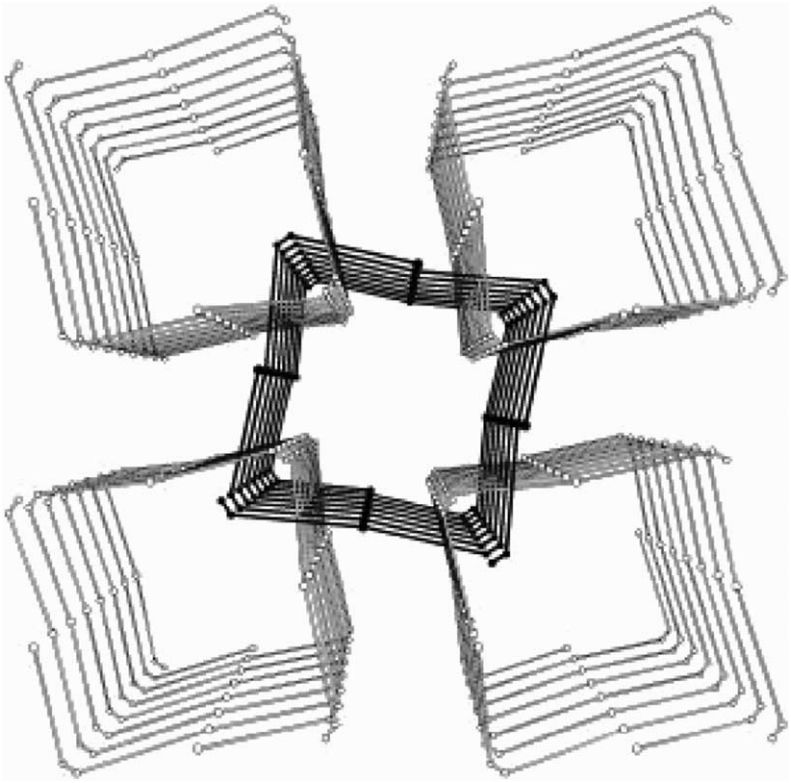

Fig. 54. The entanglement of the nanotubes (quintuple helixes) in the structure reported in [137].

on two pyridine units connected to an enantiomerically pure *iso*mannide stereoisomer and $HgCl_2$ [135].

A different type of entanglement of two 1D chains is present in $[Zn(bimb)(OAc)_2]\cdot 6H_2O$ [bimb = 4,4′-bis-(imidazol-1-ylmethyl)biphenyl, OAc^- = acetate] [136]. Two independent single-stranded wavy chains are interwoven with each other to form a double-stranded motif that looks like two 'entwined snakes' (see Fig. 53c).The dihedral angle between the two planes defined by the zinc atoms in each strand is 49.6°.

Finally, as a confirmation of the fact that novel topological types are continuously discovered, we mention here an exceptional structural motif just reported by Lin and coworkers [137]. The assembly of $Ni(acac)_2$ and 1,1-binaphthyl-6,6′-bipyridines (two C_2-symmetric ligands) has produced 4_1 helical chains, in which $Ni(acac)_2$ biconnecting units and the corner ligands alternate, with a helical pitch of 47.3 and 47.5 Å. Surprisingly, five such infinite homochiral helixes associate to form nanotubes (quintuple helixes). Moreover, the nanotubes are laterally entangled to give an unprecedented 3D chiral array, because each helix is interwoven with other four belonging to different nanotubes (see Fig. 54).

7. Conclusions

The concepts of crystal engineering and of supramolecular chemistry have thus far been employed to design and characterize a number of novel prototypical network structures based upon selected building blocks. On changing the type and number of the chemical components an almost unlimited potential for the synthesis of new systems seems on hand. As illustrated by the examples discussed above, entangled structures are becoming increasingly common within coordination polymers, and many new topologies are being reported. In the attempt to establish useful relationships between structures and properties for these species a careful analysis of the topology is unavoidable, particularly for the more complex types of entanglements, as polycatenanes, polyrotaxanes and polyknots, that have been discussed here. Some topological aspects (and also open problems) have been presented in this review, that is essentially intended as a contribution for a discussion within the scientific community. The application of topological methods is necessary to land the crystal engineering of coordination polymers on more certain mathematical bases and could also inspire new approaches for dealing with more complicated systems.

Many hypothetical (maybe exotic) examples of extended entanglements have also been proposed in this paper, that are likely to be encountered in the near future. Indeed, different network models that were anticipated on a pure theoretical background within crystal chemistry (like, for instance, the racemate of the $SrSi_2$ type [138] and the 12^3 self-penetrating net [116], discussed by Wells [23b], or the 'dense' net [139] and the 'net #97′ [140], suggested by O'Keeffe [25a] have been successively discovered in the realm of coordination polymers.

Acknowledgements

We would like to thank Dr. Silvia Rizzato for help in the preparation of the figures and for many useful discussions. We are grateful to Prof. Massimo Moret (Milano Bicocca University) for making available PACKNET, a program for the separation of nets. The Italian MIUR is also acknowledged for support to the project COFIN2000 "Solid Supermolecules".

References

[1] (a) R. Robson, B.F. Abrahams, S.R. Batten, R.W. Gable, B.F. Hoskins, J. Liu, Supramolecular architecture, in: T. Bein (Ed.), ACS Symposium Series 499, American Chemical Society, Washington, DC, 1992, p. 256;
(b) R. Robson, J. Chem. Soc. Dalton Trans. (2000) 3735;
(c) M.J. Zaworotko, Chem. Soc. Rev. 23 (1994) 283;
(d) B. Moulton, M.J. Zaworotko, Curr. Opin. Solid State Mater. Sci. 6 (2002) 117;
(e) M.J. Zaworotko, Chem. Commun. (2001) 1;
(f) M.J. Zaworotko, Nature 402 (1999) 242;
(g) C.L. Bowes, G.A. Ozin, Adv. Mater. 8 (1996) 13;
(h) P.J. Hagrman, D. Hagrman, J. Zubieta, Angew. Chem. Int. Ed. Engl. 38 (1999) 2639;
(i) M. Munakata, L.P. Wu, T. Kuroda-Sowa, Adv. Inorg. Chem. 46 (1999) 173;
(j) A.J. Blake, N.R. Champness, P. Hubberstey, W.S. Li, M.A. Withersby, M. Schroder, Coord. Chem. Rev. 183 (1999) 117;
(k) A.N. Khlobystov, A.J. Blake, N.R. Champness, D.A. Lemenovskii, A.G. Majouga, N.V. Zyk, M. Schroder, Coord. Chem. Rev. 222 (2001) 155;
(l) N.R. Champness, M. Schroder, Curr. Opin. Solid State Mater. Sci. 3 (1998) 419;
(m) M. Eddaoudi, D.B. Moler, H.L. Li, B.L. Chen, T.M. Reineke, M. O'Keeffe, O.M. Yaghi, Acc. Chem. Res. 34 (2001) 319;
(n) T.J. Barton, L.M. Bull, W.G. Klemperer, D.A. Loy, B. McEnaney, M. Misono, P.A. Monson, G. Pez, G.W. Scherer, J.C. Vartuli, O.M. Yaghi, Chem Mater. 11 (1999) 2633;
(o) M.W. Hosseini, Coord. Chem. Rev. 240 (2003) 157.

[2] General: C. Janiak, Dalton Trans. (2003) 2781;
Porosity: G.B. Gardner, D. Venkataraman, J.S. Moore, S. Lee, Nature 374 (1995) 792;
D. Venkataraman, G.B. Gardner, S. Lee, J.S. Moore, J. Am. Chem. Soc. 117 (1995) 11601;
O.M. Yaghi, G. Li, H. Li, Nature 378 (1995) 703;
O.M. Yaghi, H. Li, C. Davis, D. Richardson, T.L. Groy, Accounts Chem. Res. 31 (1998) 474;
M. Eddaoudi, H. Li, O.M. Yaghi, J. Am. Chem. Soc. 122 (2000) 1391;
S. Noro, S. Kitagawa, M. Kondo, K. Seki, Angew. Chem. Int. Engl. 39 (2000) 2081;
M.J. Zaworotko, Angew. Chem. Int. Ed. Engl. 39 (2000) 2113;
Catalysis: M. Fujita, Y.J. Kwon, S. Washizu, K. Ogura, J. Am. Chem. Soc. 116 (1994) 1151;
J.S. Seo, D. Whang, H. Lee, S.I. Jun, J. Oh, Y.J. Jeon, K. Kim, Nature 404 (2000) 982;
NLO: O.R. Evans, W. Lin, Acc. Chem. Res. 35 (2002) 511;
Magnetism: O. Kahn, Acc. Chem. Res. 33 (2000) 647, and references therein;
W. Lin, O.R. Evans, G.T. Yee, J. Solid State Chem 152 (2000) 152;
Electrical conductivity: A. Aumuller, P. Erk, G. Klebe, S. Hunig, J.U. von Schutz, H.-P. Werner, Angew. Chem. Int. Ed. Engl. 25 (1986) 740.

[3] (a) J.-M. Lehn, Supramolecular Chemistry: Concepts and Perspectives, VCH, New York, 1995;
(b) J.-M. Lehn, Angew. Chem. Int. Ed. Engl. 29 (1990) 1304;
(c) G.R. Desiraju, Crystal Engineering: Design of Organic Solids, Elsevier, Amsterdam, 1989;
(d) G.R. Desiraju, Angew. Chem. Int. Ed. Engl. 34 (1995) 311.

[4] B.F. Hoskins, R. Robson, J. Am. Chem. Soc. 112 (1990) 1546.

[5] B. Moulton, M.J. Zaworotko, Chem. Rev. 101 (2001) 1629;
T.L. Hennigar, D.C. MacQuarrie, P. Losier, R.D. Rogers, M.J. Zaworotko, Angew. Chem. Int. Ed. Engl. 36 (1997) 972;
A.J. Blake, N.R. Brooks, N.R. Champness, M. Crew, A. Deveson, D. Fenske, D.H. Gregory, L.R. Hanton, P. Hubberstey, M. Schröder, Chem. Commun. (2001) 1432

[6] C.V.K. Sharma, Cryst. Growth Des. 2 (2002) 465.

[7] M. O'Keeffe, M. Eddaoudi, H. Li, T. Reineke, O.M. Yaghi, J. Solid State Chem. 152 (2000) 3;
O.M. Yaghi, M. O'Keeffe, N.W. Ockwig, H.K. Chae, M. Eddaoudi, J. Kim, Nature 423 (2003) 705.

[8] D.M. Proserpio, R. Hoffman, P. Preuss, J. Am. Chem. Soc. 116 (1994) 9634.

[9] J.S. Miller, Adv. Mater. 13 (2001) 525.

[10] O. Ermer, Adv. Mater. 3 (1991) 608.

[11] T.M. Reineke, M. Eddaoudi, D.M. Moler, M. O'Keeffe, O.M. Yaghi, J. Am. Chem. Soc. 122 (2000) 4843.

[12] R. Kitaura, K. Seki, G. Akiyama, S. Kitagawa, Angew. Chem. Int. Ed. Engl. 42 (2003) 428.

[13] S.R. Batten, R. Robson, Angew. Chem. Int. Ed. Engl. 37 (1998) 1461.

[14] S.R. Batten, R. Robson, in: J.-P. Sauvage, C. Dietrich-Buchecker (Eds.), Molecular Catenanes, Rotaxanes and Knots: A Journey Through the World of Molecular Topology, Wiley-VCH, Weinheim, 1999, pp. 77–105.

[15] (a) S.R. Batten, Cryst. Eng. Commun. 3 (Art. 18) (2001) 67;
(b) S.R. Batten, Curr. Opin. Solid State. Mater. Sci. 5 (2001) 107.

[16] (a) J. P Sauvage, Acc. Chem. Res. 31 (1998) 611;
(b) J.C. Chambron, C.O. Dietrich-Buchecker, J.P. Sauvage, Top. Curr. Chem. 165 (1993) 131;
(c) J.P. Sauvage, Acc. Chem. Res. 23 (1990) 319;
(d) J.-P. Sauvage, C.O. Dietrich-Buchecker, Molecular Catenanes, Rotaxanes and Knots, Wiley-VCH, Weinheim, 1999;
(e) C.O. Dietrich-Buchecker, J.-P. Sauvage, Angew. Chem. Int. Ed. Engl. 28 (1989) 189.

[17] (a) D.B. Amabilino, J.F. Stoddart, Chem. Rev. 95 (1995) 2725;
(b) F.M. Raymo, J.F. Stoddart, Chem. Rev. 99 (1999) 1643;
(c) M.C.T. Fyfe, J.F. Stoddart, Acc. Chem. Res. 30 (1997) 393;
(d) S.A. Nepogodiev, J.F. Stoddart, Chem. Rev. 98 (1998) 1959.

[18] (a) K. Mislow, Croatica Chem. Acta 69 (1996) 485;
(b) K. Mislow, Bull. Soc. Chim. Belg. 86 (1977) 595.

[19] D.M. Walba, Tetrahedron 41 (1985) 3161.

[20] R.W. Gable, B.F. Hoskins, R. Robson, J. Chem. Soc., Chem. Commun. (1990) 1677 (CSD refcode: JEZRUB).

[21] P.R. Ashton, I. Baxter, M.C.T. Fyfe, F.M. Raymo, N. Spencer, J.F. Stoddart, A.J.P. White, D.J. Williams, J. Am. Chem. Soc. 120 (1998) 2297.

[22] M. Moret, PACKNET, 2000, University of Milano-Bicocca.

[23] (a) A.F. Wells, Structural Inorganic Chemistry, fifth ed., Oxford University Press, Oxford, 1984;
(b) A.F. Wells, Three-Dimensional Nets and Polyhedra, Wiley, New York, 1977;
(c) A.F. Wells, Further Studies of Three-Dimensional Nets, ACA Monograph 8, 1979.

[24] (a) J.V. Smith, Chem. Rev. 88 (1988) 149;
(b) J.V. Smith, Tetrahedral Frameworks of Zeolites, Clathrates and Related Materials, Landolt-Börnstein New Series IV/14, Subvolume A, Springer, Berlin, 2000

[25] (a) M. O'Keeffe, B.G. Hyde, Crystal Structures. I. Patterns and Symmetry, Mineral. Soc. Am., Washington, 1996;

(b) M. O'Keeffe, Z. Kristallogr. 196 (1991) 21;
(c) M. O'Keeffe, B.G. Hyde, Phil. Trans. R. Soc. Lond. 295 (1980) 553.
[26] M. O'Keeffe, EUTAX, Local modified PC version by D.M. Proserpio.
[27] M. Kondo, M. Shimamura, S.-I. Noro, S. Minakoshi, A. Asami, K. Seki, S. Kitagawa, Chem. Mater. 12 (2000) 1288.
[28] E. Cannillo, F. Mazzi, G. Rossi, Acta Crystallogr. 21 (1966) 200.
[29] D.E. Palin, H.M. Powell, J. Chem. Soc. (1947) 208;
H.M. Powell, J.Chem. Soc. (1950) 300.
[30] Y. Kinoshita, I. Matsubara, T. Higuchi, Y. Saito, Bull. Chem. Soc. Jpn. 32 (1959) 1221.
[31] L. Carlucci, G. Ciani, D.M. Proserpio, S. Rizzato, Chem. Eur. J. 8 (2002) 1520.
[32] D.S. Reddy, T. Dewa, K. Endo, Y. Aoyama, Angew. Chem. Int. Ed. Engl. 39 (2000) 4266.
[33] M. Eddaoudi, J. Kim, N. Rosi, D. Vodak, J. Wachter, M. O'Keeffe, O.M. Yaghi, Science 295 (2002) 469.
[34] K.A. Hirsch, S.R. Wilson, J.S. Moore, Chem. Eur. J. 3 (1997) 765.
[35] L. Carlucci, G. Ciani, M. Moret, D.M. Proserpio, S. Rizzato, Angew. Chem. Int. Ed. Engl. 39 (2000) 1506 (WISVID).
[36] A.W. Sleight, R.J. Bouchard, Inorg. Chem. 12 (1973) 2314.
[37] (a) J.Y. Lu, A.M. Babb, Chem. Commun. (2001) 821;
(b) Y.-C. Jiang, Y.-C. Lai, S.-L. Wang, K.-H. Lii, Inorg. Chem. 40 (2001) 5320;
(c) D.M. Shin, I.S. Lee, Y.K. Cheung, M.S. Lah, Chem. Commun. (2003) 1036.
[38] H. Dodziuk, K.S. Nowinski, Tetrahedron 54 (1998) 2917.
[39] (a) O. Delgado Friedrichs, M. O'Keeffe, O.M. Yaghi, Acta Cryst. A59 (2003) 22;
(b) O.D. Friedrichs, M. O'Keeffe, O.M. Yaghi, Solid State Sci. 5 (2003) 73;
(c) B. Chen, M. Eddaoudi, S.T. Hyde, M. O'Keeffe, O.M. Yaghi, Science 291 (2001) 1021;
(d) R. Nesper, S. Leoni, Chem. Phys. Chem. 2 (2001) 413;
(e) V.A. Blatov, Acta Cryst. A56 (2000) 178;
(f) O.D. Friedrichs, M. O'Keeffe, Acta Cryst. A 59 (2003) 351.
[40] E. Flapan, When Topology Meets Chemistry, University Press, Cambridge, 2000.
[41] (a) C. Liang, K. Mislow, J. Math. Chem. 16 (1994) 27;
(b) P. Cromwell, E. Beltrami, M. Rampichini, Math. Intelligencer 20 (1998) 53 (see also http://www.liv.ac.uk/~spmr02/rings/index.html).
[42] L. Carlucci, G. Ciani, D.M. Proserpio, Cryst. Eng. Commun. 5 (2003) 269.
[43] (a) S. Leininger, B. Olenyuk, P.J. Stang, Chem. Rev. 100 (2000) 853;
(b) M. Fujita, K. Ogura, Coord. Chem. Rev. 148 (1996) 249.
[44] M. Fujita, Acc. Chem. Res. 32 (1999) 53.
[45] W.R. Wikoff, L. Liljas, R.L. Duda, H. Tsuruta, R.W. Hendrix, J.E. Johnson, Science 289 (2000) 2129;
J. Chen, C.A. Rauch, J.A. White, P.T. Englund, N.R. Cozzarelli, Cell 80 (1995) 61.
[46] N.C. Seeman, Angew. Chem. Int. Ed. Engl. 37 (1998) 3220;
N. C Seeman, Annu. Rev. Biophys. Biomol. Struct. 27 (1998) 225.
[47] (a) P. Losier, M.J. Zaworotko, Angew. Chem. Int. Ed. Engl. 35 (1996) 2779;
(b) K.S. Min, M.P. Suh, Solid State Chem. 152 (2000) 183;
(c) M.A. Withersby, A.J. Blake, N.R. Champness, P.A. Cooke, P. Hubberstey, W.S. Li, M. Schroder, Inorg. Chem. 38 (1999) 2259;
(d) O.M. Yaghi, H. Li, T.L. Groy, Inorg. Chem. 36 (1997) 4292.
[48] H.-F. Zhu, J. Fan, T. Okamura, W.-Y. Sun, N. Ueyama, Chem. Lett. (2002) 898.
[49] (a) A.J. Blake, N.R. Champness, A. Khlobystov, D.A. Lemenovskii, W.-S. Li, M. Schroder, Chem. Commun. (1997) 2027 (NIWVUK);
(b) M. Maekawa, H. Konaka, Y. Suenaga, T. Kuroda-Sowa, M. Munakata, J. Chem. Soc., Dalton Trans. (2000) 4160.
[50] (a) L. Carlucci, G. Ciani, D.M. Proserpio, J. Chem. Soc., Dalton Trans. (1999) 1799;
(b) B. Dong, R.C. Layl, N.G. Pschirer, M.D. Smith, U.H.F. Bunz, H.-C. zur Loye, Chem. Mater. 11 (1999) 1413 (EBEHAU);
(c) Y.-B. Dong, R.C. Layland, M.D. Smith, N.G. Pschirer, U.H.F. Bunz, H.-C. zur Loye, Inorg. Chem. 38 (1999) 3056 (LOCXEG);
(d) J. Tao, X. Yin, R. Huang, L. Zheng, Inorg. Chem. Commun. 5 (2002) 1000.
[51] (a) M. Fujita, Y.J. Kwon, O. Sasaki, K. Yamaguchi, K. Ogura, J. Am. Chem. Soc. 117 (1995) 7287;
(b) M. Fujita, O. Sasaki, K.-Y. Watanabe, K. Ogura, K. Yamaguchi, New J. Chem. 22 (1998) 189 (ZALTOV, ZALTOV01, SEQMUW).
[52] (a) K. Biradha, K.V. Domasevitch, B. Moulton, C. Seward, M.J. Zaworotko, Chem. Commun. (1999) 1327;
F.H. Herbstein, Acta Cryst. B57 (2001) 517;
(b) K. Biradha, A. Mondal, B. Moulton, M.J. Zaworotko, J. Chem. Soc., Dalton Trans. (2000) 3837.
[53] F.-Q. Liu, T.D. Tilley, Inorg. Chem. 36 (1997) 5090 (NORDAZ).
[54] E.-Q. Gao, Z.-M. Wang, C.-S. Liao, C.H. Yan, New J. Chem. 26 (2002) 1096.
[55] D.J. Chesnut, A. Kusnetzow, R. Birge, J. Zubieta, Inorg. Chem. 38 (1999) 5484 (HOXRUH).
[56] J.M. Knaust, S. Lopez, S.W. Keller, Inorg. Chim. Acta 324 (2001) 81.
[57] X.-M. Zhang, X.-M. Chen, Eur. J. Inorg. Chem. (2003) 413.
[58] S. Banfi, L. Carlucci, E. Caruso, G. Ciani, D.M. Proserpio, Cryst. Growth Des., in press.
[59] M.L. Tong, X.-M. Chen, B.-H. Ye, L.-N. Ji, Angew. Chem. Int. Ed. Engl. 38 (1999) 2237 (HOFXOP, HOFXUV).
[60] J. Tao, X.-M. Zhang, M.-L. Tong, X.-M. Chen, J. Chem. Soc., Dalton Trans. (2001) 770 (XENCUO).
[61] S.M.-F. Lo, S.S.-Y. Chui, L.-Y. Shek, Z. Lin, X.X. Zhang, G. Wen, I.D. Williams, J. Am. Chem. Soc. 122 (2000) 6293 (LOLQUOS).
[62] Y. Fu, X.-T. Wu, J.-C. Dai, L.-M. Wu, C.-P. Cui, S.-M. Hu, Chem. Commun. (2001) 1856 (VOGQUIR).
[63] J.Y. Lu, A.M. Babb, Inorg. Chem. 40 (2001) 3261 (IBITOC).
[64] Y. Diskin-Posner, G.K. Patra, I. Goldberg, Chem. Commun. (2002) 1420.
[65] L. Carlucci, G. Ciani, P. Macchi, D.M. Proserpio, S. Rizzato, Chem. Eur. J. 5 (1999) 237 (GEHQEP, GEHTAO).
[66] S.R. Batten, A.R. Harris, P. Jensen, K.S. Murray, A. Ziebell, J. Chem. Soc., Dalton Trans. (2000) 3829 (LOTQUG).
[67] L. Carlucci, G. Ciani, D.M. Proserpio, S. Rizzato, Chem. Commun. (2000) 1319 (MEBBIE).
[68] Z.-Y. Fu, X.-T. Wu, J.-C. Dai, S.-M. Hu, W.-X. Du, N. J. Chem. 26 (2002) 978.
[69] A.C. Benyei, P.I. Coupar, G. Ferguson, C. Glidewell, A.J. Longh, P.R. Meehan, Acta Crystallogr., Sect. C 54 (1998) 1515 (POVJAL).
[70] S.V. Jablan, Forma 14 (1999) 269.
[71] (a) H.L. Frisch, E. Wassermann, J. Am. Chem. Soc. 83 (1961) 3789;
(b) N. van Gulick, N. J. Chem. 17 (1993) 619.
[72] C. Mao, W. Sun, N.C. Seeman, Nature 386 (1997) 137.
[73] S. Muthu, J.H.K. Yip, J.J. Vittal, J. Chem. Soc., Dalton Trans. (2002) 4561.
[74] D.B. Leznoff, B.-Y. Xue, R.J. Batchelor, F.W.B. Einstein, B.O. Patrick, Inorg. Chem. 40 (2001) 6026 (ICIWOG).
[75] M.P. Suh, H.J. Choi, S.M. So, B.M. Kim, Inorg. Chem. 42 (2003) 676.
[76] R. Liantonio, P. Metrangolo, T. Pilati, G. Resnati, Cryst. Growth Des. 3 (2003) 355.
[77] (a) M. Kondo, T. Yoshitomi, K. Seki, H. Matsuzaka, S. Kitagawa, Angew. Chem. Int. Ed. Engl. 36 (1997) 1725;
(b) K.N. Power, T.L. Hennigar, M.J. Zaworotko, N. J. Chem. 22 (1998) 177;
(c) C.J. Kepert, M.J. Rosseinsky, Chem.Commun. (1999) 375.
[78] L.R. MacGillivray, S. Subramanian, M.J. Zaworotko, J. Chem. Soc., Chem. Commun. (1994) 1325 (LETWAI).

[79] (a) D. Whang, K. Kim, J. Am. Chem. Soc. 119 (1997) 451;
(b) K.-M. Park, D. Whang, E. Lee, J. Heo, K. Kim, Chem. Eur. J. 8 (2002) 498 (REKHIY);
(c) D. Whang, Y.-M. Jeon, J. Heo, K. Kim, J. Am. Chem. Soc. 118 (1996) 11333;
(d) D. Whang, J. Heo, C.-A. Kim, K. Kim, Chem. Commun. (1997) 2361;
(e) E. Lee, J. Heo, K. Kim, Angew. Chem. Int. Ed. Engl. 39 (2000) 2699.

[80] (a) J.-F. Ma, J.-F. Liu, Y. Xing, H.-Q. Jia, Y.-H. Lin, J. Chem. Soc., Dalton Trans. (2000) 2403;
(b) Y.-B. Dong, M.D. Smith, H.-C. zur Loye, Inorg. Chem. 39 (2000) 4927;
(c) N.R. Brooks, A.J. Blake, N.R. Champness, J.W. Cunningham, P. Hubberstey, S.J. Teat, C. Wilson, M. Schroder, J. Chem. Soc., Dalton Trans. (2001) 2530;
(d) J. Fan, H.-F. Zhu, T. Okamura, W.-Y. Sun, W.-X. Tang, N. Ueyama, Inorg. Chem. 42 (2003) 158.

[81] (a) H.-P. Wu, C. Janiak, L. Uehlin, P. Klufers, P. Mayer, Chem. Commun. (1998) 2637;
(b) M.A. Withersby, A.J. Blake, N.R. Champness, P.A. Cooke, P. Hubberstey, A.L. Realf, S.J. Teat, M. Schroder, J. Chem. Soc., Dalton Trans. (2000) 3261;
(c) C. He, B.-G. Zhang, C. Duan, J. Li, Q.-J. Meng, Eur. J. Inorg. Chem. (2000) 2549;
(d) M. Kondo, M. Shimamura, S. Noro, S. Minakoshi, A. Asami, K. Seki, S. Kitagawa, Chem. Mater. 12 (2000) 1288;
(e) D.M. Ciurtin, Y-B. Dong, M.D. Smith, T. Barclay, H-C. zur Loye, Inorg. Chem. 40 (2001) 2825;
(f) Y-H. Liu, C-S. Lin, S-Y. Chen, H-L. Tsai, C-H. Ueng, K-L. Lu, J. Solid State Chem. 157 (2001) 166;
(g) P.S. Mukherjee, S. Dalai, G. Mostafa, E. Zangrando, T.-H. Lu, G. Rogez, T. Mallah, N.R. Chaudhuri, Chem. Commun. (2001) 1346;
(h) G. De Munno, F. Cipriani, D. Armentano, M. Julve, J.A. Real, N. J. Chem. 25 (2001) 1031;
(i) M.B. Zaman, M.D. Smith, H.-C. zur Loye, Chem. Mater. 13 (2001) 3534;
(j) S. Noro, R. Kitaura, M. Kondo, S. Kitagawa, T. Ishii, H. Matsuzaka, M. Yamashita, J. Am. Chem. Soc. 124 (2002) 2568;
(k) A. Dimos, D. Tsaousis, A. Michaelides, S. Skoulika, S. Golhen, L. Ouahab, C. Didierjean, A. Aubry, Chem. Mater. 14 (2002) 2616;
(l) L. Carlucci, G. Ciani, M. Moret, D.M. Proserpio, S. Rizzato, Chem. Mater. 14 (2002) 12;
(m) L. Carlucci, G. Ciani, D.M. Proserpio, S. Rizzato, Cryst. Eng. Commun. 4 (2002) 413.

[82] M.J. Plater, M.R.J. St. Foreman, T. Gelbrich, S.J. Coles, M.B. Hursthouse, J. Chem. Soc., Dalton Trans. (2000) 3065.

[83] L. Carlucci, G. Ciani, D.M. Proserpio, N. J. Chem. (1998) 1319 (MAHYID).

[84] K. Biradha, K.V. Domasevitch, C. Hogg, B. Moulton, K.N. Power, M.J. Zaworotko, Cryst. Eng. 2 (1999) 37.

[85] C.B. Aakeroy, A.M. Beatty, D.S. Leinen, Angew. Chem. Int. Ed. Engl. 38 (1999) 1815 (GOKMOI).

[86] N. Moliner, C. Munoz, S. Letard, X. Solans, N. Menendez, A. Goujon, F. Varret, J.A. Real, Inorg. Chem. 39 (2000) 5390 (QOVYEF).

[87] M. Kondo, M. Shimamura, S. Noro, S. Minakoshi, A. Asami, K. Seki, S. Kitagawa, Chem. Mater. 12 (2000) 1288 (REBWUQ).

[88] L. Carlucci, G. Ciani, D.M. Proserpio, S. Rizzato, Cryst. Eng. Commun. 5 (2003) 190.

[89] D. Hagrman, R.P. Hammond, R. Haushalter, J. Zubieta, Chem. Mater. 10 (1998) 2091 (FAKQIR).

[90] B.F. Hoskins, R. Robson, E.E. Sutherland, unpublished results, quoted in ref. [13].

[91] K.A. Hirsch, S.R. Wilson, J.S. Moore, Chem. Commun. (1998) 13 (PACQOZ).

[92] J.A. Kolnaar, Ph.D. thesis, Leiden University, Leiden, 1998, mentioned in J.G. Haasnoot, Coord. Chem. Rev. 200–202 (2000) 131.

[93] C.J. Kuehl, F.M. Tabellion, A.M. Arif, P.J. Stang, Organomet. 20 (2001) 1956 (XIKJIK).

[94] C.S.A. Fraser, M.C. Jennings, R.J. Puddephatt, Chem. Commun. (2001) 1310 (XIBLEZ).

[95] B.F. Hoskins, R. Robson, D.A. Slizys, J. Am. Chem. Soc. 119 (1997) 2952 (RIZZEF).

[96] M.E. Kosal, J.-H. Chou, K.S. Suslick, J. Porph. Phthal. 6 (2002) 377.

[97] (a) C.V.K. Sharma, G.A. Broker, J.G. Huddleston, J.W. Baldwin, R.M. Metzger, R.D. Rogers, J. Am. Chem. Soc. 121 (1999) 1137;
(b) C.V.K. Sharma, G.A. Broker, R.D. Rogers, J. Solid State Chem. 152 (2000) 253.

[98] G.-F. Liu, B.-H. Ye, Y.-H. Ling, X.-M. Chen, Chem. Commun. (2002) 1442.

[99] M.J. Plater, M.R.St.J. Foreman, T. Gelbrich, M.B. Hursthouse, Cryst. Eng. 4 (2001) 319 (ODAHEG).

[100] B.F. Hoskins, R. Robson, D.A. Slizys, Angew. Chem. Int. Ed. Engl. 36 (1997) 2336 (NEBSUI).

[101] D.M.L. Goodgame, S. Menzer, A.M. Smith, D.J. Williams, Angew. Chem. Int. Ed. Engl. 34 (1995) 574 (YOCPEL).

[102] C.V.K. Sharma, R.D. Rogers, Chem. Commun. (1999) 83 (GOZBAY).

[103] M.-L. Tong, Y.-M. Wu, J. Ru, X.-M. Chen, H.-C. Chang, S. Kitagawa, Inorg. Chem. 41 (2002) 4846.

[104] M.B. Zaman, M.D. Smith, H.-C. zur Loye, Chem. Commun. (2001) 2256 (ICIDUT, ICIFAB).

[105] K. Biradha, M. Fujita, Chem. Commun. (2002) 1866.

[106] S. Banfi, L. Carlucci, E. Caruso, G. Ciani, D.M. Proserpio, J. Chem. Soc., Dalton Trans. (2002) 2714.

[107] L. Carlucci, G. Ciani, D.M. Proserpio, Chem. Commun. (1999) 449 (JUQFUW).

[108] M.-L. Tong, H.-J. Chen, X.-M. Chen, Inorg. Chem. 39 (2000) 2235 (MEDRIW, MEDROC).

[109] B. Hayes, Am. Scientist 85 (1997) 506.

[110] M.A. Withersby, A.J. Blake, N.R. Champness, P.A. Cooke, P. Hubberstey, M. Schroder, J. Am. Chem. Soc. 122 (2000) 4044 (MARKOF).

[111] D.J. Price, S.R. Batten, B. Moubaraki, K.S. Murray, Chem. Eur. J. 6 (2000) 3186 (WOGROZ).

[112] M. O'Keeffe, Nature 392 (1998) 879 (however, taking into account our definition of self-penetration, for Ice IV the self-penetrating six- and ten-membered circuits are not both "shortest rings").

[113] M.J. Plater, M.R.J. St. Foreman, T. Gelbrich, M.B. Hursthouse, J. Chem. Soc., Dalton Trans. (2000) 1995 (WETWIB).

[114] B.F. Abrahams, M.J. Hardie, B.F. Hoskins, R. Robson, E.E. Sutherland, J. Chem. Soc. Chem. Commun. (1994) 1049 (HEHHED, HEHHAD, HEHHIL).

[115] J. Kim, K. Kim, Cryst. Eng. 3 (2000) 1 (WOFNET).

[116] B.F. Abrahams, S.R. Batten, M.J. Grannas, H. Hamit, B.F. Hoskins, R. Robson, Angew. Chem. Int. Ed. Engl. 38 (1999) 1475 (GOQWOY).

[117] T. Schareina, C. Schick, B.F. Abrahams, R. Kempe, Z. Anorg. Allg. Chem. 627 (2001) 1711 (RAKBIO).

[118] L. Carlucci, G. Ciani, D.M. Proserpio, S. Rizzato, J. Chem. Soc., Dalton Trans. (2000) 3821 (XASDUQ, XASFAY).

[119] L. Carlucci, G. Ciani, F. Porta, D.M. Proserpio, Angew. Chem. Int. Ed. Engl. 42 (2003) 317.

[120] P. Jensen, S.R. Batten, B. Moubaraki, K.S. Murray, J. Chem. Soc., Dalton Trans. (2002) 3712.

[121] H.O. Stumpf, L. Ouahab, Y. Pei, D. Grandjean, O. Kahn, Science 261 (1993) 447;
H.O. Stumpf, L. Ouahab, Y. Pei, P. Bergerat, O. Kahn, J. Am. Chem. Soc. 116 (1994) 3866 (YAPTUE);

M.G.F. Vaz, L.M.M. Pinheiro, H.O. Stumpf, A.F.C. Alcantara, S. Golhen, L. Ouahab, O. Cador, C. Mathoniere, O. Kahn, Chem. Eur. J. 5 (1999) 1486;
M.G.F. Vaz, H.O. Stumpf, N.L. Speziali, C. Mathoniere, O. Cador, Polyhedron 20 (2001) 1761–1769.
[122] P.M. Van Calcar, M.M. Olmstead, A.L. Balch, J. Chem. Soc. Chem. Commun. (1995) 1773 (NUJTUH).
[123] L. Carlucci, G. Ciani, A. Gramaccioli, D.M. Proserpio, S. Rizzato, Cryst. Eng. Commun. (2000) 29 (WOPNOE).
[124] I. Ino, J.C. Zhong, M. Munakata, T. Kuroda-Sowa, M. Maekawa, Y. Suenaga, Y. Kitamori, Inorg. Chem. 39 (2000) 4273 (XAKCIV).
[125] E.A. Axtell III, J.-H. Liao, M.G. Kanatzidis, Inorg. Chem. 37 (1998) 5583.
[126] M.A. Withersby, A.J. Blake, N.R. Champness, P. Hubberstey, W.S. Li, M. Schroder, Angew. Chem. Int. Ed. Engl. 36 (1997) 2327 (NEBUEV).
[127] I.G. Dance, L.J. Fitzpatrick, A.D. Rae, M.L. Scudder, Inorg. Chem. 22 (1983) 3785 (CEPKIR).
[128] R. Bau, J. Am. Chem. Soc. 120 (1998) 9380 (HEQKAP).
[129] L. Carlucci, G. Ciani, D. Wolf v. Gudenberg, D.M. Proserpio, Inorg. Chem. 36 (1997) 3812 (RORJEN).
[130] A. Erxleben, Inorg. Chem. 40 (2001) 2928 (QOZSON).
[131] O. Mamula, A.V. Zelewsky, T. Bark, G. Bernardinelli, Angew. Chem. Int. Ed. Engl. 38 (1999) 2945 (CINCEH).
[132] X.-M. Chen, G.F. Liu, Chem. Eur. J. 8 (2002) 4811.
[133] A. Jouaiti, M.W. Hosseini, N. Kyritsakas, Chem. Commun. (2003) 472.
[134] S. Sailaja, M.V. Rajasekharan, Inorg. Chem. 39 (2000) 4586 (QAJWUT).
[135] P. Grosshansa, A. Jouaitia, V. Bulacha, J.-M. Planeixa, M.W. Hosseini, J.-F. Nicoudb, Chem. Commun. (2003) 1336.
[136] H.-F. Zhu, W. Zhao, T. Okamura, B.-L. Fei, W.-Y. Sun, N. Ueyama, N. J. Chem. 26 (2002) 1277.
[137] Y. Cui, S.J. Lee, W. Lin, J. Am. Chem. Soc. 125 (2003) 6014.
[138] See e.g. L. Carlucci, G. Ciani, D.M. Proserpio, A. Sironi, Chem. Commun. (1996) 1393;
B.F. Abrahams, S.R. Batten, H. Hamit, B.F. Hoskins, R. Robson, Chem. Commun. (1996) 1313.
[139] L. Carlucci, G. Ciani, P. Macchi, D.M. Proserpio, Chem. Commun. (1998) 1837.
[140] See e.g. L. Carlucci, G. Ciani, N. Cozzi, M. Moret, D.M. Proserpio, S. Rizzato, Chem. Commun. (2002) 1354;
I. Boldog, E. B. Rusanov, A.N. Chernega, J. Sieler, K.V. Domasevitch, J. Chem. Soc., Dalton Trans. (2001) 893.